University of Southern Queensland

Faculty of Engineering and Surveying

Use of Vibration Signature in Structural Health Monitoring (Composite/Internal Damages)

A dissertation submitted by

Erin Heaton

in fulfilment of the requirements of

Courses ENG4111 and ENG4112 Research Project

towards the degree of

Bachelor of Engineering (Mechanical)

Submitted: October, 2011

Abstract

This dissertation develops and analyses the use of vibration signature as a method to detect damage in composite structures. A glass fibre pultrusion square hollow section member was used in this analysis.

The member was subjected to a forced oscillation produced by a shaker. The response of the system was gathered by an accelerometer at several data acquisition points along the length of the member. The force and acceleration data obtained was then post processed to create fast Fourier transformations and frequency response functions. This process was completed for the undamaged section and several damaged scenarios. The frequency response functions of each of these scenarios at each node were then cross-referenced with the relating undamaged data using a finite difference approach. This finite difference approach produced damage index values for each node at every damage level tested. This provided an indication of the position of any potential damages. The damage indexes at each level for a known damage were then used to create an arbitrary scale that could be used to determine the extent of damage sustained.

This method was completed with inherent issues pertinent to interpolation, a small data sample frequency and initial delamination of the composite. However, despite these issues the vibration damage detection technique did correctly identify damages and damage levels when a node was directly damaged. Detection of damages between data acquisition nodes was less successful.

Through further code optimisation and an increase in computing power this method may provide results accurate enough to be used in engineering endeavours. It is intended that this method be used to detect damages in structures used in low safety factor situations such as in the aerospace industry. It may be used to alert maintenance to particular points of interest and alert operators of anomalous damages before catastrophic failure occurs.

University of Southern Queensland

Faculty of Engineering and Surveying

ENG4111 Research Project Part 1 &
ENG4112 Research Project Part 2

Limitations of Use

The Council of the University of Southern Queensland, its Faculty of Engineering and Surveying, and the staff of the University of Southern Queensland, do not accept any responsibility for the truth, accuracy or completeness of material contained within or associated with this dissertation.

Persons using all or any part of this material do so at their own risk, and not at the risk of the Council of the University of Southern Queensland, its Faculty of Engineering and Surveying or the staff of the University of Southern Queensland.

This dissertation reports an educational exercise and has no purpose or validity beyond this exercise. The sole purpose of the course pair entitled "Research Project" is to contribute to the overall education within the student's chosen degree program. This document, the associated hardware, software, drawings, and other material set out in the associated appendices should not be used for any other purpose: if they are so used, it is entirely at the risk of the user.

Professor Frank Bullen

Dean

Faculty of Engineering and Surveying

Certification

I certify that the ideas, designs and experimental work, results, analyses and conclusions set out in this dissertation are entirely my own effort, except where otherwise indicated and acknowledged.

I further certify that the work is original and has not been previously submitted for assessment in any other course or institution, except where specifically stated.

Erin Heaton

Student Number: 0050085655

_____

Signature

_____

Date

Acknowledgements

This research was carried out under the principal supervision of Dr. Jayantha Epaarachchi. I would like to thank Dr. Epaarachichi for his guidance, direction and words of wisdom over the course of this project.

I would also like to thank my father, Robert Heaton, for the support he provided.

Gratitude needs to be expressed to two of my friends, William McHugh and Iain Brookshaw, for providing advice when various hurdles were experienced during the course of this research project.

Table of Contents

List of Figures

List of Tables

List of Appendices

Nomenclature

Abbreviations

The following abbreviations have been used throughout the text:

APS	Autopower Spectrum
CEPS	Cepstrum Function
COF	Curvature of Frequency
COH	Average Coherence Function
ESD	Energy Spectral Density
FEA	Finite Element Analysis
FFT	Fast Fourier Transformation
FRF	Frequency Response Function
Gxy	Averaged Cross Spectrum
GxyN	Cross Power Spectrum
PSD	Power Spectral Density
WIN	Windowed

Equation Variable Symbols

The following variable symbols have been used in the text:

A	Cross-Sectional Area of the Beam [m^2]
a	Initial Point [-]
$\alpha_{i,j}(\omega)$	FRF Taken at Node i with an Forced Oscillation at Position j
$\alpha_{i+1,j}(\omega)$	FRF Taken at node i +1 with an oscillating force at position j
$\alpha_{i-1,j}(\omega)$	FRF Taken at Node i -1 with an oscillating force at position j
$\alpha''_{i,j}(\omega)_D$	Curvature of Frequency at a Damaged Node and Particular Damage Extent
$\alpha''_{i,j}(\omega)$	Curvature of Frequency at an Undamaged Node and Particular Damage Extent
$\alpha''_{i,j}(\omega)$	Curvature of Frequency
b	Final Point [-]

$\beta_{i,j}(\omega)$	Damage Index at a Node and Particular Damage Extent
E	Young's modulus [Pa]
f_n	Natural Frequency [Hz]
h	Node Spacing [m]
I	Moment of Inertia of the Cross Section of the Beam [m^4]
i	Node Number Counter
j	Position of the Oscillating Force
k	Damage Extent Counter
L	Total Length of the Beam [m]
N	Number of Natural Frequency
N	Maximum Value of i, Total Node Number
n	Number of Trapezoid Sections Between a and b [-]
Ω_n	Frequency Coefficient
ρ	Density [kg/m^2]
x	Acceleration or Velocity [$m.s^{-2}$ or $m.s^{-1}$];

Chapter 1 **Introduction**

Structural damage detection techniques are evolving to suit modern engineering applications. This evolution is required as the older techniques are unable to detect damage efficiently. Essentially these techniques use highly localised, destructive and are a highly operator and time dependant means of damage detection. Therefore it is the intention of the researcher to gather data pertinent to new avenues of damage detection. These methods utilise the vibration characteristics of damaged and undamaged composite structures.

This new method of damage detection using vibration characteristics presents a number of beneficial attributes. It is a non-destructive, comprehensive technique that reduces the requirement for experienced operators, large amounts of money and time. Real time damage detection is also a viable option with this method, as Microelectromechanical Systems are small sensors that can be imbedded into structures providing acceleration data while the structure is being used.

Vibration characteristics of structures can be used to determine the position and extent of a damaged section within a structure. The technique that has been chosen correlates the flexibility matrix of an undamaged structure with that of a damaged structure. This was achieved by obtaining acceleration and force data at a number of node points located on the structure and using this to gain frequency response function data. This data was then used in a finite difference type algorithm in an attempt to determine the position and extent of the damage sustained.

1.1 Background

Damage detection is a significant part of the engineering world. It is used to determine when a particular structure requires maintenance and whether a structure is safe for use. This process saves lives and money by protecting from disaster.

There are many different types of damage detection currently being used. These include X-Ray, ultrasonic, coin tap, dye penetration and visual inspection. The majority of these techniques require a skilled operator and some rendition of visual inspection as X-Ray and Ultrasonic are used with a display. These processes are also localised and therefore take a large amount of time to completely test a large structure. Visual detection is also difficult when using a composite material as composites are created from many materials that are bonded together. Because of this an operator may not be able differentiate between a legitimate crack and a line of a different material. Therefore other damage detection techniques must be discovered in order to detect damages in composite materials.

For these reasons a different method of detecting damage utilising vibration was proposed. Damage detection using vibration has many desirable properties such as being a non-destructive, quick, cheap and easy method of damage detection. There are many different vibration damage detection techniques available. This includes frequency change using fast Fourier transformation. This method changes the data obtained through experimentation from being time dependant to being frequency dependant, which provides the natural frequencies of the structure. The small differences between the natural frequencies of a structure being tested and a known undamaged structure are used to determine whether the test structure is damaged. Change in modal strain energy, change in mode shape, neural network, residue force indicator and changes in the flexibility matrix may also be used. Essentially each of these uses a change in a vibration characteristic of a material to determine whether the structure is damaged or not. Factors used to describe these characteristics include acceleration, velocity, deflection, force, strain and mode shapes.

The vibration damage detection method chosen utilised the small differences in flexibility matrix using frequency response functions to detect damage. This method converted force data and deflection data at various points along the structure into frequency response functions which were then used in a finite difference algorithm. This algorithm produced a damage index at various data acquisition nodes on the

structure that were subjected to increasing levels of damage. This index gave an indication of the position of these damages. Extent of damage was quantified with an arbitrary scale of damage which was created by tabulating damage indexes at known damage levels.

This method was chosen as the literature reviewed suggested that it was highly robust, cheap, reliable, accurate and has the ability to detect numerous damages in a single structure. The location of the excitation force is also irrelevant so the testing apparatus can be set up with ease. It also removes the requirement for an experienced operator as the position and extent of the damage is identified automatically using algorithms in a post processing program.

1.2 Aims and Objectives

During the operational lifetime of a structure the vibration signature changes due to material property degradation. As such, vibration signatures can be used as an index of residual lifetime of the structure or component. This project investigated the change of vibration signature of a composite structure due to dynamic loading. Tasks that have been completed consist of an extensive literature review, sample preparation, measurement of vibration characteristics of composite components and validation using finite element analysis.

1.3 Process

The general processes conducted by the researcher in order to complete this analysis are outlined in the following:

- Conducted research pertinent to the background material relevant to composite vibration modelling, the composite material being tested and vibration data acquisition
- Designed and manufactured a device that was used to connect the excitation apparatus to the testing material
- Data collection pertinent to the forced vibration of defective and faultless fibre composite members
- Numerically solve for the natural frequencies and frequency response functions of the faultless material and the various levels of defective material

- Conducted the damage detection process using the finite difference algorithm
- Created an arbitrary scale of damage using the output of the finite difference algorithm
- Completed a computational finite element analysis of the member to confirm the numerical results
- Evaluated whether this process was accurate enough to be a viable means of defect detection in composite materials

1.4 Chapter Overview

1.4.1 Chapter 2 Literature Review

Chapter 2 consisted of a review of the literature pertinent to the various current damage detection methods available. Sensor variants, composite materials, signal processing and integration methods were also presented. The different damage detection techniques available were discussed.

1.4.2 Chapter 3 Vibration Analysis Methodology

Chapter 3 outlined the components of the apparatus and vibration damage detection method chosen. Damage index and the type of test damage that was used were also defined and discussed. A brief overview of the post processing program was also presented

1.4.3 Chapter 4 Apparatus

The various components that were used to conduct the experimentation were presented and discussed in chapter 4. The construction process required to use the apparatus and the operation steps were also outlined.

1.4.4 Chapter 5 System Verification

The various system verification methods used were outlined in chapter 5. These consisted of finite element analysis, hand calculations and using LMS Express to perform data checks while the experimentation was occurring.

1.4.5 Chapter 6 Data Analysis

Chapter 6 explains the processes involved in the post processing program including the damage detection and post processing constituents.

1.4.6 Chapter 7 Discussion and Results

Chapter 7 presented and analysed the various data plots produced in the post processing procedure. These included the presentation and examination of the raw data, FFT, FRF, damage index and scale of damage.

1.4.7 Chapter 8 Conclusions

The accuracy and viability of the damage detection system was discussed in Chapter 8. The way in which the project specifications are met was discussed and the future work required to achieve a reliable system were presented.

Chapter 2 **Literature Review**

This chapter offers a brief review of the research conducted and the decisions made using this knowledge. It will cover a selection of the existing techniques that are viable in relation to damage detection as well as the different integration methods and the different sensors that can be used in this type of application. Signal processing will also be discussed briefly.

2.1 Existing Techniques for Damage Detection

Damage detection techniques have existed for many years. The general types of damage detection include ultrasonic, X-Ray and visual inspection techniques such as dye penetration. These are successful and useful avenues of damage detection, however they all have merits and detrimental aspects pertinent to particular applications.

2.1.1 Dye Penetration

Dye penetration is a visual inspection technique used to identify surface damages by introducing dye onto the surface of a material (Munns 2009). The dye is left to penetrate the surface of the specimen where the defects have occurred. The excess dye is then wiped away leaving the dye in the defects. The defects can then be visually identified by eye. Dye penetration damage detection can only detect the damages on the outer surface of the material (Munns 2009). Therefore, this method was deemed an inaccurate and operator dependant technique and therefore was not considered.

2.1.2 Ultrasonic

Ultrasonic damage detection is used in the engineering industry as a local damage detection technique (Tsuda 2006). This method involves investigating the changes in ultrasonic signal through a damaged structure in comparison to an undamaged

specimen. This allows the position of the damage and an indication of the extent of damage to be found. This method was improved upon by Dutta (2010). It was proposed that a non-baseline method be used in order to determine whether damage has occurred in a structure without prior undamaged test specimens. This method utilises Lamb waves and modal data which is created and gathered using piezoelectric wafer transducers. Therefore as both of these methods require many components that may not be easily obtained, this method will not be used.

2.1.3 X-Ray

Damage detection using X-Rays is described as a non-destructive method (Bathias & Cagnasso 1992). This method involves using X-Ray tomography to inspect the complete structure. While the X-Ray process is taking place the structure is rotated 180 degrees. The specimen is tridimensionally reconstructed on a computer presenting its local density makeup (Bathias & Cagnasso 1992). This image is then used by an operator to determine where the damages exist and to what extent. This method was not used as it requires numerous expensive components and a relatively experienced operator in order to work accurately.

2.1.4 Damage Detection Method Selection

These typical methods of damage detection were deemed to be time consuming, inaccurate and generally operator dependant. Therefore a new damage detection technique utilising vibration characteristics was formulated.

2.2 Existing Vibration Damage Detection Methods

Many techniques have been created to detect damage in structures. These include X-ray, ultrasonic, magnetic resonance, coin tap, dye penetration and visual inspection. Most of these techniques are localised techniques which require a substantial amount of time and money to perform. In this application a composite pultrusion will be used and as such, visual and magnetic detection techniques are not viable. This is because the composite material is created from a number of materials that have been bonded together. This mix of materials and bonding action make it impossible to correctly identify cracks and damages with these techniques. Therefore a less time consuming, accurate and preferably non-destructive technique of damage detection in composite and bonded materials is required. It is proposed that vibration damage detection be used to detect damage in the composite member.

There are numerous techniques available for determining the existence, location and magnitude of damage in structures using vibration techniques. These techniques do not usually require prior knowledge of the general location of the damage, do not destroy the structure and do not require disassembly of the structure. These techniques include frequency changes, modal strain energy, mode shapes, neural network, residue force indicator of damage and changes in the flexibility matrix.

2.2.1 Changes in Frequency

The first set of methods considered relates to the differences of frequencies between damaged and undamaged structures. Through the correlation of damaged and undamaged channel section test data it was discovered that general changes in frequency profile may occur when damage exists (Chen, Spyrakos & Venkatesh 1995).

Chen et al. (1995) used an accelerometer and an impact loading in order to obtain test data pertinent to the damaged and undamaged sections. Linear regression was used to filter out background noise and a fast Fourier transformation algorithm was then used to change the data function from being time dependant to frequency dependant. The data from each section was then graphed in order to visually recognise any changes in natural frequency that had occurred between the two sections. Chen et al. (1995) discovered that the results they obtained "indicate a reduction in frequencies with increase in damage" (Chen et al. 1995, pg 1203).

Salawu (1999) suggests that a frequency shift of approximately 5% is necessary to confidently determine whether a structure is damaged. However, Salawu also concludes that a 5% frequency shift is not always an indication of damage in a structure. Ambient condition changes throughout the day may result in greater frequency changes in excess of 5% in certain structures (Salawu 1997). Therefore this method is proposed to be an avenue that can be used to detect large amounts of damage in structures. However, it cannot be relied upon for the detection of small defects as Salawu (1997) concludes it "may not be sufficient for the unique identification of the location of structural damage" (Salawu 1997, pg 721).

2.2.2 Change in Modal Strain Energy

The second set of damage detection methods considered relates to the change of modal strain energy. Shi et al. (1998, 2000) presented a technique that used the changes in modal strain energy to detect multiple structural damages without prior knowledge of damage locations. It was found that when damage is present in a structure the stiffness

matrix is affected while the mass matrix remains unaffected. With the use of finite element modelling it was also found that the undamaged elements in the structure would not have a significant change in stiffness and the damaged elements would.

Therefore Shi et al. (1998, 2000) used these characteristics to create a modal energy change ratio algorithm. This algorithm utilises the stiffness matrices of damaged and undamaged structures and correlates the two over a particular node spacing to determine the differences in modal strain energy. It was found that the undamaged elements did not undergo a significant modal strain energy change while the damaged elements did. However, it was also found that the nodes of the structure that correspond to the particular mode shape introduced errors into the data. These readings gave either large values or small values for the modal strain energy change. This may cause incorrect identification of where damage would occur or may cause them to be disregarded altogether. In order to increase the accuracy of the results obtained from the algorithm Shi et al. (1998) used multiple modes instead of just one. It was also found that "the Modal Strain Energy Change in higher modes do not contribute much in the identification of the damage location" (Shi, Law & Zhang 1998, pg 831).

2.2.3 Mode Shapes

The third set of damage detection methods considered utilises mode shapes to detect damage in structures. Maia et al. (2003) presented four different methods of mode shape utilisation in order to detect damage in structures. These consisted of mode shape, mode shape slope, mode shape curvature and mode shape curvature squared. These methods are interrelated as they are either the first or second derivative of the original mode shape. These mode shapes are created by the discovery of the natural frequencies of the damaged and undamaged structures by means of experimentation.

Each of these methods can be used to detect the position and to some extent the degree of damage imposed on the structure with the use of the damage index method. Kim et al. (2002) used this damage index method which utilises an algorithm to correlate the damaged and undamaged test data at nodal points along the structure. This provides a damage index of which can be plotted and the position of damages can be visually identified by recognising the peaks in the plot. Although this is a prospective method Maia et al. (2003) describe the process of modal identification as time-consuming and fraught with unavoidable errors pertaining to the curve fitting method. Therefore this method was not considered in depth.

2.2.4 Residue Force Indicator

The fourth method of damage detection utilises residue forces to determine the location and extent of the damage. Ricles and Kosmatka (1992) used this method to determine the position and extent of damage in structures. This method involves the use of modal test data and an analytical structure model to locate damaged regions using residual modal force vectors (Ricles & Kosmatka 1992). Then with the use of a weighted sensitivity analysis the damage extent was found using the changes in mass or stiffness of the structure (Ricles & Kosmatka 1992).

2.2.5 Frequency Response Function

The fifth damage detection method considered uses the frequency response function, FRF, curvature of a structure. Sampaio et al. (1999) and Maia et al. (2003) tested this technique's viability in comparison to other damage detection avenues, primarily mode shape methods.

It was found that the FRF based technique was similar to the mode shape methods previously mentioned. However, as this technique uses a large range of different frequencies, which could also include natural frequencies, it was shown that it is far more accurate (Maia et al. 2003) (Sampaio, Maia & Silva 1999). The frequency response functions, of both the undamaged and damaged structures, are calculated with the use of several sets of nodal deflection data and oscillating force data. This is achieved by dividing the displacement data by the force data, which is essentially creating a flexibility matrix (He & Fu 2001). The FRF data is then used in a similar damage index algorithm as in the mode shape circumstance. This involves the correlation of the FRF data of the damaged and undamaged sections in order to detect the large local differences in flexibility between the two structures. It is then possible to determine where multiple damages have occurred by observing where large changes in flexibility have occurred.

This technique increases in accuracy as the nodal spacing decreases (Sampaio, Maia & Silva 1999). Sampaio et al. (1999) tested the influence of changes in frequency range, input force location and what impact noise had on the accuracy of this method. It was found that by using smaller frequency ranges the accuracy of the damage detection is increased. This is because as the frequency range increases the number of modal frequencies included in the calculations is increased. However an accuracy decrease is associated with the increase in the number of resonances and anti-resonances. This is

because the curvature of the FRF becomes "less significant when compared with the amplitude difference arising from the resonances' frequency shift, because of the loss of stiffness" (Sampaio, Maia & Silva 1999, pg 1033). Therefore it was proposed that a frequency range before the first resonance or anti-resonance frequency should be used. The influence of the input force location was found to be irrelevant. Therefore the excitation oscillation force could be placed anywhere on the structure without effecting the damage detection process. The influence of noise on the accuracy of the damage detection method was also considered. In order to test this factor Sampaio et al. (1999) introduced noise into their test data. It was found that this damage detection method demonstrated resilience to the introduction of noise, by continuing to correctly locate and indicate the extent of damage in the structure.

Other techniques that are described as parameter estimation are similar to this technique. Different parameters are used in these damage detection methods, for example Yao et al. (1992) successfully used strain frequency response functions in order to detect damage.

2.2.6 Neural Network

The neural network damage detection method was also considered. Ortiz et al. (1997) used this technique in order to find damage present in a cantilever beam. This technique involved splitting the structure into several sections that consisted of several Timoshenko beam elements (Ortiz, Ferregut & Osegueda 1997). The neural network algorithms and resonant frequency information sets were then used in conjunction with this model to produce damage locations.

2.2.7 Vibration Damage Detection Selection

In order to solve for the location and damage extent of a pin-pinned beam subjected to an oscillating force each of these methods were considered. Although each method is a viable means of damage detection in structures, the frequency response function method was chosen. The literature suggests that this method is robust, reliable and has the ability to detect multiple damages in a particular structure without issue. Therefore the frequency response method of damage detection was utilised in the research.

2.3 Methods of Integration

The acceleration data provided by the experimentation requires 2 sets of integration to change it into deflection data. There are many avenues available for the integration of

the acceleration data. These include the Trapezoidal rule, Simpson's rule and the Midpoint rule.

2.3.1 Trapezoidal Rule

The Trapezoidal rule (Fink & Mathews 2004), (Faires & Burden 2003) is one avenue available for the integration of data. This method approximates the area underneath a curve, or several data points, by transforming this area into a number of trapezoids. This then allows for the integral to be found. Mathews and Fink (2004) later provided a revised version of this method that uses error analysis. This version produces far more accurate integrated data as it incorporates the error into the integration technique. It was found that this method was a possible means of data integration.

2.3.2 Midpoint Rule

The Midpoint rule (Fink & Mathews 2004), (Faires & Burden 2003) is an additional technique used to integrate data. This method uses two points and an equation for the midpoint between these points to find the integral of the data. This method can be improved by factoring in the error associated with this method (Fink & Mathews 2004).

2.3.3 Simpson's Rule

Simpson's rule (Fink & Mathews 2004), (Faires & Burden 2003) is another method used to integrate data. This method uses the quadratic polynomial and Lagrange polynomial interpolation in order to find the integral. As Faires and Burden (2003) states "Simpson's rule (is) significantly superior to the Midpoint and Trapezoidal rules in almost all situations".

2.3.4 Integration Method Selection

It was found that Simpson's rule provides the most accurate integration method. Therefore this method will be used to integrate the data as necessary.

2.4 Sensor Variants

The data required for damage detection using vibration techniques is varied. Therefore many different sensors are available for vibration data acquisition. These include laser Doppler vibrometers, accelerometers, Microelectromechanical Systems, hammers and shakers.

2.4.1 Laser Doppler Vibrometers

Laser Doppler vibrometers are used to gain instantaneous velocity data of structures that undergo oscillating loads (Castellini & Revel 2000). The velocity information is collected by the laser Doppler vibrometer through the measurement of the diffusion of a laser beam due to the movement of the surface of the structure. These instantaneous diffusions can then be translated into the relating velocities of the surface. Accurate velocity data obtained from this method can then be used in many different damage detection techniques. As this method is a highly accurate method of data acquisition it is preferred. However, this method is unavailable as the facilities available do not include laser Doppler vibrometer technology. The components required are also expensive and would not be a cost effective means of damage detection.

2.4.2 Accelerometers

Accelerometers are an affordable and easily set up sensor available for vibration data acquisition (PCB 2009). Essentially, an accelerometer is created from a housing, a mass, piezoelectric material and signal leads. The acceleration associated with vibration testing is collected by measuring the electrical output of the piezoelectric material, such as quartz, when the acceleration is applied to the mass. As accelerometers are cheap and available they will initially be used in the data acquisition process.

2.4.3 Microelectromechanical Systems

Microelectromechanical Systems are a relatively new type of sensor that can be used in many different applications (Vittorio 2001). This new technology can be used to create accelerometers, miniature robots, microengines, inertial sensors and microtransmitters, etc (Vittorio 2001). In order to gain the required vibration data a Microelectromechanical Systems accelerometer should be used. This type of accelerometer acts in the same way a normal accelerometer, as previously discussed, by using piezoelectric properties. However, the materials are micro machined into thin films in order to create an extremely small sensor. It is thought that these sensors are small enough to be placed into composite materials for real time damage detection.

2.4.4 Force Creation and Sensors

In order to collect the force data required for vibration damage detection either impact hammers (PCB 2009) or shakers (NVMS 2011) are used. Both of these components generate their force data using piezoelectric materials. These materials are used as they

output an electrostatic charge when the force is applied to the apparatus. This charge is then used to determine the force applied to the apparatus and the structure being tested (PCB 2009). Impact hammers consist of a hammer head of a known weight with a force sensor on its tip. A shaker is generally created from a transducer which allows it to oscillate in and out of its casing causing oscillating forces at various frequencies (NVMS 2011). A force and acceleration sensor is placed onto the shaker to gather the required data. As impact hammers are generally used for impact scenarios and shakers are used to generate oscillation data, a shaker will be used in this circumstance.

2.5 Signal Processing

Signal processing describes a number of methods used "for the generation, transformation, and interpretation of information" (SPS 2011). The vibration analysis method chosen requires assignment of certain signal generation parameters and the implementation of noise reduction techniques. The input frequency, sample frequency, type of signal waveform and noise filtering techniques were investigated.

2.5.1 Waveforms

There are various types of waveforms available pertinent to signal generation. The general waveforms available were periodic, rectangular and triangular waveforms (Storr 2011). Each of these produces a different type of response when used as an input signal for the shaker. Therefore as each waveform produces a different response the ideal signal was chosen in order to produce a reliable response in the composite structure.

Periodic waveforms are cyclical in nature and are used to describe various signals (Storr 2011). Over time these signals increase and decrease in accordance with their period and amplitude. These factors are used to describe the scale and frequency of the signal used (Storr 2011). The use of this set of waveforms also enables ease of integration and differentiation as the result of both of these processes are periodic in nature (James 2007).

Rectangular waveforms are created by several positive and negative pulses. An initial pulse heightens the signal to its maximum amplitude. The signal remains at this amplitude until a second negative impulse is created reducing the signal to its original position (Storr 2011). These waveforms are used extensively in the electronic and in microelectronic circuits for timing purposes (Storr 2011).

Triangular waveforms are a group of oscillating signals that generally produce a symmetrical triangular shape. These triangles oscillate at equal amplitude above and below a centreline (Storr 2011).

The research that has been conducted required an input signal for the oscillating force. Signal processing of this oscillating force and the response to this force was of paramount importance. Therefore as periodic functions are easily integrated and differentiated with a known outcome, periodic functions were used in this analysis (Storr 2011).

2.5.2 Filtering

Signal filtering is a process used to reduce the unwanted constituents, or noise, of a signal to "extract a desired signal" (Orfanidis 2010, pg 382). High and low pass filters are commonly used to reduce this noise. High and low pass filters are used by setting a cut off frequency. High pass filters discard any signal that is below the cut off frequency and low pass filters discard any frequencies that are above the cut off frequency (Orfanidis 2010). Therefore with enough information pertinent to the experimentation occurring, such as several natural frequencies, a particular range of frequencies can be set. It is intended that this process increases the accuracy of the analysis by solely analysing data relating to the particular experimental range.

2.5.3 Input Frequency

In order to produce an accurate and reliable output a particular shaker input frequency was determined. With the use of preliminary finite element analysis, in ANSYS, performed the initial natural frequencies were determined pertinent to the composite structure (ANSYS 2011). It was decided that reliable data would be produced if the excitation frequency was lower than the second natural frequency of the composite structure. As the second natural frequency of the system was found to be 145 Hz, using ANSYS (refer to section 7.2.1), it was decided that the input frequency should be 60 Hz. Therefore the frequency of the input was 60 Hz and was periodic in nature.

2.5.4 Sample Frequency

The correct sampling rate is of paramount importance in numerical analysis. It was found that "the sampling rate must be at least twice the bandwidth of the signal, or else there will be distortion" (Nise 2008). Therefore a sampling frequency will be used in excess of twice the input frequency.

While higher sampling rates produce more accurate results the amount of data produced is extremely large. Therefore a sampling rate must be chosen that will accommodate for the required accuracy while reducing size of data and processing time.

As the input frequency was 60 Hz a sampling frequency in excess of twice this must be used in the numerical analysis. Therefore a sampling rate of 5120 Hz was chosen. As this frequency is more than 85 times larger than the input frequency and will produce data small enough to process efficiently it was used.

2.6 Composite Material

Composite materials are advanced materials that are used in various engineering applications as they exhibit a mixture of desirable properties. They are light weight, incredibly strong, durable, resistant to corrosion and electrically inert (USQ 2008). As these materials will play a significant role in the future of engineering endeavours, quality control and damage detection methods must be created to suit them. Generally fibre composite materials are described by their fibre and resin.

The general fibres used in engineering applications are glass, carbon and aramid. These long thin fibres are imbedded into a resin matrix to create a material that has high strength and stiffness (USQ 2008). The fibres act as reinforcement and carry the primary loads acting on the material. The resin matrix is used to fix the fibres in situ ensuring the fibres carry the primary loads.

2.6.1 Glass Fibre

Glass reinforcement fibres are “the most common synthetic reinforcing fibre available in today’s composite industry” (USQ 2008, pg 3.10). This material has many advantages and disadvantages. These will be outlined in the following lists adapted from ENG8803 Mechanics and Technology of Fibre Composites (USQ 2008):

The advantages of glass fibre reinforcement include:

- Low cost in comparison to other fibres
- Widely available in a plethora of different shapes and components
- Experienced glass fibre manufacturers exist, as this material has been used for many years
- High tensile strength
- Resistant to heat and can therefore be used in structural applications in high temperature environments
- Dimensional stability when exposed to heat

- High chemical resistance
- Highly resistant to moisture
- Fire resistant
- Electrically inert
- Compatible with various polymer resins

The disadvantages of glass fibre include:

- Low modulus of elasticity
- Low load carrying capacity in relation to its density in comparison to other fibres
- Low fatigue performance in comparison to other fibres
- Health risks associated with its handling

Factors that affect the strength of glass fibres:

- Incompatibility with organic resins, does not create good bonds between resin and fibre (this can be remedied with a coupling agent however)
- Has a lower load carrying capacity in relation to its density than other fibres
- Long term strength is an issue due to fatiguing problems of glass fibre

2.6.2 Carbon Fibre

Carbon reinforcement fibres are "the "high-performance" reinforcement for modern composites" (USQ 2008, pg 3.18). This material has many advantages and disadvantages. These will be outlined in the following lists adapted from ENG8803 Mechanics and Technology of Fibre Composites (USQ 2008):

The advantages of carbon fibre include:

- High fibre stiffness
- High strength capacity
- Low density meaning high strength to weight ratio
- Good long-term load performance.

The disadvantages of carbon fibre include:

- Expensive in comparison to other fibres
- Has resin compatibility issues – epoxy resins are usually used, which increases the cost of the finished product
- Carbon fibre is not as readily available as other fibres

2.6.3 Aramid fibre

Aramid reinforcement fibres are used "where other reinforcement cannot supply the required impact performance" (USQ 2008, pg 3.29). This material has many

advantages and disadvantages. These will be outlined in the following lists adapted from ENG8803 Mechanics and Technology of Fibre Composites (USQ 2008):

The advantages of aramid fibre include:

- High toughness and impact performance (around 2-4 times that of carbon fibre)
- High tensile strength
- Flame resistant
- Chemical resistance (except high concentration chemicals)

The disadvantages of aramid fibre include:

- Low strength in compression circumstances (tend to micro-buckle in compression)
- Fails when transverse tension is applied due to the weak hydrogen bonds between fibres
- Ultraviolet radiation damages these fibres
- Absorbs moisture

2.6.4 Fibre Chosen for Analysis

The damage detection analysis requires a cheap and readily available fibre composite material. As glass fibre is an easily accessible and cheap material it will be used in this analysis. The glass fibre material chosen was a pultruded square hollow section manufactured by Wagners CFT Manufacturing Pty Ltd (Wagners 2009). This material is formed from 76% glass fibre, 20% vinylester resin and 4% "other non-hazardous ingredients" (Wagners 2009, pg 2). A report outlining various aspects of this composite pultrusion can be viewed in appendix B.2. The material specifications can be viewed in appendix B.1.

2.6.5 Factors that Affect the Strength of Fibre Composites

There are many properties that affect the strength of composite materials. These are generally related to the way in which they are manufactured and the loading circumstances imparted upon the material (USQ 2008). Manufacturing faults, damages and incorrect loading may result in catastrophic failure of the composite material.

Matching the correct fibre and resin is an important manufacturing decision that may affect the performance of a composite material. Factors such as the strength of the bond between fibre and resin, direction and angle of the fibre weave and fibre resin compatibility effect the materials performance greatly (USQ 2008). The bonding of an

incompatible fibre and resin may result in the introduction of moisture, delamination and destruction of the fibre due to a corrosive resin (USQ 2008) (Christensen 2009).

Delamination is a particularly problematic situation as it may occur internally, reducing the strength of the material without warning. Essentially delamination is a process that uncouples the fibre from the matrix reducing the strength of the material drastically (Christensen 2009). This failure mode may be caused by a reduction in the bond between resin and fibre, through out of plane loading and by general damages (USQ 2008) (Christensen 2009). The damage detection analysis chosen may be affected by the delamination of the material, due to sustained damages. This may cause errors in the damage detection readings and will be further investigated.

Chapter 3 **Vibration Analysis Methodology**

In order to complete a research task a number of processes must be completed. In this circumstance these tasks include reviewing literature to determine an ideal method, performance of this method and confirmation of the results using other methods. Therefore this chapter will outline the techniques that have been performed in order to complete the research task.

3.1 Vibration Damage Detection Technique Selection

In order to determine the ideal method of damage detection using vibration, numerous sources were reviewed. The information detailed within these sources was then combined to form a literature review. The assisted in choosing what type of vibration damage detection technique would be effective in this particular situation. Frequency response function, FRF, data pertinent to a composite beam structure would be used. It was intended that this data be compiled for a damaged and an undamaged section. This FRF data was then converted into a damage index by placing it into a finite difference algorithm. This algorithm outputted data that enabled the identification of the extent and position of the damage with the use of damage index (Maia et al. 2003).

3.2 Apparatus selection

Experimental data was required in order to complete the damage detection analysis. The technique chosen requires deflection and force data at certain points on a structure in order to detect the damage. Therefore sensors, data acquisition and excitation apparatus were required. The appropriate components were chosen after an extensive review of literature. The chosen components were an accelerometer, shaker, signal generator, signal amplifier and data acquisition component which were used in conjunction with a computer.

3.3 Damage Index

Position of damage can be easily determined through the use of a node system. The extent of damage is more difficult to determine. To give an indication of how damaged a structure is, the researcher has used an algorithm that outputs a damage index (Maia et al. 2003). Damage index cross-references between the undamaged initial structure and the present damaged structure. In order to quantify the damage index the researcher has damaged the structure several times and to varying degrees. The damage index output of these was then used to determine the range in which the structure would be damaged when damage extent is unknown. Therefore, this system can then, theoretically, be used to determine the extent and position of damages in a particular structure.

3.4 Type of Damage

Several types of damages will be tested using the vibration damage detection technique chosen. The fibre composite material was artificially damaged at and between nodes. This was completed to establish the effect position of damage, in relation to the sensor, would have on the damage detection method. Damages will also be implemented prior to the damage detection method to determine the effect they will have on the damage detection method.

3.4.1 Artificial damage

To test the damage detection technique artificial damages were introduced into the test structure. To achieve this it was decided that the most accurate avenue was to introduce 1mm wide cracks into the member. These cracks were created with a hacksaw.

The method chosen to introduce damage into the section was determined to be the removal of material. This was quantified by area or moment of inertia. As the area of the section is reduced at that particular point of damage it is believed that a relative amount of damage was introduced into the section. Therefore the percentage of area removed through the introduction of the crack is proportional to the percentage damage imparted upon the section. The damage levels and corresponding cut depths used can be viewed in the following table, Table 3.4.1.1.

Table 3.4.1.1 Damage Levels

Damage Levels	
Percentage Damaged (%)	Depth of 1 mm Cut (mm)
5	1
10	2
20	4
30	12
40	31
50	50
60	69
80	96

3.4.2 Position of Damage

The effect of the position of the damages relative to the sensor was also tested. This test was conducted to aid in establishing the accuracy of the analysis. This process consisted of damaging the fibre composite material at and between sensor data collection nodes. The method outlined in section 4.3 was completed for each of these circumstances.

3.4.3 Previously Damaged Section

The fibre composite section was also damaged before analysis. This was to determine what effect this would have on the system. It was thought that these damages may have a significant effect on the characteristics of the material and therefore have a profound effect on the damage detection method. If this were to occur the damages that were intended to be found may be hidden in this previous damage and therefore will not be found or at least masked.

3.5 Post Processing Program

The post processing program was created to perform the required mathematical operations to determine the damages in the structure. A brief outline of this program is provided in this section. Full explanation of the program can be viewed in Chapter 6.

3.5.1 Post Processing

As deflection and force data is required by the analysis process, a Matlab script was created. This script was created to understand how the data was processed and have ultimate control over it.

3.5 Post Processing Program Vibration Analysis Methodology

One purpose of this script is to integrate the acceleration data provided by the accelerometer twice. This provided the required deflection data and the force data was directly provided by the shaker. The script then performed fast Fourier transformation on both the deflection and force data in order to convert it from being time dependant to being frequency dependant. This process provided the natural frequencies of the system. The natural frequencies were then checked through correlation of the acquired data and a finite element analysis, using ANSYS (ANSYS 2011).

3.5.2 Damage Detection

FRF data was then created using the FFT data and checked with the LMS express post processing program. This process was performed at particular points along the structure. It was decided that this nodal mesh would have a spacing of 20 mm (refer to section 6.1.1). With the FRF data at each point along the structure obtained, the data was then placed into the finite difference algorithm in order to determine the position of the damage. This process was then repeated after the section had been intentionally damaged. Essentially, this process correlates the differences in flexibility matrix between the damaged and undamaged structure at each nodal point. This difference was then used as a damage index in order to determine the position of the damage and to an extent the degree of damage sustained. In order to gauge the extent of damage an arbitrary damage scale was created. This entailed completing the damage detection processes several times with differing degrees of damage imparted upon the structure. Therefore, with this arbitrary scale the position and extent of damage was determined.

Chapter 4 **Apparatus**

Certain apparatus were required to obtain the necessary vibration data used to test the damage detection technique. The purpose of this chapter is to explain the necessity of each of these components and briefly explain their functions.

4.1 Apparatus Chosen

Various components were required and chosen for the purpose of gathering acceleration and force data pertinent to the vibration characteristics of the composite member. These components consist of an accelerometer, shaker, signal generator, signal amplifier, data acquisition component, shaker attachment apparatus, stands, computer, LMS express post processing program, Matlab and the structure that is to be tested.

4.1.1 Composite Structural Member

The composite structural member chosen for this analysis process was a 100 mm by 100 mm by 5 mm thick glass fibre and resin square section. This member has been previously damaged and will therefore test the robustness of the post processing program. Wagners produced the composite structural member that will be tested (Wagners 2011).

The analysis of this structure was achieved through using 82 data acquisition nodes along its surface. 81 of these nodes were used as the damage detection data acquisition positions. These nodes were spaced 20 mm apart along the 1.6 m section. The additional node point was used to collect data pertinent to the vibration directly on top of the oscillating force point. Additional information pertinent to the choice of nodal spacing and number of nodes can be viewed in section 6.1.1. The member may be

viewed in appendix C.1. The specifications of this material can be viewed in appendix B.2.

4.1.2 Stands

The performance of this analysis required the composite structure to have 1.6 m of its length suspended in the air. This was achieved with the use of multi-height stands. The height of these stands can be adjusted by rotating their top section. Therefore the composite structure was placed onto these stands. This was achieved by placing the stands 1.6 m apart and placing the composite structure onto the circular sections of the stands.

4.1.3 Shaker Attachment Apparatus

In order to perform the vibration analysis the composite structure must be attached to the shaker. This device was required to translate vibration well, exhibit robustness, and had to have the ability to be attached to the section at varying points. To achieve this, a shaker attachment apparatus was created by the researcher.

Attaching the shaker to the composite structure was required. Therefore the researcher created an attachment apparatus with the use of 4 mm carbon steel plate, 3 steel G-clamps and a small piece of carbon steel angle section. An angle grinder was used to cut the plate into a square that was 250 mm by 250 mm a smaller square, 150 mm by 150 mm, was then cut out of the centre of this square. The G-clamps were then prepared by removing the threaded section and handle of each, discarding the remaining pieces of the G-clamp. Each G-clamp section was then welded using a MIG welder to the square piece of plate at the centre of the top, right and left sides of the front face, each threaded section being perpendicular to their corresponding side. The small piece of angle iron had a 5 mm hole drilled into the centre of one of its flanges, which was countersunk. This component was then welded onto the untouched side of the square component.

The shaker attachment apparatus can be seen in appendix C.2. It was designed so the square composite section would slide through the centre of the square piece of plate. When the apparatus arrives at the required position the apparatus is fixed to the structure. This is achieved by tightening the g-clamp mechanisms, locking the section between the two side clamps and between the base of the plate and the top clamp. The angle iron component is then used to attach the shaker by means of a threaded rod and

two M4 nuts. The two nuts work against each other to lock the shaker onto the angle iron and therefore the composite structure.

4.1.4 Shaker

Industrial shakers are expensive devices used to impart varying degrees of forced vibration onto a structure or material (NVMS 2011). This equipment is capable of recording the oscillating force and acceleration at the point of excitation. As forced vibration must be imparted upon the composite structure in order to gather the pertinent data for damage detection a shaker will be used. As was stated in sections 2.5.1 and 2.5.3 the input signal into the shaker will be periodic and will oscillate at 60 Hz. The shaker that was made available was the PCB shaker which may be viewed in appendix C.3. The specifications and cross-section view of this device can be viewed in appendices C.4 and C.5 respectively.

4.1.5 PCB Accelerometer

The accelerometer was an integral part of the vibration apparatus design. Through the use of piezoelectric materials the accelerometer allows acceleration data to be obtained (PCB 2009). This application required the use of a single axis accelerometer capable of recording acceleration data in the positive and negative y axis. This data was then used to perform the damage detection process

Portability, accuracy and availability were the factors affecting the choice of the single axis accelerometer. The available accelerometers included a large, robust, cylindrical thread and nut mounted accelerometer capable of recording g-force readings. A slightly smaller cylindrical accelerometer was also available it was a small cubic accelerometer, 10 mm by 10 mm, and was capable of measuring acceleration within a range of 0 ± 5000 g. The smaller cubic PCB accelerometer was chosen as the optimum accelerometer in this circumstance. This decision was made as this accelerometer was readily available, was accurate enough to record the small vibration responses in the structure and had the ability to be mounted with the use of wax. The specifications of this accelerometer can be found in appendix C.6.

4.1.6 Microelectromechanical Systems

Due to time strict time constraints Microelectromechanical Systems were not tested. They are however, a sensor that may be used in real time damage detection as they can be imbedded into various materials (Vittorio 2001).

4.1.7 Signal Generator

Signal generation at a particular chosen frequency is an important aspect of the data formation process. This particular analysis system required the generation of an oscillating signal, which was transformed into an oscillating force with the use of the shaker and signal amplifier. The composite structure was then subjected to this oscillating force and the response was recorded by the accelerometer. Therefore in order for a reliable analysis to be performed it was paramount that each data set acquired from all of the nodal points located on the composite structure was obtained through the same signal frequency and type.

Devices that are capable of creating the required signal frequency and type are called signal generators. The signal generator available for this research was the Function Generator HM8030-4. This device can be used to generate a large range of frequencies from 0.25 Hz to 3500 kHz. Various signal waveforms can also be chosen which include periodic, triangular and rectangular waveforms. It is important that the correct oscillating frequency and signal be sent to the shaker. The signal generation unit used can be viewed in appendix C.7.

4.1.8 Signal Amplifier

Amplification of the oscillating signal generated was required as the signal generator was limited to producing low amplitude signals. Signal amplifiers are used to boost signals that have previously been produced.

The signal amplification unit available for this analysis was the LDS PA25U Power Amplifier. Gains produced by this device are within 0 to 10 times larger than the original signal. As the signal generated was too small to be used the signal was amplified using the signal amplifier before it was then sent to the shaker. The signal amplifier used can be viewed in appendix C.8.

4.1.9 Data Acquisition Unit

Acquisition of the acceleration and force data produced by the system was one of the most important tasks completed. Processes such as these are performed using data acquisition units, in conjunction with computers and software, that convert the physical form of signals into quantitative data. This data can then be used further to describe how a particular system is acting.

The data acquisition component that was available for this system was the LMS SCM05 Serial: 46080207. To obtain the required sensor signal data this unit was used in conjunction with LMS Express vibration signal processing software available on the laboratory computer (LMS 2010). This unit had the ability to process signals produced by up to 16 sensors at one time while boosting each of these signals with an internal amplification unit. This amplification was a means of reducing the effect of external undesirable noise that may be present in the signal. The data acquisition unit can be viewed appendix C.9.

4.1.10 Computer

Computing power was required for this data intensive analysis. It was decided that two computers were required for this study, a laboratory computer and a personal computer. The laboratory computer was used to collect the force and acceleration data using the LMS Express software (LMS 2010). The powerful personal computer was used for the vast amount of numerical calculations required using Matlab (MathWorks 2011).

4.1.11 LMS Express

LMS Express software is a data acquisition and processing program used in vibration analysis of systems (LMS 2010). Essentially LMS Express is a graphical user interface used to run the data acquisition unit and process the data obtained.

The LMS Express software is used to perform many tasks in the research process. These processes include starting and stopping the analysis, obtainment of data, visual representation of data and the exportation of data into Text ".txt" files. Additional data post processing techniques, used as verification methods for the post processing program, are also available in this software package. These include CEPS, FFT, APS, Gxy, GxyN, FRF, COH, WIN, PSD and ESD analyses.

4.1.12 Matlab

Matlab is a powerful program that is generally used to "perform computationally intensive tasks" (MathWorks 2011). This software enables the user to create programs to perform various tasks ranging from simple calculations to the simulation of complex systems.

The researcher has used this software to produce a program that performs the various steps required to detect position and extent of damage in the composite structure.

Acceleration and force data at particular points on the structure obtained from the apparatus was imported into the program and the damage index of each node is displayed graphically. The calculations and data analysis will be discussed further in Chapter 6.

4.2 Construction of the Apparatus

The apparatus required by this damage detection process must be connected in a particular fashion. The construction of the system is as follows:

1. Place the structure onto the stands which are 1.6 m apart
2. Place the shaker attachment apparatus onto the structure
3. Attach the shaker to the bottom of the shaker attachment apparatus
4. Place the accelerometer at the first nodal position that is required
5. Connect the signal generator to the signal amplifier
6. Connect the signal amplifier to the shaker
7. Connect the shaker and accelerometer to the data acquisition component
8. Connect the data acquisition component to the computer
9. Plug in all necessary components into the mains power
10. Turn on all components and the computer, excluding the signal amplifier
11. Open the LMS express program
12. Calibrate each component accordingly

A complete set up picture of this system can be found in appendix C.10. LMS express then outputs the data into a ".txt" file which can be read by the Matlab script. This script is run and the damage position and extent is shown.

4.3 Operation of Apparatus

Operating this system required a number of steps that were performed periodically. These steps were conducted after each artificial damage was performed. The artificial damages were decided to be 5%, 10%, 20%, 30%, 40%, 50%, 60% and 80%. These damages were performed at data acquisition node 23 and between nodes 54 and 55. Damages of 60% were also introduced at nodes 30, 40 and 48 and between nodes 15 and 16 and also between nodes 60 and 61 to determine the effect previous damages would have on this damage detection method. The sequence of operation steps is as follows:

4.3 Operation of Apparatus Apparatus

1. Assemble the apparatus as outlined in 4.2
2. Place the wax on the accelerometer
3. Place the accelerometer onto node 1, shaker position/ forced oscillation point
4. Turn the signal amplifier on and place the dial to the required gain
5. Press the record button located in the LMS Express graphical user interface
6. Repeat step 3 - 5 for the remaining 81 nodes, taking samplings of LMS Express generated FFT data for later comparison and verification.
7. Turn signal amplifier dial to the off position
8. Export the data as ".txt" files
9. Disconnect all equipment connected to the composite structure and shaker attachment apparatus
10. Artificially damage the section at or between predetermined nodes
11. Perform steps 1-10 until all damage percentages have been investigated
12. Import data into the Matlab post processing program
13. Perform the analysis

Chapter 5 **System Verification**

Verification of the numerical analysis is required to ensure the program is performing correctly. The researcher has performed three different techniques to verify the output of the Matlab program. The LMS Express post processing of the FFT data was used as an initial data verification measure. Hand calculations of the first natural frequencies have been performed. These were then used to cross-reference with the natural frequencies obtained with the numerical processing program. Finite element analysis of the square section composite structure was performed in the finite element analysis program ANSYS (ANSYS 2011). These analyses were performed in order to obtain an estimate of a number of the natural frequencies associated with the structure. These natural frequencies were then use to verify the numerical analysis of the shell.

5.1 Finite Element Analysis

Finite element analysis, FEA, is a method used in various types of analysis to solve complex engineering problems (Martin & Carey 1973). Analyses of complex structural, modal and thermal problems are simplified greatly using this method (ANSYS 2011). This mathematically intensive method is generally performed using computers as achieving a finite element analysis of even a simple system is laborious and time consuming. This method will be used to verify the numerical method outlined in chapter 6.

The finite element method consists of the transformation of a complex model into a mesh consisting of numerous elements and nodes (Martin & Carey 1973). Elements are considered as the components of the mesh that translate the inputs of a system. Nodes are the connecting points between elements where the reactions to the inputs are calculated. Meshing is considered as an accurate estimation of a complex model

(Martin & Carey 1973). This allows a mathematically simple, accurate estimation of the required reactions to the external inputs of the system to be found. External inputs such as theoretical forces, pressures and various node restrictions are applied to simulate the actions of the model when environmental interaction occurs. To determine the response to these environmental interactions the required output, deformation or stress for example, is obtained through calculating the reactions at each node through each element.

Certain factors affect the accuracy of a finite element analysis. Element size and shape of mesh used in the analysis greatly affect this accuracy. Reducing the element size in a finite element analysis increases the precision of the output as the mesh becomes finer and represents the model more accurately (Biomesh 2010). Decreasing the elements size does, however, increase the amount of mathematic processes required and therefore the time required to analyse a system. There are also various different mesh shapes available when conducting an FEA. These typically involve changing how many elements connect to nodes and in what way. Different shapes are used to describe certain shapes and orientations of models more accurately.

Verification of the correct natural frequencies of the composite structure was required. Therefore in order to verify the numerical analysis, finite element analyses will be performed pertinent to each level of damage sustained. These analyses were performed using the finite element software package ANSYS to reduce mathematic operation time (ANSYS 2011).

5.1.1 Creation of the Solid Model

Finite element analysis using computer software requires a solid model of the structure that is to be analysed. Therefore a solid model of the composite structure was created in order to perform the FEA.

ANSYS (ANSYS 2011) was used to model this section by means of drawing the cross-section of the member, two concentric squares the first 100 mm by 100 mm and the second 90 mm by 90 mm with 5 mm rounds, and extruding it to 1.6 m. As a finite element analysis was required for each damage level, undamaged to 80%, 9 models were created. Each of these models were damaged in accordance with their percentage damage. This was achieved through placing 1 mm thick cuts into the material at the particular depths outlined in section 3.4. As the section that is being analysed is

previously damaged the initial damages were also modelled. The model representing the 50% damaged level can be viewed in Figure 5.1.1.1 and Figure 5.1.1.2.

Figure 5.1.1.1 Side View of ANSYS Model

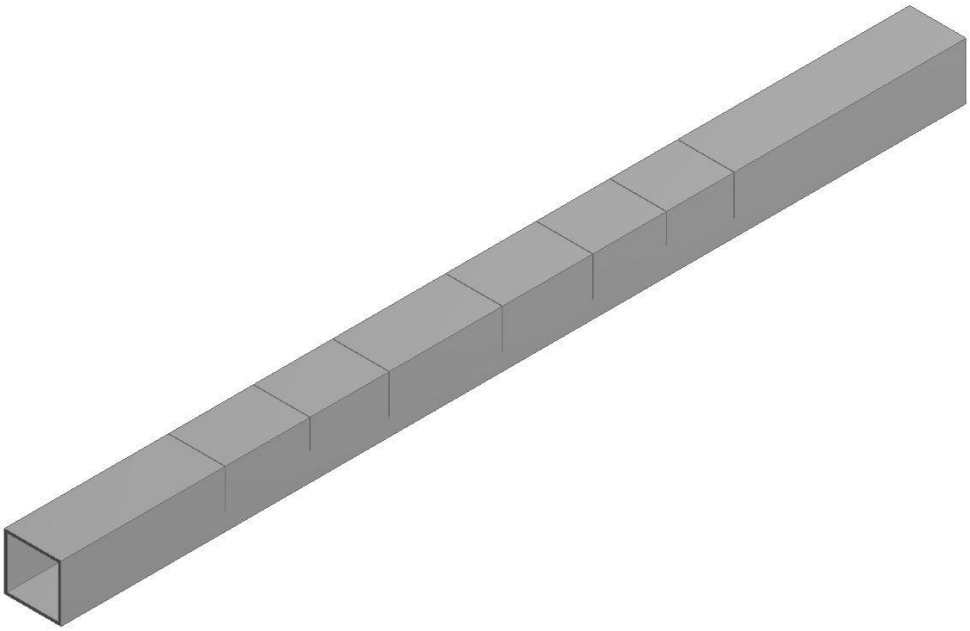

Figure 5.1.1.2 Isometric View of ANSYS Model

5.1.2 Conduction of the Finite Element Analysis

The finite element analysis was performed in ANSYS to verify the information provided by the post processing program (ANSYS 2011). This analysis was completed 9 times in order to check each damage level was producing the correct natural frequencies. The following outlines the steps taken to perform the finite element analysis:

1. Opened ANSYS and clicked and dragged “modal analysis” into the work space
2. Inputted the material properties
3. Created the solid model using ANSYS
4. Generated the mesh
5. Constrained the model at its ends, pinned-pinned
6. Performed the modal finite element analysis
7. Saved the modal analysis data outputted, natural frequencies
8. Repeated steps 1-6 for each of the models

The information provided by these modal finite element analyses was then tabulated. The natural frequencies of each of the damages can be viewed in section 7.2.1. As can be seen the natural frequencies generally lower when damages are introduced into the system. This is also a method of damage detection, however, it does not identify where the damage and to what extent has taken place.

5.2 Hand Calculations

Hand calculations were also performed in order to verify the first natural frequency of the undamaged section. This was performed to verify the finite element analysis verification method. Essentially the performance of this method is a simple calculation that determines the first natural frequency of the member using the following equation:

$$f_n = \frac{\left(\sqrt{\frac{E}{\rho}}\right)\left(\sqrt{\frac{I}{A}}\right)\Omega_{\mathrm{n}}^2}{2\pi L^2}$$

where E is the Young's modulus [Pa]

ρ is the density [kg/m^2]

I is the moment of inertia of the cross section of the beam [m^4]

A is the cross-sectional area of the beam [m^2]

Ω_{n} is the frequency coefficient

n is the number of natural frequency [1]

L is the total length of the beam [m]

f_n is the natural frequency [Hz]

Figure 5.1.2.1 Natural Frequency Equation (Balachandran & Magrab 2009)

5.3 LMS Express FFT

To further verify the numerical method performed in Chapter 6 the post processing program available in LMS Express was also used. LMS Express has the ability to perform fast Fourier transformations on the data that it is acquiring. FFT data was checked as the data obtainment operation was performed to ensure the correct range of frequencies was being collected.

Chapter 6 **Data Analysis**

Post processing and damage detection of the composite structure was conducted using a user created Matlab program. This program was designed to convert the provided data into usable damage detection data. Therefore two main sections of the script were created. These were the post processing section and the damage detection section. The post processing section converted the data provided by the apparatus into the data form required for the damage detection process. Subsequently the damage detection section then placed this data into a finite difference type algorithm. It was intended that the combination of these sections and the data collected be used to accurately estimate the extent and position of damage sustained by a structure.

6.1 Matlab Program Part 1 – Post Processing

Section one of the Matlab data analysis program involved the conversion of data into the required data form. The damage detection process required deflection and force data with respect to frequency (He & Fu 2001). As the apparatus used provides acceleration and force data with respect to time a number of processes had to be completed. These included inputting the required data and initial parameters, performing interpolation and integration and converting the data into frequency domain data with the use of fast Fourier transformation.

6.1.1 Inputs

Various inputs are required for the successful use of the post processing program. The first section of this program was designed to assign and import this information in order to organise it for use. These inputs comprise of the importation of the raw apparatus data to the input of various constants required for operations such as data windowing and filtering.

6.1 Matlab Program Part 1 – Post Processing Data Analysis

Data generated by the apparatus outlined in Chapter 4 was imported for use in subsequent calculations. The raw data output was provided as uniquely named text files. For ease of use the post processing program was designed to run independently after the initial user inputs. Therefore to achieve this, the data text files were renamed to denote the node position. Undamaged node data was renamed "Data_U_x" and the damaged data was renamed "Data_D_x", where x was the data acquisition node number. Furthermore these files were then placed into unique folders to organise the data of each damage extent. With the use of this organisation system the program then imported the data by means of the "importdata" function (MathWorks 2011). This provided a large matrix with acceleration, force and time data present. Therefore each set of node data for each extent of damage was split into respective acceleration, force and time constituents for later use.

The post processing program required various constant inputs to function effectively. These include assigning values for:

- Total number of nodes (82)
- Distance between nodes (0.02m)
- Total number of damaged data sets (8)
- First windowing time value (user defined)
- Final windowing time value (user defined)
- Total sample time (3s)
- Low frequency filter parameter (80Hz)
- High frequency filter parameter(500Hz)
- Substitution filtering factor ($1x10^{18}$)
- Sampling frequency (calculated from input)

The assignment of the total number of nodes used in the data acquisition process was required. This initial user input was necessary as it was used to determine the number of iterations required for a large number of the subsequent processes. Such processes included the importation of the raw apparatus data, assignment of this data, interpolation and integration, performance of fast Fourier transformations and the creation of the damage index. As finer meshes provide increased accuracy the mesh size, or number of nodes along the composite member, chosen was the smallest possible (Biomesh 2010). The accelerometer used to gather the raw apparatus data was 10 mm wide and 10 mm long. As the determination of the accuracy of this damage detection method was required, artificial damages were introduced at and between nodes. Therefore the smallest possible node spacing, using this accelerometer, was

found to be 20 mm. This nodal spacing would ensure the entire section would be analysed while leaving enough space between nodes to test the accuracy of damages present between nodes. Therefore the total number of nodes chosen was 82, inclusive of the initial force node, refer to section 4.1.1. Figure 6.1.1.1 and Figure 6.1.1.2 depict the nodal spacing placed on the composite structure.

Figure 6.1.1.1 Full Node Spacing

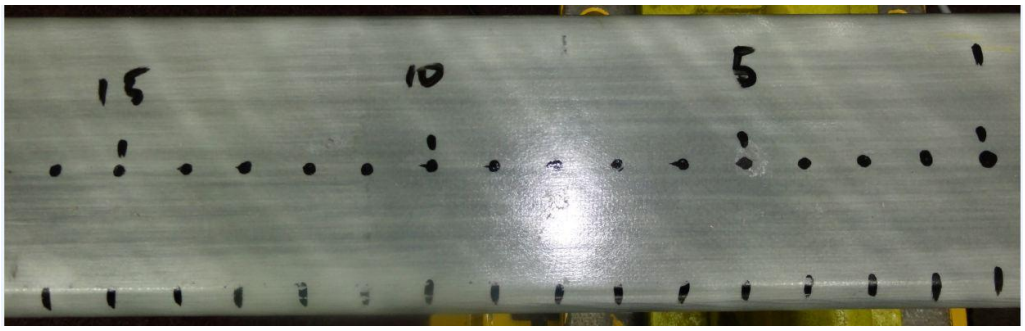

Figure 6.1.1.2 Close-Up of Node Spacing

The total number of damaged data sets was required as it acted as a counter for the damaged data importation and post processing. As the damages investigated were 5%, 10%, 20%, 30%, 40%, 50%, 60% and 80% the number of damaged data sets in this circumstance was 8. This value was used by the program to determine how many damaged data importations and processes to perform and in what order. In this circumstance the initial value, 5%, was provided with the reference number 1 and all subsequent damages were provided reference numbers in ascending order, where the maximum,80%, was 8.

Windowing of data was used in order to reduce the amount of memory required and hasten the computational process. The first windowing value refers to the starting time parameter, beginning of computations, and the final windowing value refers to the end time, finish of computations. The input of total sample time is required as it is used to create the windowing parameters for the data. For example if one required a 3 s long data set to be windowed from 1 s to 1.5 s, the first windowing value would be 1 s and the final windowing value would be 1.5 s. Setting these parameters in this manner would decrease the computation time and amount of memory required by 83%, which is important when using large sampling frequencies.

6.1 Matlab Program Part 1 – Post Processing Data Analysis

Each set of data was provided with a unique set of full length time data. As the raw time data output was only accurate to 2 significant figures several force and acceleration data points "shared" time data. As this was not acceptable new time data was created. This data was created by forming a 1 line matrix whose values were set to range from 0 to the total time at increments of total time divided by the number of data acquisitions in this time frame. The position of each windowing value was then found by multiplying each of the input values by the length of the time matrix divided by the total time. These position values were then used to window the data between the user defined windowing parameters.

Additional filtering was performed in order to provide results with increased accuracy. As this analysis considers the initial few natural frequencies of the system, all other frequency information was considered as noise and was disregarded. This was achieved through defining the low and high frequency filtering parameters. These parameters were determined through extensive modal finite element analysis, hand calculations and LMS Express output. From these verification methods it was determined that the first few natural frequencies would almost exclusively occupy frequencies ranging from 80Hz to 500Hz. Therefore the low frequency filter parameter was set at 80Hz and the high frequency filter parameter was set at 500Hz.

Filtering was achieved using the low and high frequency filtering parameters and the substitution filtering factor. In order to ensure the first few natural frequencies were exclusively used in the subsequent computations, amplitudes of all frequencies outside of the low to high filtering range were set to a small number. This was performed in both the force and deflection data following the fast Fourier process, frequency domain conversion. As the frequency response function was calculated by dividing the deflection by the force, while in the frequency domain, values of 1 would be found outside of the specified range with this method. Furthermore this method ensured these frequencies did not impinge on the damage detection process.

Sampling frequency describes the rate of data acquisition performed. This value is calculated for each new analysis by dividing the amount of data acquisitions by the total acquisition time. It was used in the frequency domain conversion of data to determine the frequency of each acceleration and force amplitude.

6.1.2 Simpsons Rule Loops

Deflection and force data with respect to frequency was required to perform the frequency response function calculations. Therefore as the raw data consisted of acceleration and force data, the acceleration data was converted into deflection data prior to the domain change. This was completed with the use of a function file created to perform interpolation and integration on set of data.

The function file "Simpsons.m" was created to perform the required interpolation and integration steps required in the acceleration to deflection conversion. This function file completes these processes on any data that also has time data present with it. Initially interpolation was required to transform the data into usable data that could be integrated. This process involved utilising the "interp" function provided by Matlab (MathWorks 2011). In order to produce the most accurate data possible all points were interpolated in sets of 9. As the counter of this data increases by 1 the data connects itself automatically.

Simpsons rule was then used as the integration method to gain the required data (Fink & Mathews 2004). This was completed using the interpolated data provided by the interpolation process. This process was performed using 2 trapezoids for each calculation. The calculations continue until the data end of the data inputted into the function. The following equation was used to achieve this (Fink & Mathews 2004):

$$\int_a^b f(x)dx = \frac{b-a}{3n}\left[f(a) + 4f\left(\frac{a+b}{2}\right) + f(b)\right]$$

where x is acceleration or velocity [m.s^{-2} or m.s^{-1}];
a is the initial point [-]
b is the final point [-]
n is the number of trapezoid sections between a and b [-]

Figure 6.1.2.1 Integration: Simpson's Rule

This method approximates the integral of the data inputted with the use of quadratic polynomials, refer to section 2.3.3. The constants b and a describe the starting and ending positions of the process and $f(a)$ and $f(b)$ are the values at these positions. This process is run twice to change the acceleration data into velocity data and then the velocity data into deflection data. The created function file can be viewed in appendix D.2.

6.1.3 Fast Fourier Transformation

Fast Fourier transformation is a technique used to transform time domain data into frequency domain data. This process was required as the determination of natural frequencies and calculation of frequency response function data requires frequency domain data. Therefore the FFT function was used in Matlab to achieve the fast Fourier transformation of the deflection and force data of all damage extents (MathWorks 2011).

Fast Fourier transformation is used to divide a set of data into a set of frequencies that when used together, algorithmically describe the data set (Rao 2005). This operation was used to determine the natural frequencies of the data input, for verification, and to create the frequency response data. This was achieved by setting the resolution of the process which is achieved through calculating the next power of the length of the time matrix. This is then used with the deflection or force data to obtain the fast Fourier transformation, using the "fft" function in Matlab (MathWorks 2011). Frequency data was also created to plot the data for verification.

Filtering was then applied to the fast Fourier transformation data as described in section 6.1.1.

6.2 Matlab Program Part 2 – Damage Detection

The damage detection constituent of the program was formed to determine the extent and the position of damage in the composite structure. The data transformed in the previous post processing program was used to achieve this by calculating the frequency response functions of the data. The frequency response functions were then used in a finite difference type algorithm to achieve a damage index value pertinent to each node at each damage extent.

6.2.1 Creation of Frequency Response Function Data

Frequency response function, FRF, data is easily obtainable and is used in a far more robust damage detection method in comparison to others (refer to 2.2). This method was used in this analysis. FFT data, pertinent to force and deflection, gathered from the post processing section is used to create the FRF data.

The fast Fourier transformation of the deflection data and the force data was used to calculate the FRF data at each node and damage extent of the composite structure. This was achieved by dividing the frequency domain deflection data by the frequency

domain force data (He & Fu 2001). FRF was then used to calculate the damage index at each node of each damage extent. This method was used as it was found to be far more accurate than simply using the changes in natural frequency at each node. The process of dividing the deflection data by the force data ensures that any errors attributed to the data collection processes do not affect the damage detection outcome. For example, if the operator were to set slightly different amplitudes of signal sent to the shaker, causing larger or smaller oscillation forces, this method would disregard this error.

6.2.2 Damage Index Algorithm

Damage index is a dimensionless factor that can be used to describe the amount of damage in a structure (Sampaio, Maia & Silva 1999) (Maia et al. 2003). The FRF data calculated was used in conjunction with this method to obtain the position of damage in the structure. The extent of damage was to be quantified through imparting the differing damage extents onto the structure and obtaining a different damage index for each. It was thought that an arbitrary scale could then be created to obtain an indication of the extent of damage the structure had endured.

The damage index method utilises the differences in a vibration characteristic of a structures nodes to determine the position and extent of damage present. This analysis used the frequency response data collected in the post processing program to form the damage index pertinent to the composite structure. This was achieved through the use of the following equation (Maia et al. 2003):

$$\beta_{i,j}(\omega) = \frac{\left(\alpha''_{i,k}(\omega)_D{}^2 + \sum_{i=1}^{N} \alpha''_{i,k}(\omega)_D{}^2\right) \sum_{i=1}^{N} \alpha''_{i,k}(\omega)^2}{\left(\alpha''_{i,k}(\omega)^2 + \sum_{i=1}^{N} \alpha''_{i,k}(\omega)^2\right) \sum_{i=1}^{N} \alpha''_{i,k}(\omega)_D{}^2}$$

where i is the node number counter

k is the damage extent counter

$\beta_{i,j}(\omega)$ is the damage index at a node and particular damage extent

$\alpha''_{i,j}(\omega)_D$ is the curvature of frequency at a damaged node and particular damage extent

$\alpha''_{i,j}(\omega)$ is the curvature of frequency at an undamaged node and particular damage extent

N is the maximum value of i, total node number

Figure 6.2.2.1 Damage Index Equation (Maia et al. 2003)

Where the values of the curvature of frequencies were obtained with the use of the following equation (Sampaio, Maia & Silva 1999):

$$\alpha''_{i,j}(\omega) = \frac{\alpha_{i+1,j}(\omega) - 2\alpha_{i,j}(\omega) + \alpha_{i-1,j}(\omega)}{h^2}$$

where i is the node number counter

j is the position of the oscillating force

$\alpha''_{i,j}(\omega)$ is the curvature of frequency

$\alpha_{i,j}(\omega)$ is the FRF taken at node i with an oscillating at position j

$\alpha_{i+1,j}(\omega)$ is the FRF taken at node i+1 with an oscillating force at position j

$\alpha_{i-1,j}(\omega)$ is the FRF taken at node i-1 with an oscillating force at position j

h is the node spacing

Figure 6.2.2.2 Curvature of Frequency Equation (Sampaio et al. 1999)

The curvature of frequencies, COF, equation was used to obtain the required input into the damage index equation. Essentially this equation is a finite difference method that is used to calculate an estimate of the curvature of frequency at each node point. It uses FRF values before and after the current node point to achieve this.

With the curvature of frequency information for each extent of damage, including undamaged, the damage index at each node and extent of damage was then found. The numerator of the damage index equation sums the COF squared of each damage extent and adds the current node COF squared to this. The result is then multiplied by the sum of the undamaged COF squared. The denominator is similar to the numerator except the sum the undamaged COF squared is added to the undamaged COF of the current node. This is then multiplied by the sum of the COF squared of the current damaged data being used. This method of damage index formulation identified values that were greatly different than the average (Sampaio, Maia & Silva 1999). Damaged nodes provided a large damage index value in comparison to other nodes.

Finally the Matlab program constructed a plot that grants the ability to visually determine the position and extent of damage. A copy of the full program, post processing and damage detection, can be viewed in appendix D.1.

Chapter 7 **Discussion and Results**

7.1 Post Processing Program Results

To complete the damage detection method various post processing procedures were carried out. As outlined in Chapter 6 the procedures included the acquisition of acceleration and force data which was used to obtain velocity, deflection, FFT, FRF and a damage index. The damage index was then further used to create a relative damage index, which may be used to quantify damages sustained in various circumstances.

Over 3000 data sets have been used to produce the damage index as there is acceleration, velocity, deflection and force for each node at each damage level. Additional FFT, FRF and damage index data sets were also created increasing the total results. Therefore as there are a great number of results available a selection of these results will be presented in the following figures. Information relating to the directly damaged node is presented together with single representatives of undamaged and internodal damaged nodes. Therefore results obtained from nodes 23, 54 and 40 will be presented. The corresponding internodal damaged node, node 55, results were not included as they produce practically identical results to node 54.

7.1.1 Experimentation

Acceleration and force were initially obtained from the apparatus as outlined in section 4.3. The following graphs are small sections, 0.05 s, of the larger 3 seconds of force and acceleration data gathered from the apparatus. The acceleration data was then processed to produce 0.05 seconds of velocity and deflection data to provide a graphical representation.

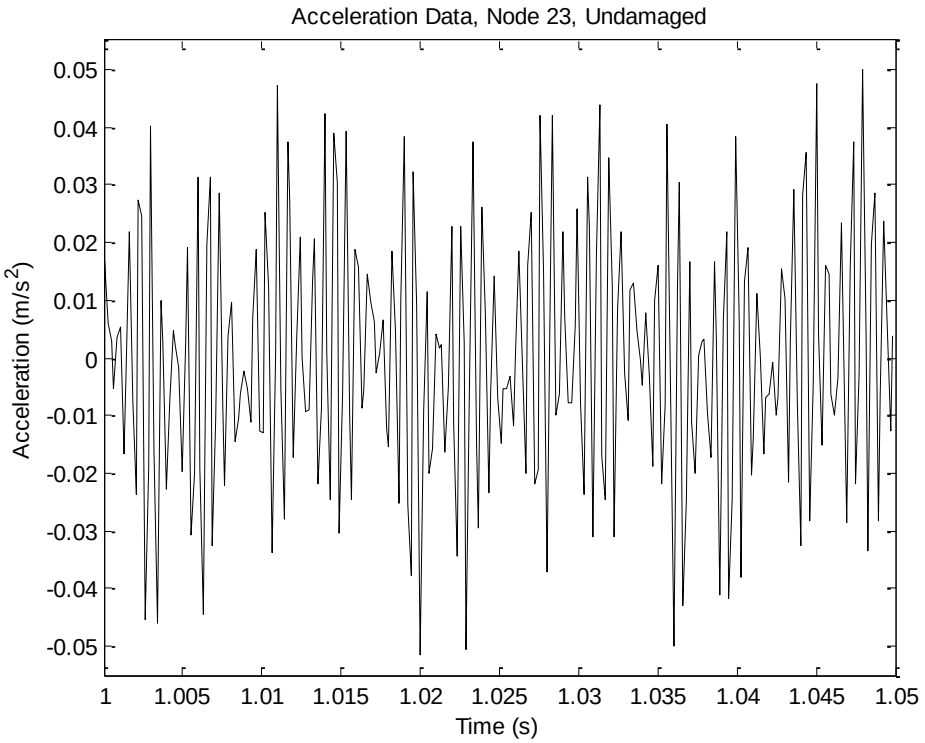

Figure 7.1.1.1 Acceleration Data, Node 23, Undamaged

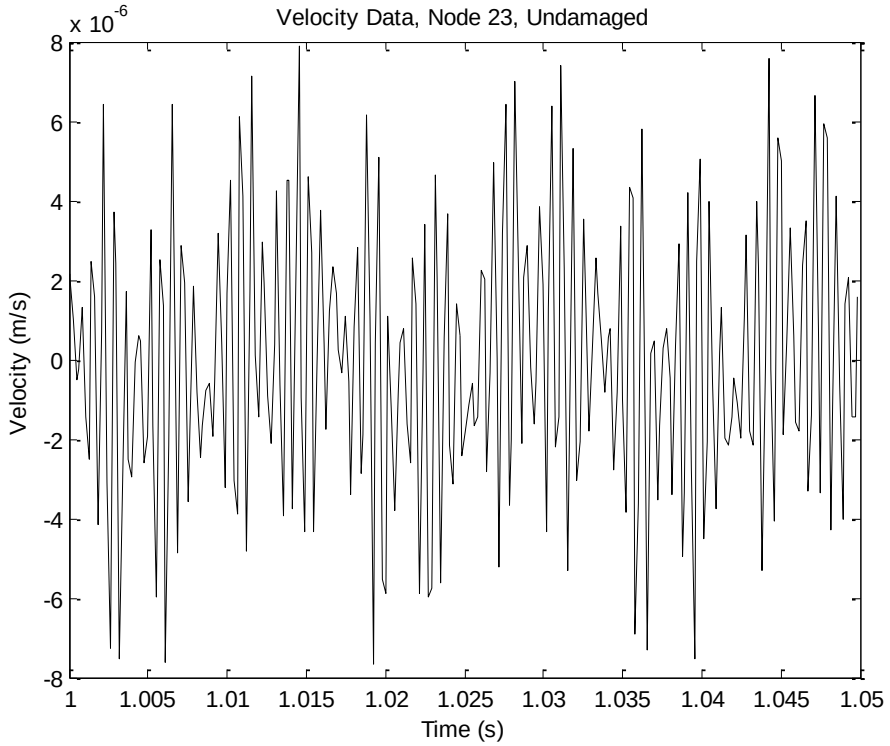

Figure 7.1.1.2 Velocity Data, Node 23, Undamaged

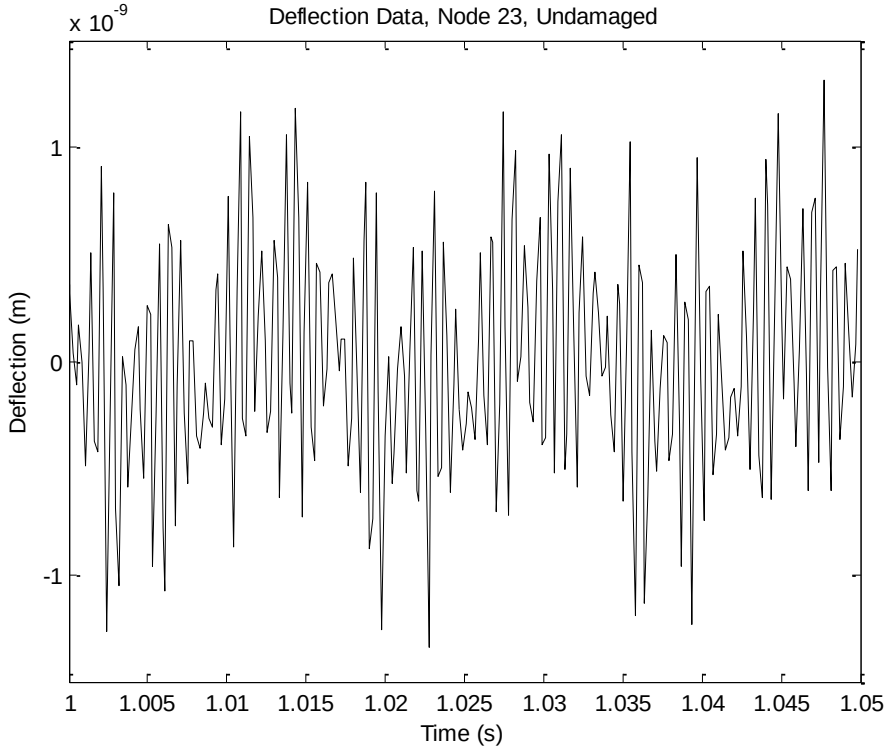

Figure 7.1.1.3 Deflection Data, Node 23, Undamaged

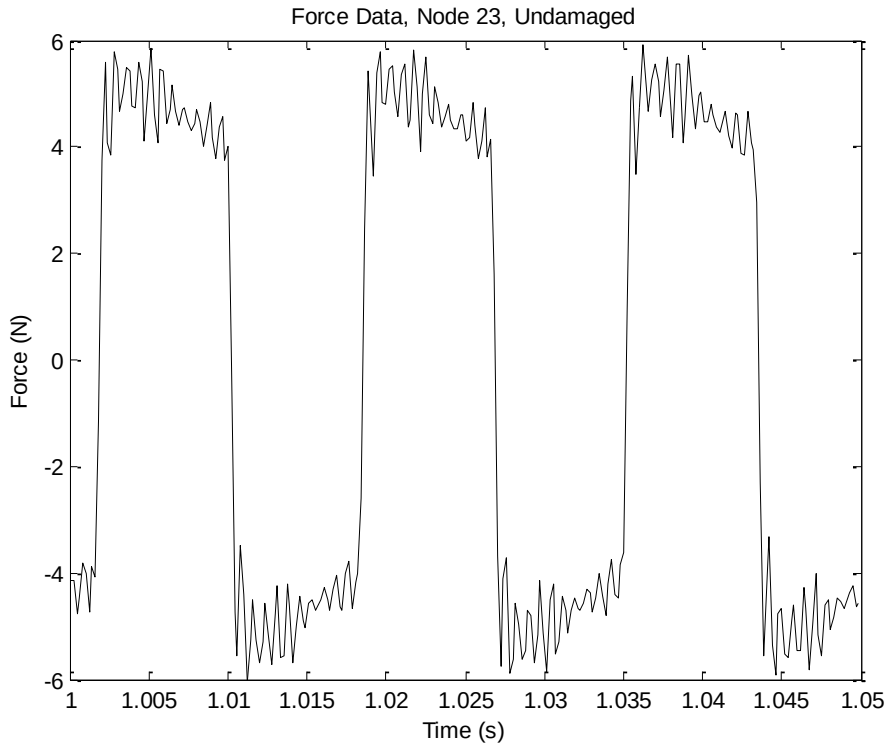

Figure 7.1.1.4 Force Data, Node 23, Undamaged

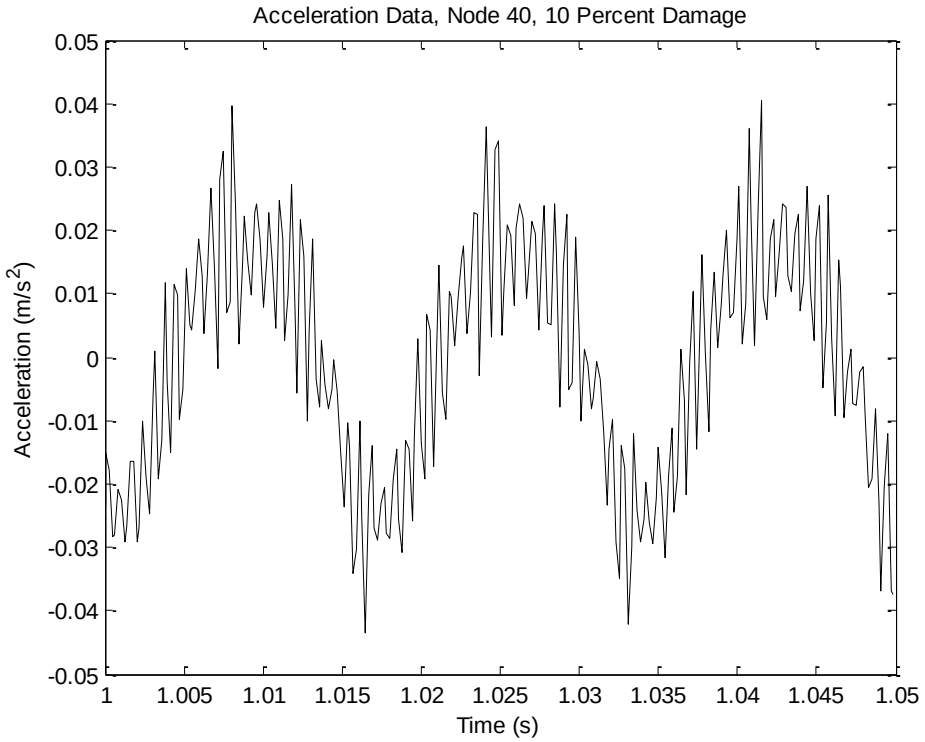

Figure 7.1.1.5 Acceleration Data, Node 40, 10 Percent Damage

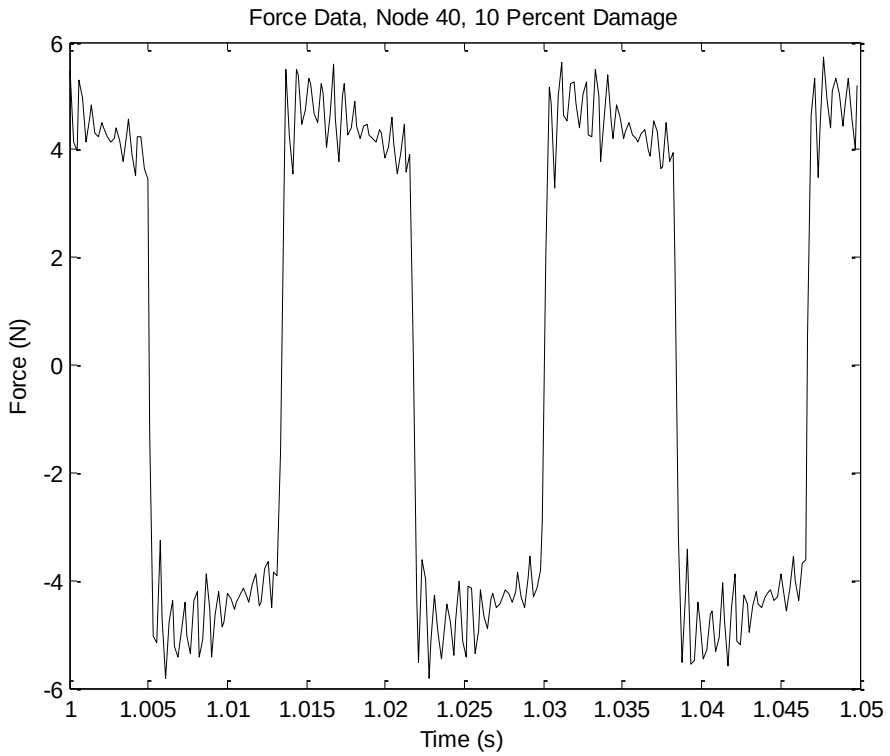

Figure 7.1.1.6 Force Data, Node 40, 10 Percent Damage

7.1.2 FFT

Various FFT analyses were conducted in order to complete the damage index method. The FFT of deflection and force were required to obtain the frequency response function of the system at a particular node point. Therefore these processes were completed for each of the data sets obtained from the 82 nodes and the 9 different damage levels, resulting in over 700 different FFT plots. A small sample of these will be presented in this section to convey the differences in the FFT between damages.

Firstly, as the damages were created at node 23 and between nodes 54 and 55, a selection of FFT plots will be presented. As a control the FFT of the undamaged node 40 will also be presented and discussed.

Fast Fourier transformations were completed for each set of force data in order to perform the frequency response function calculations. As each of the force data sets obtained was only minutely different, the FFT of each was also almost identical. An example of the force FFT may be viewed in figure 7.1.2.1.

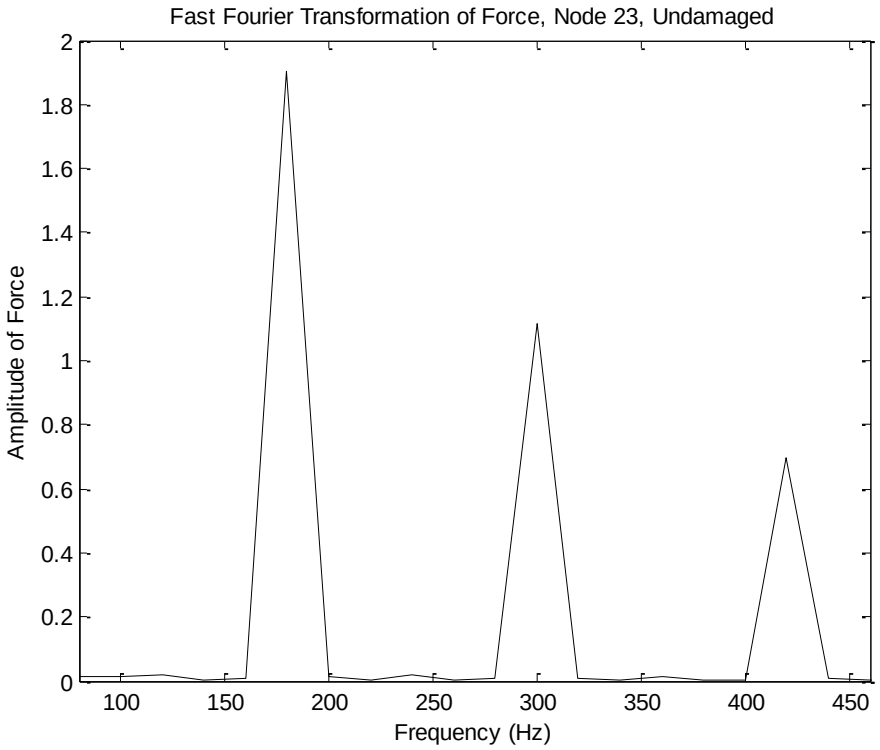

Figure 7.1.2.1 FFT of Force, Node 23, Undamaged

Due to inaccuracies, the differences between the FFT of the internodal damage nodes, 54 and 55, within the range of 5 to 60 percent are only small amplitude discrepancies. Therefore the undamaged, 5 percent damage and 80 percent damage results have been presented for each node as the differences in the intermediate results between 5 and 60

percent were virtually undiscernible. This can be viewed in figures 7.1.2.2, 7.1.2.3, 7.1.2.4 and 7.1.2.5 using node 23 as an example.

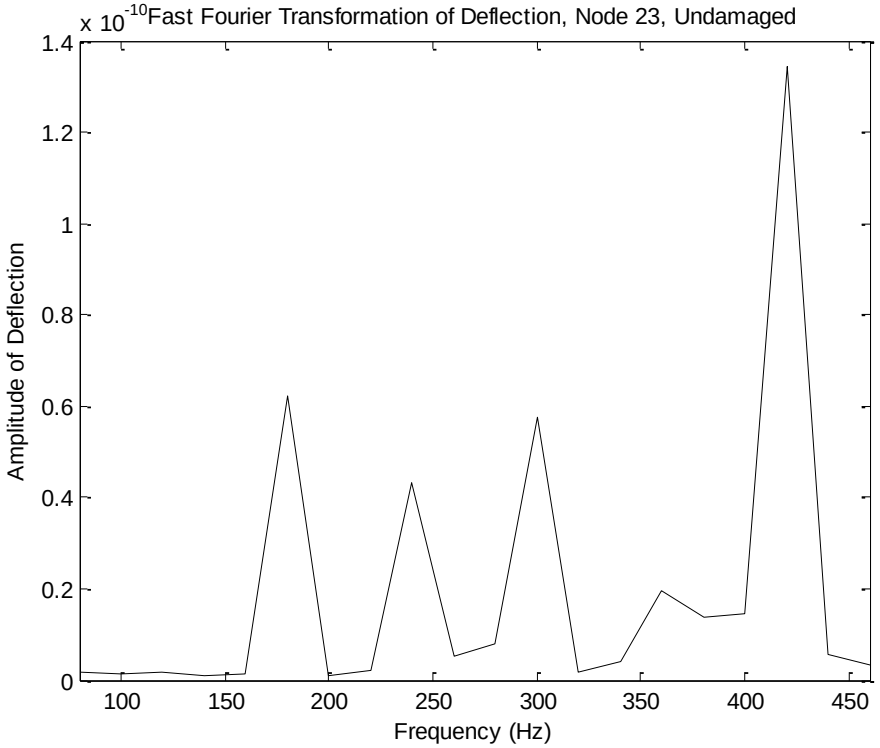

Figure 7.1.2.2 FFT of Deflection, Node 23, Undamaged

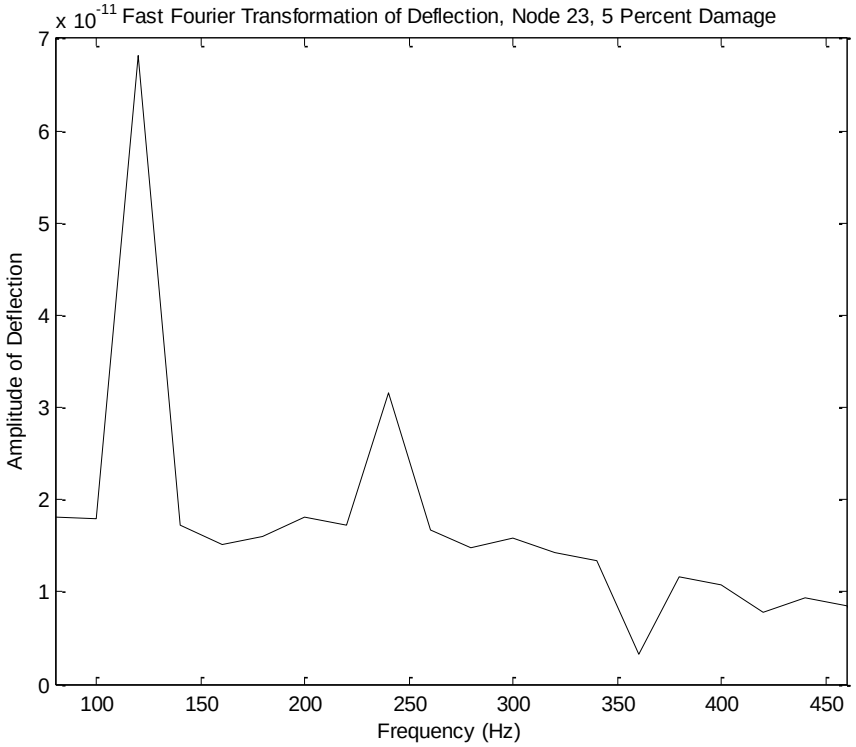

Figure 7.1.2.3 FFT of Deflection, Node 23, 5 Percent Damage

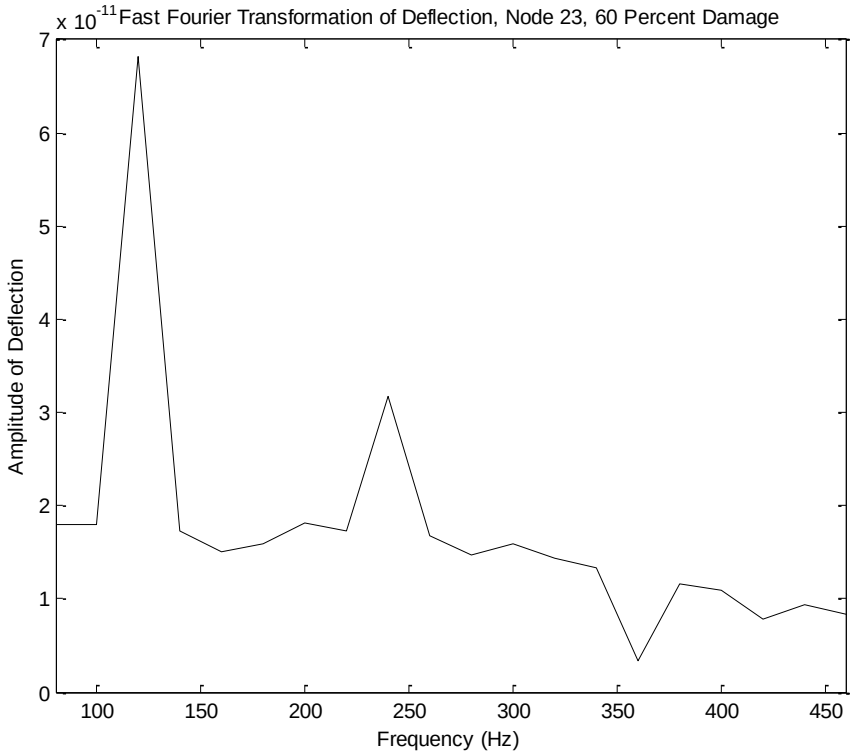

Figure 7.1.2.4 FFT of Deflection, Node 23, 60 Percent Damage

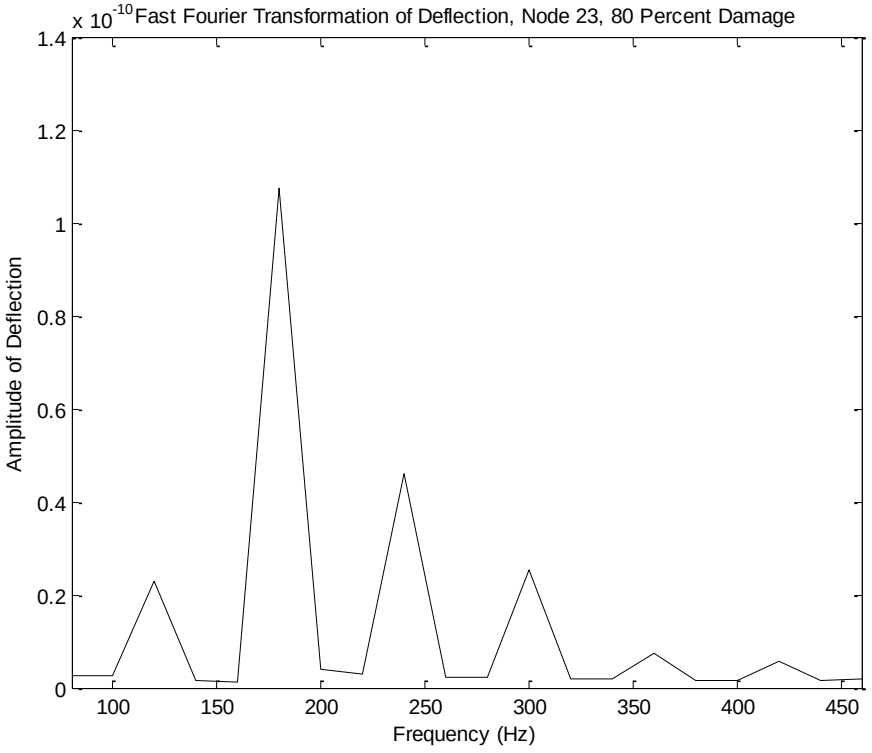

Figure 7.1.2.5 FFT of Deflection, Node 23, 80 Percent Damage

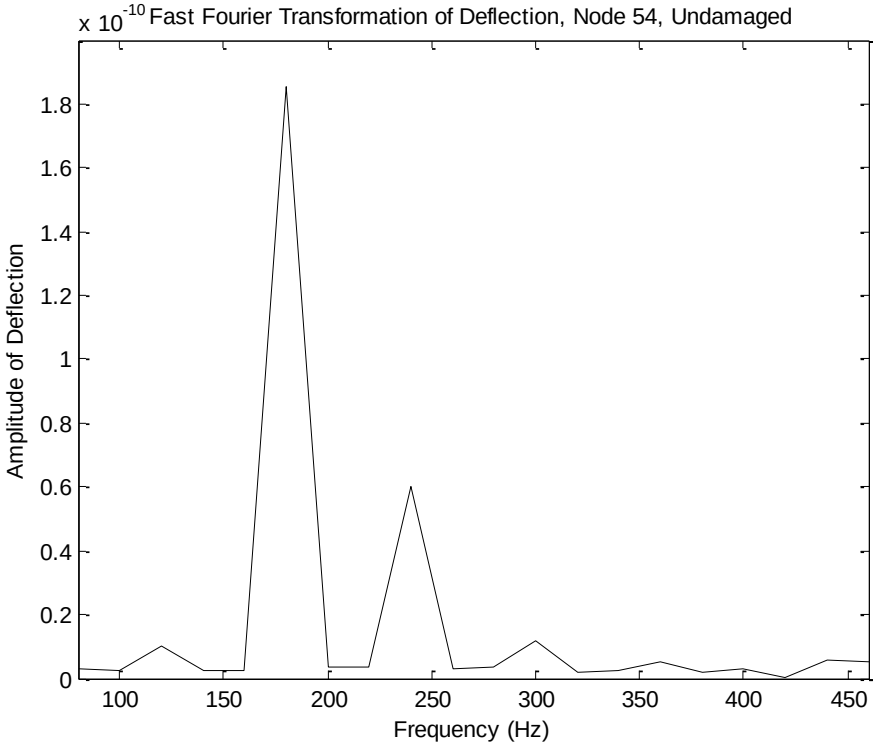

Figure 7.1.2.6 FFT of Deflection, Node 54, Undamaged

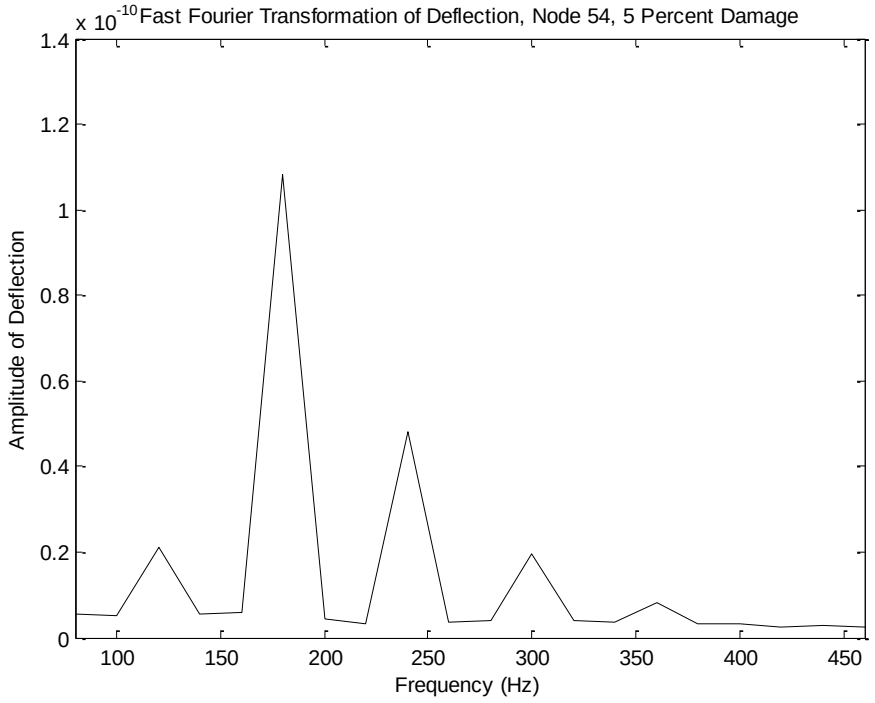

Figure 7.1.2.7 FFT of Deflection, Node 54, 5 Percent Damage

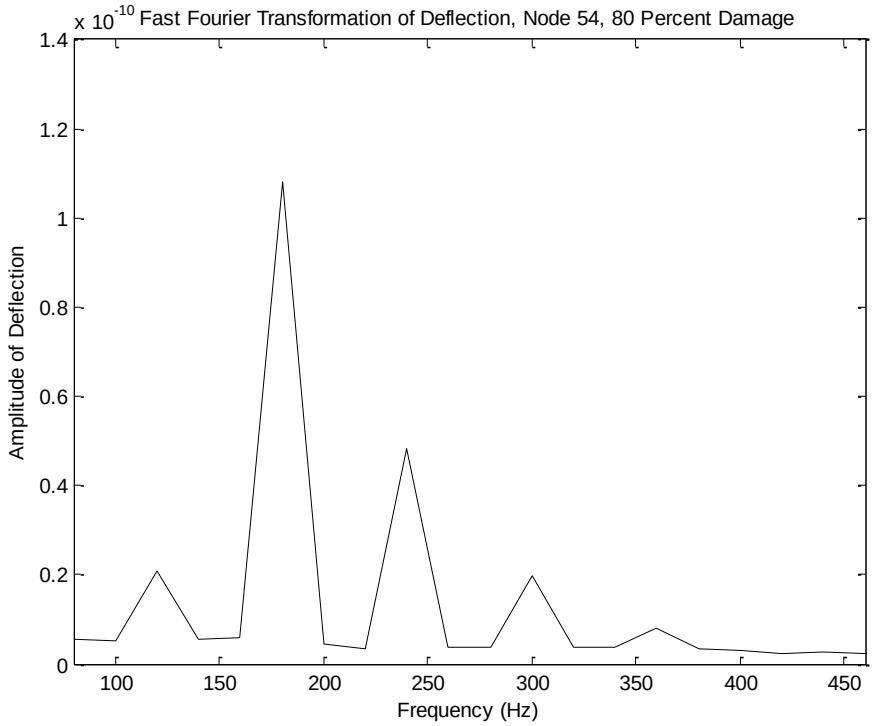

Figure 7.1.2.8 FFT of Deflection, Node 54, 80 Percent Damage

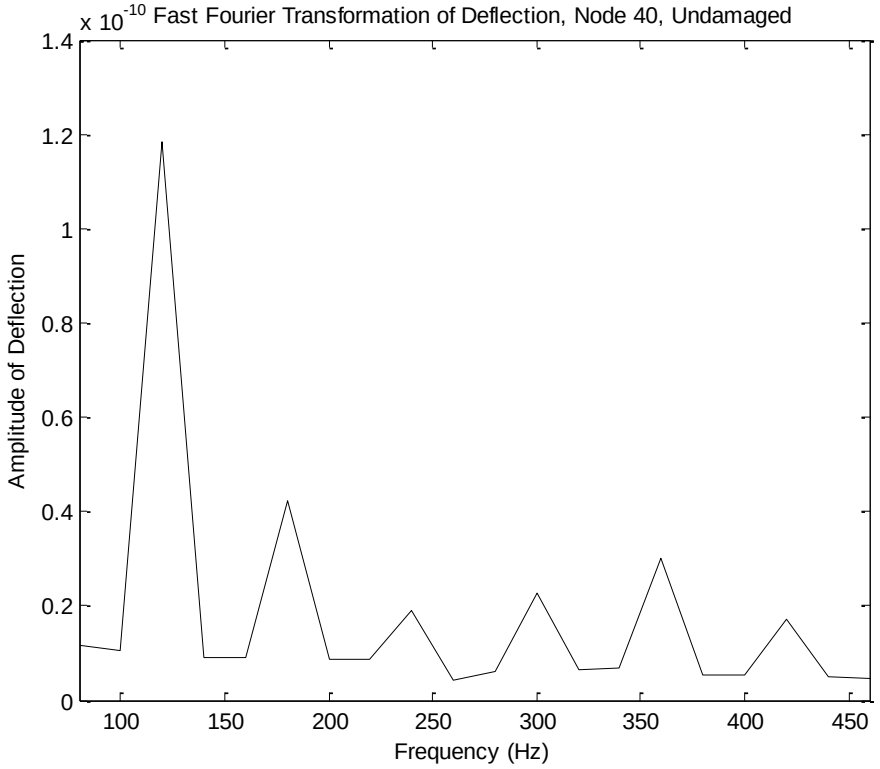

Figure 7.1.2.9 FFT of Deflection, Node 40, Undamaged

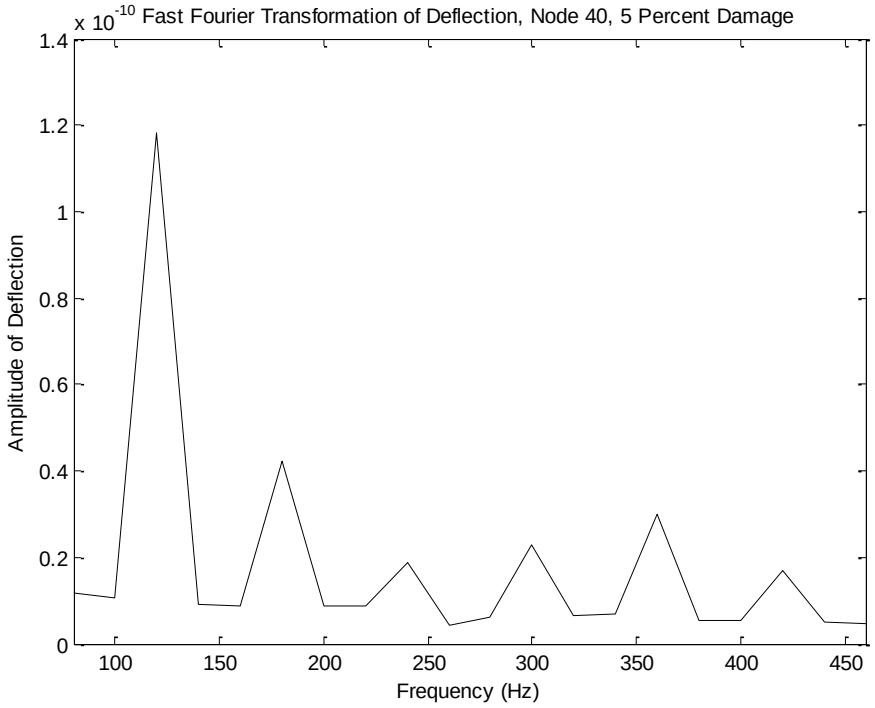

Figure 7.1.2.10 FFT of Deflection, Node 40, 5 Percent

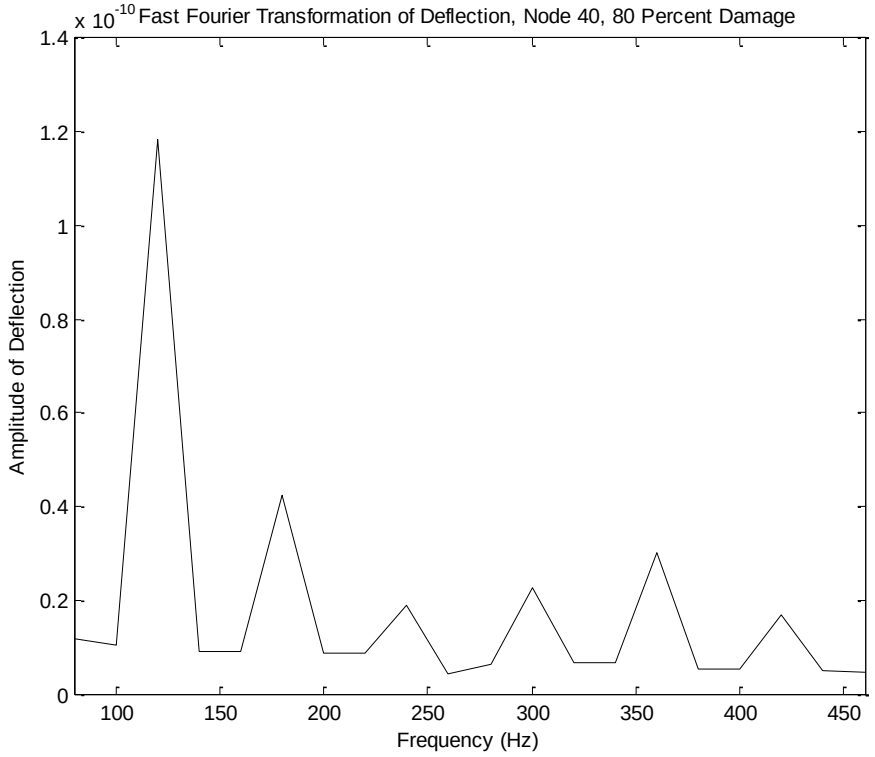

Figure 7.1.2.11 FFT of Deflection, Node 40, 80 Percent Damage

7.1.3 FRF

The following are plots of the FRF data gained by dividing the deflection by the force. These correspond to the FFT plots in 7.1.2. Therefore the undamaged, 5 percent damage and 80 percent damage results have been presented for each node as the differences in the intermediate results between 5 and 60 percent were virtually undiscernible. As the inaccuracies do not affect the directly damaged node to the extent of the internodal damaged nodes, 60 percent damage FRF data will be presented for node 23.

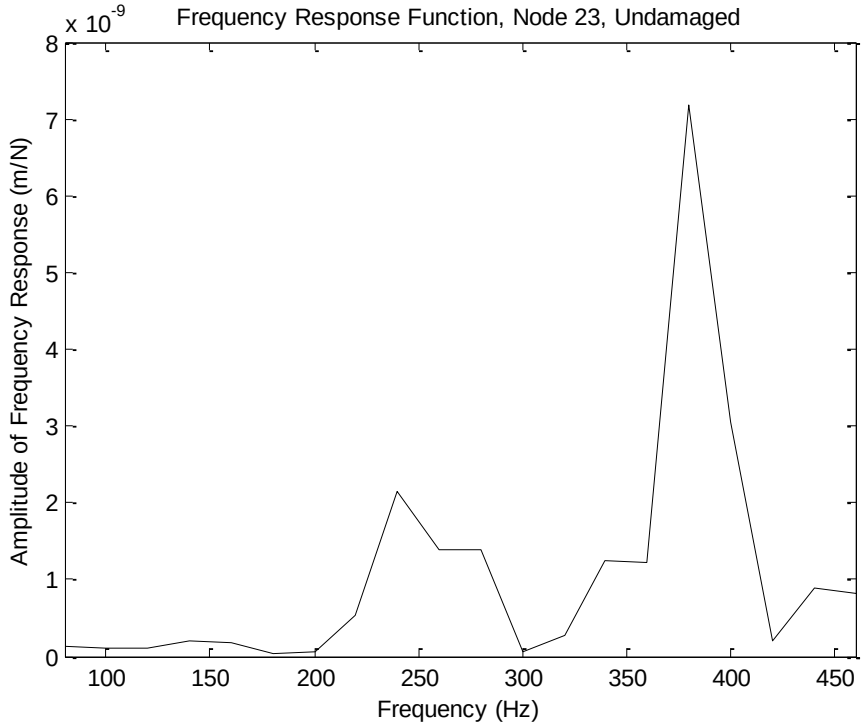

Figure 7.1.3.1 Frequency Response Function, Node 23, Undamaged

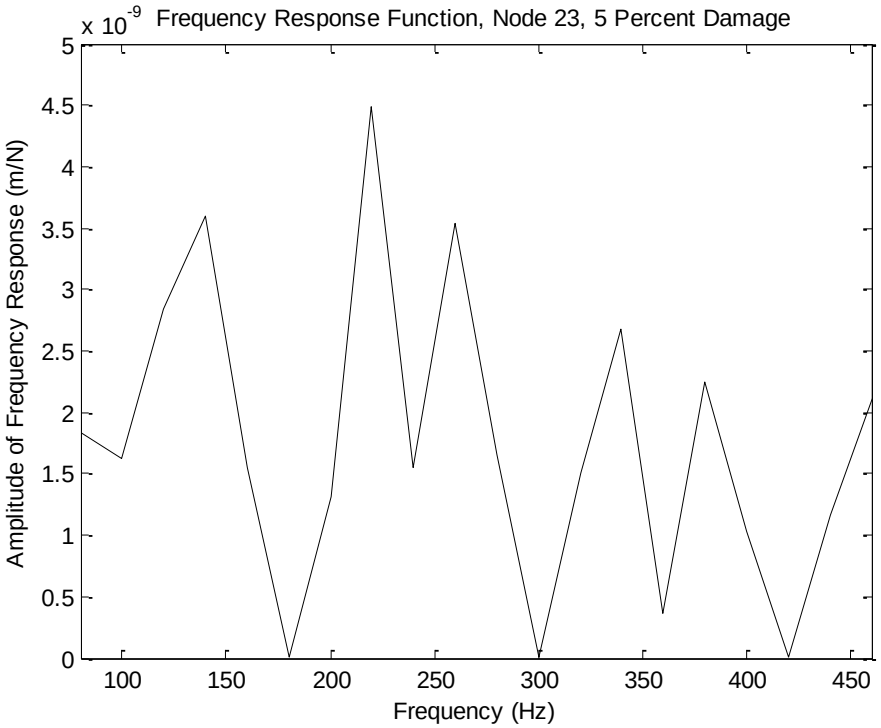

Figure 7.1.3.2 Frequency Response Function, Node 23, 5 Percent Damage

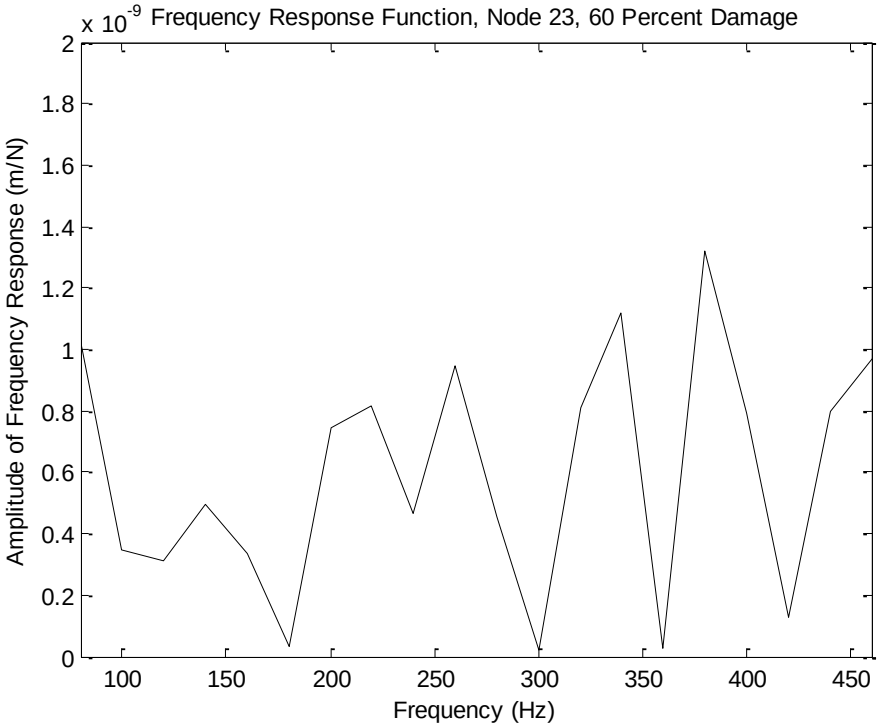

Figure 7.1.3.3 Frequency Response Function, Node 23, 60 Percent

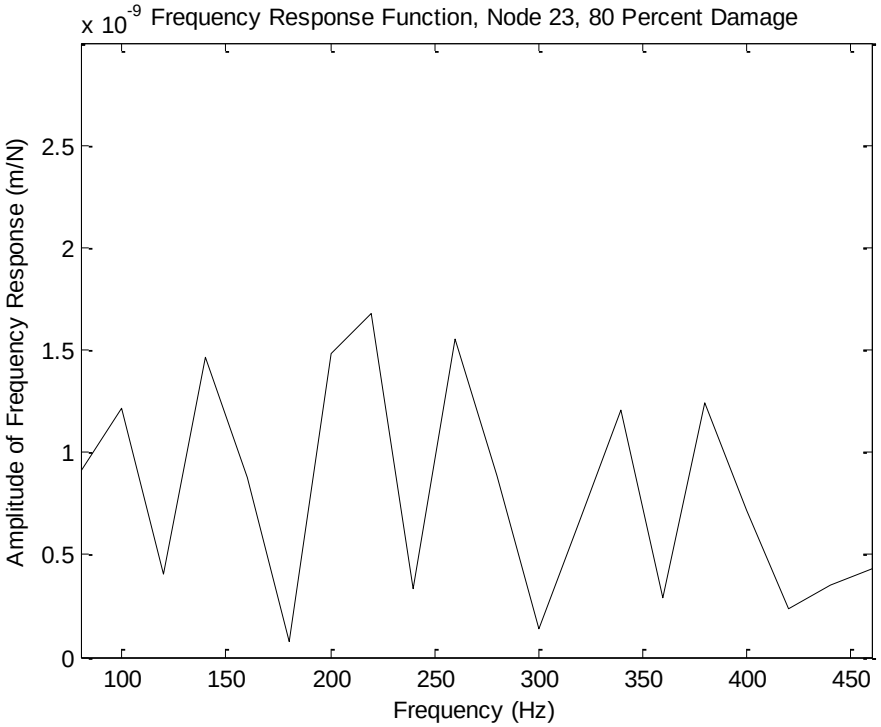

Figure 7.1.3.4 Frequency Response Function, Node 23, 80 Percent Damage

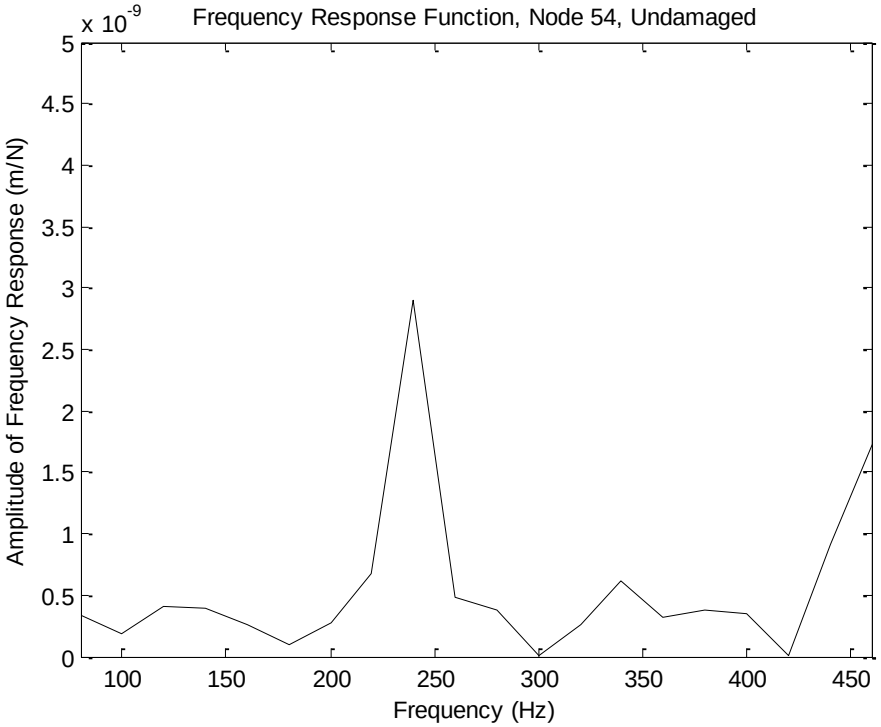

Figure 7.1.3.5 Frequency Response Function, Node 54, Undamaged

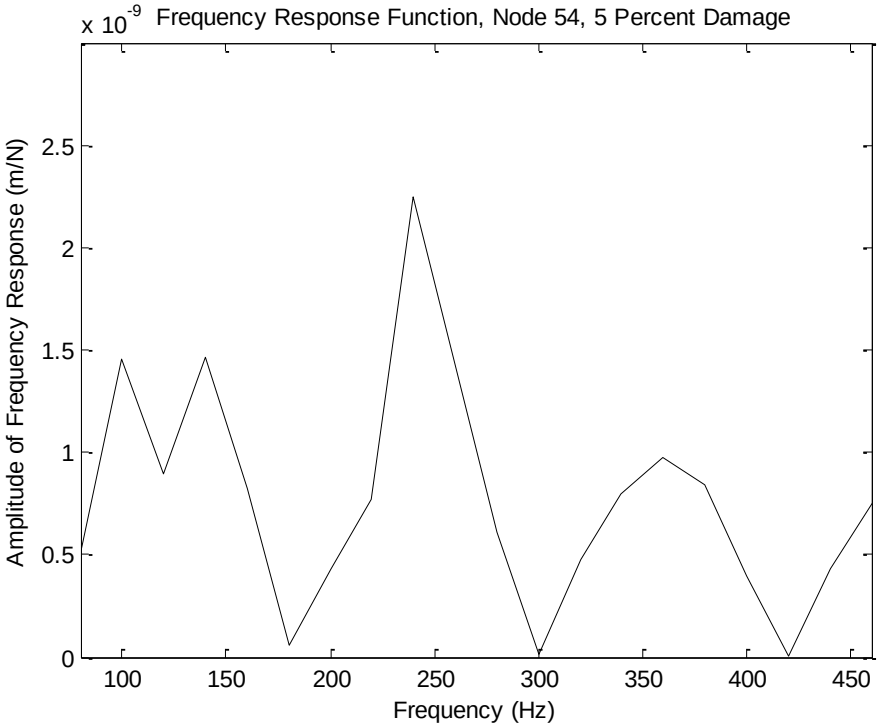

Figure 7.1.3.6 Frequency Response Function, Node 54, 5 Percent Damage

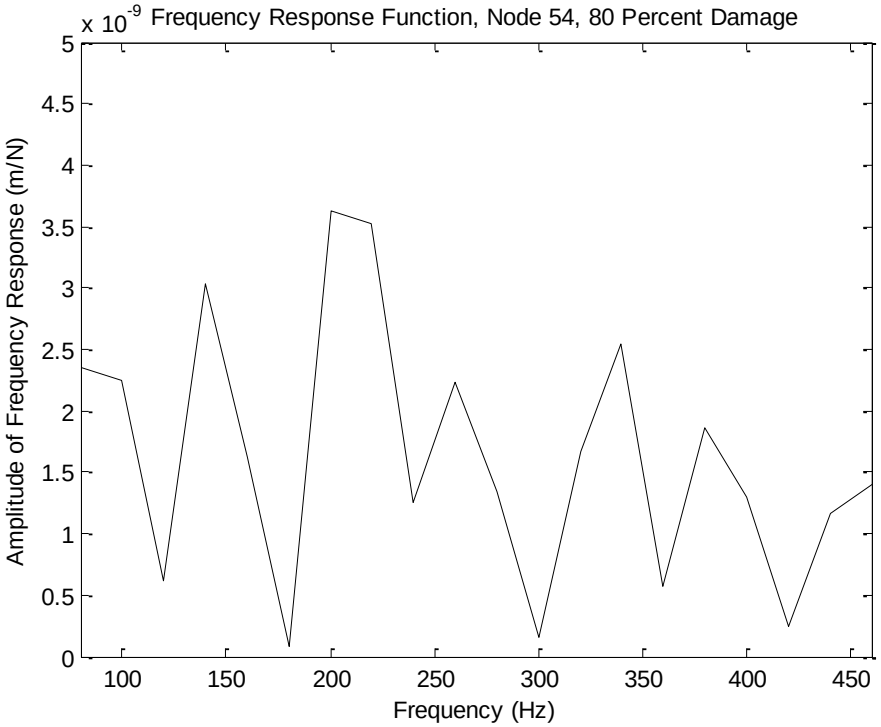

Figure 7.1.3.7 Frequency Response Function, Node 54, 80 Percent Damage

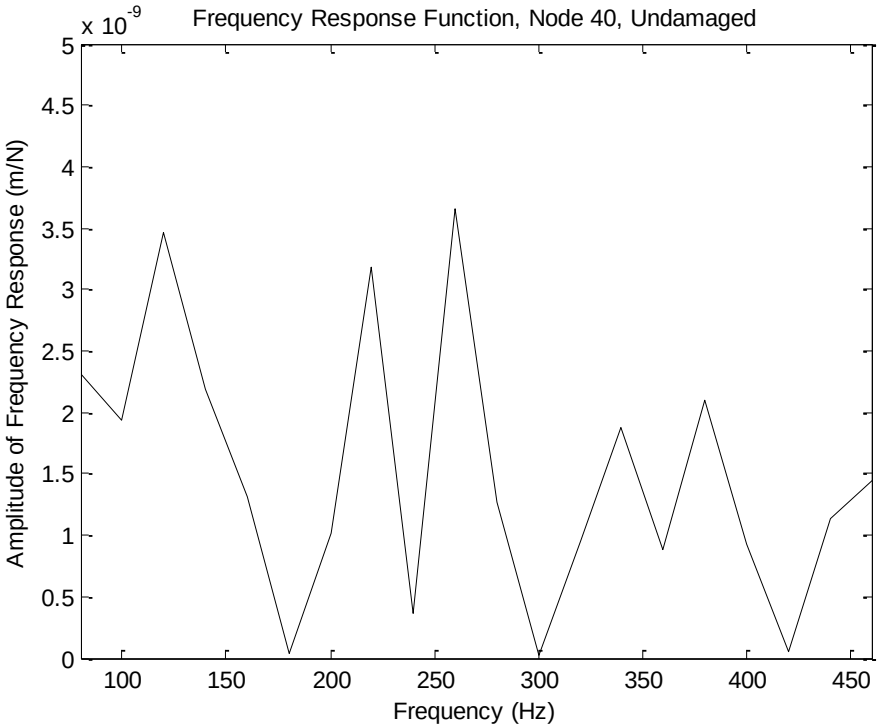

Figure 7.1.3.8 Frequency Response Function, Node 40, Undamaged

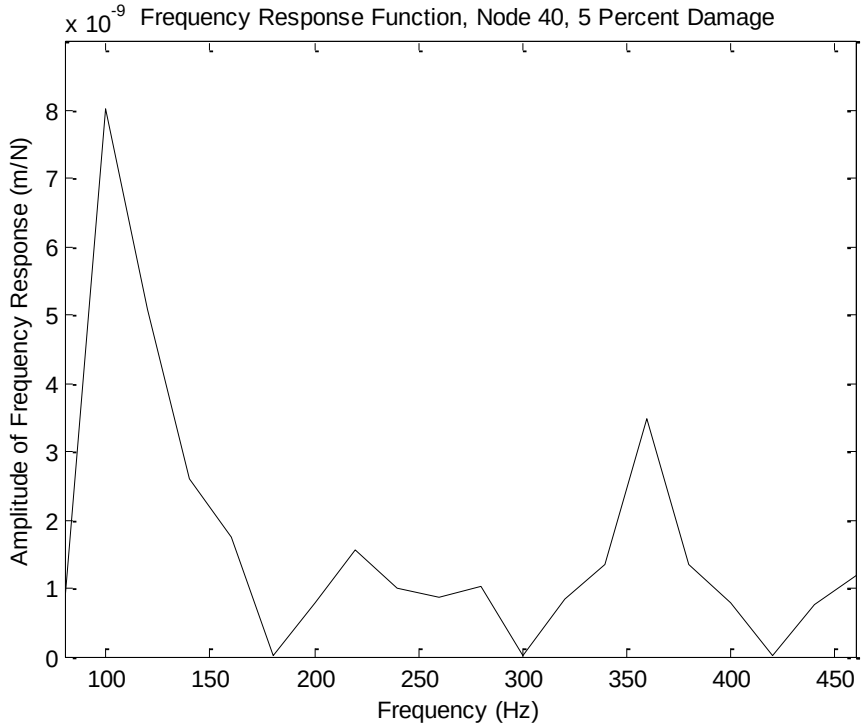

Figure 7.1.3.9 Frequency Response Function, Node 40, 5 Percent Damage

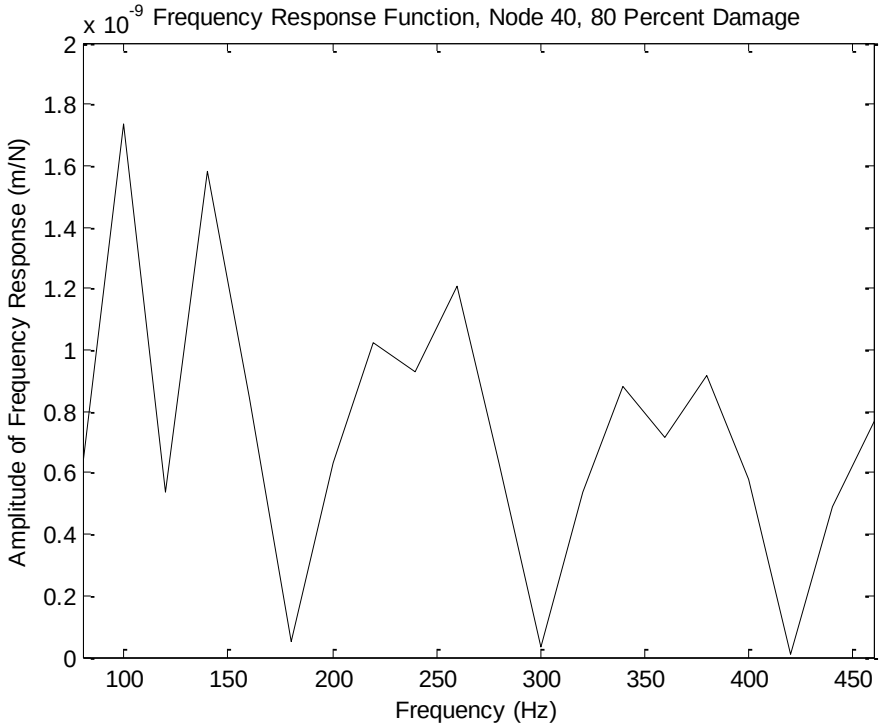

Figure 7.1.3.10 Frequency Response Function, Node 40, 80 Percent Damage

7.1.4 Damage Index

The damage index is a dimensionless factor and is used to indicate the extent of damage sustained by a node. It was intended that this factor be used to quantify the damage that had taken place with the use of the percentage damage levels. The following plots present the damage index at each node at each damage level imparted upon the composite member. The damage index at node 23 at each damage level, was then used in an attempt to create an arbitrary damage index scale, due to this node's damage index consistency.

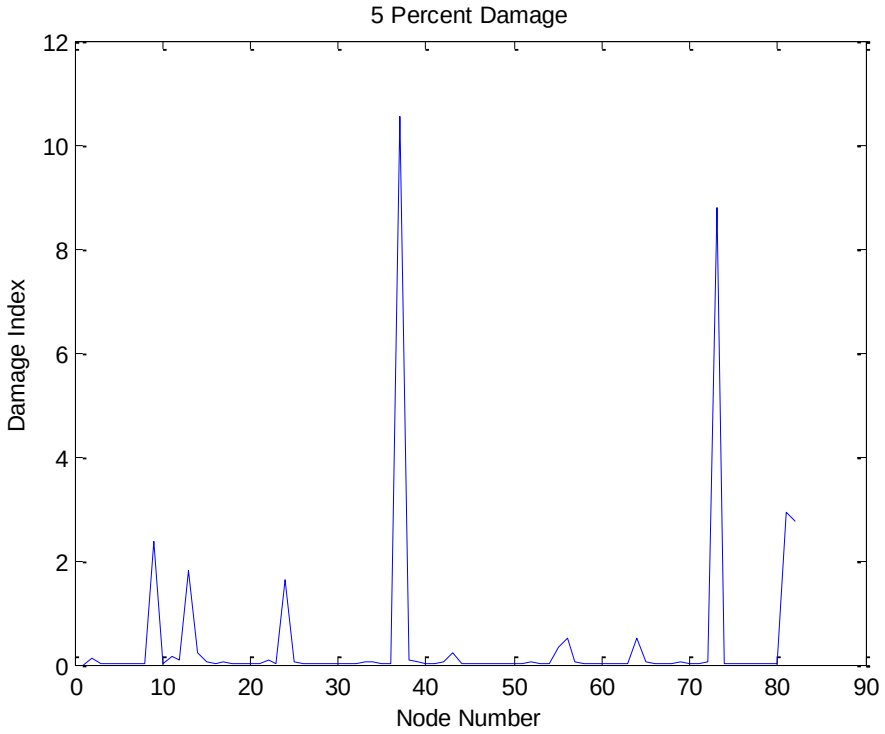

Figure 7.1.4.1 Damage Index – 5 Percent Damage

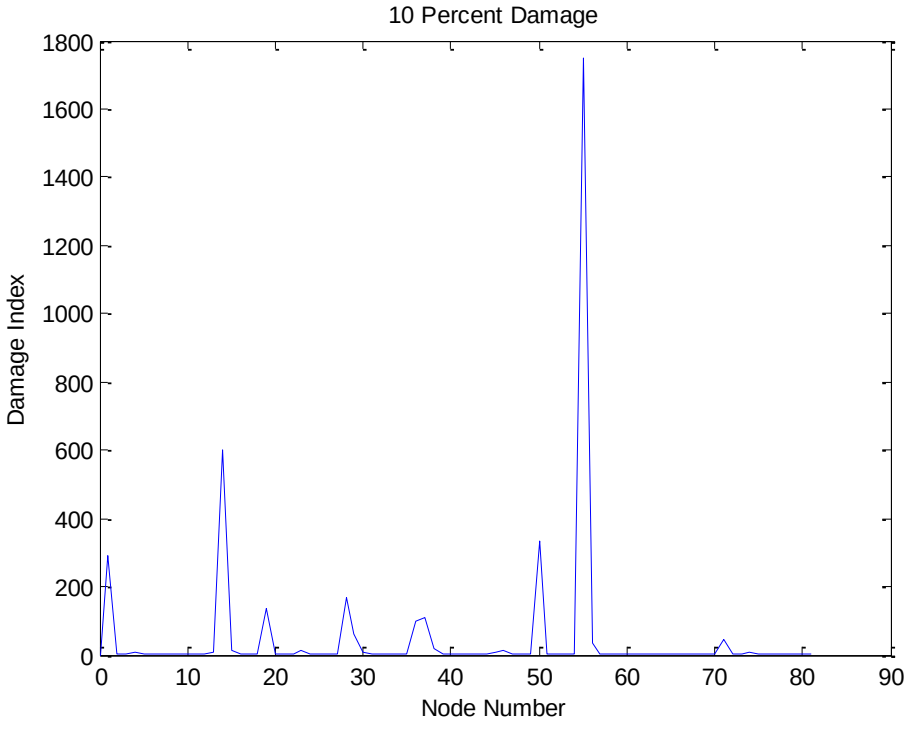

Figure 7.1.4.2 Damage Index – 10 Percent Damage

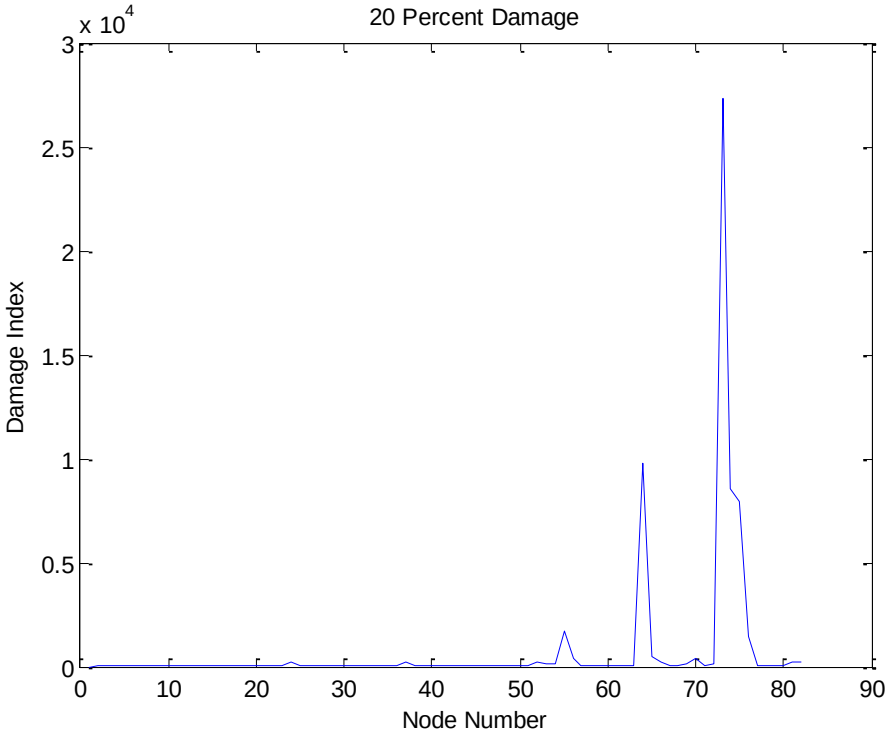

Figure 7.1.4.3 Damage Index – 20 Percent Damage

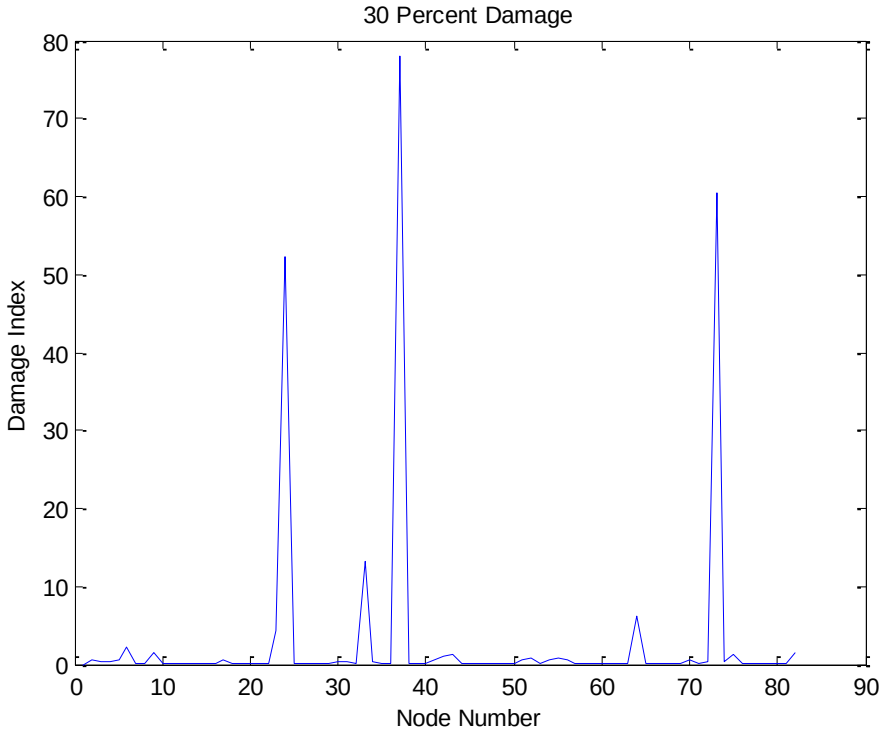

Figure 7.1.4.4 Damage Index – 30 Percent Damage

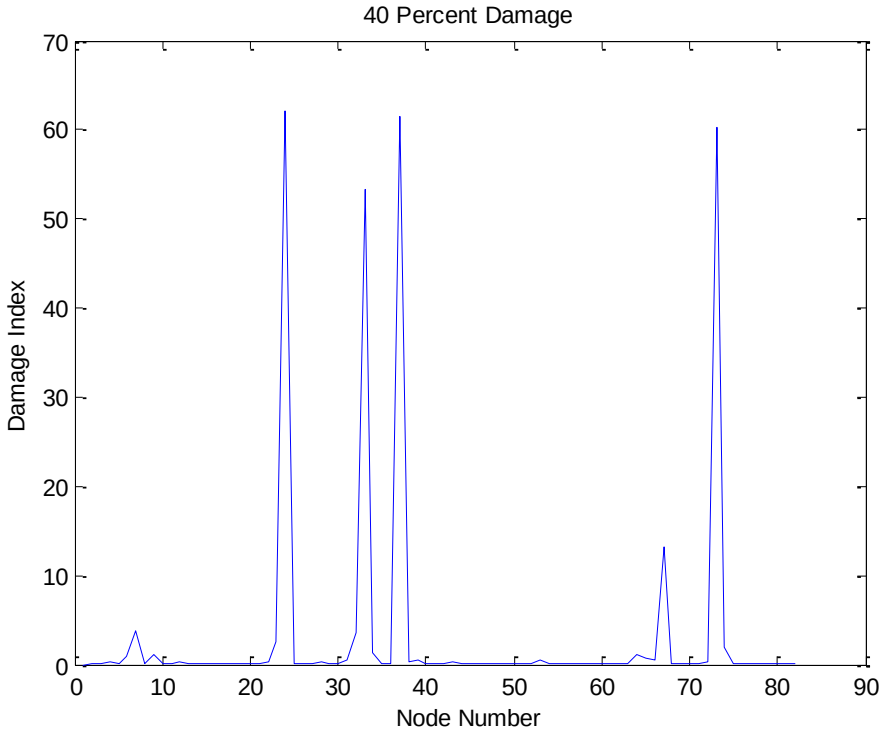

Figure 7.1.4.5 Damage Index – 40 Percent Damage

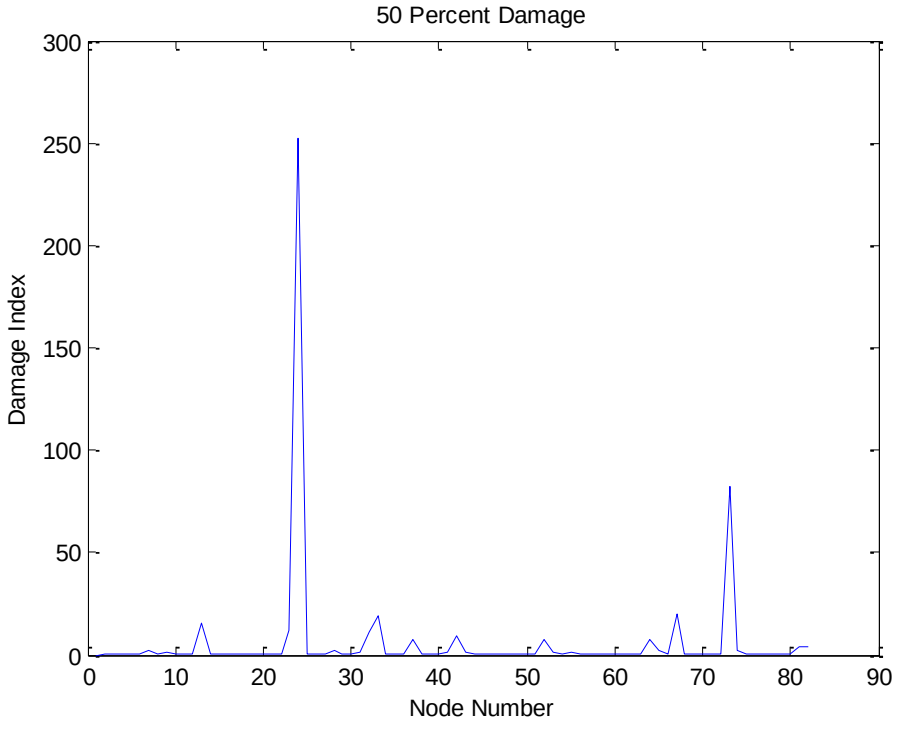

Figure 7.1.4.6 Damage Index – 50 Percent Damage

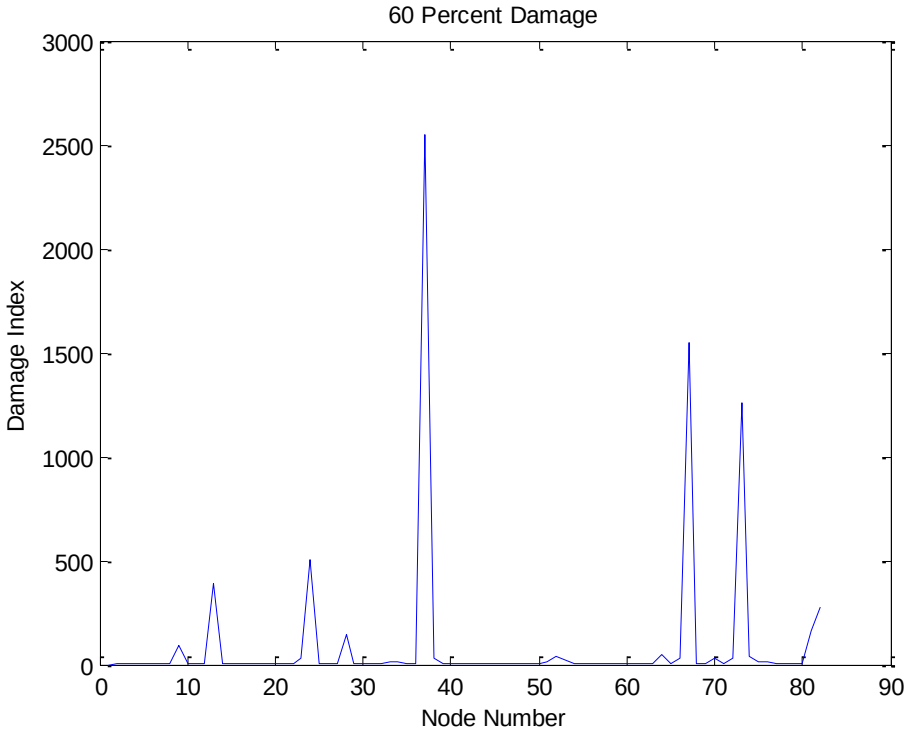

Figure 7.1.4.7 Damage Index – 60 Percent Damage

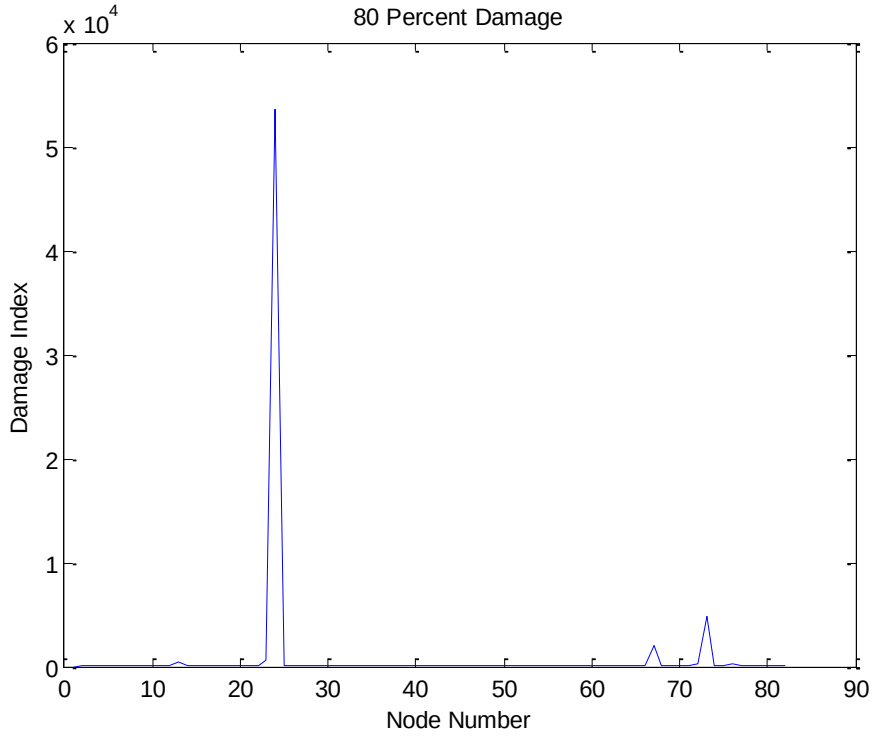

Figure 7.1.4.8 Damage Index – 80 Percent Damage

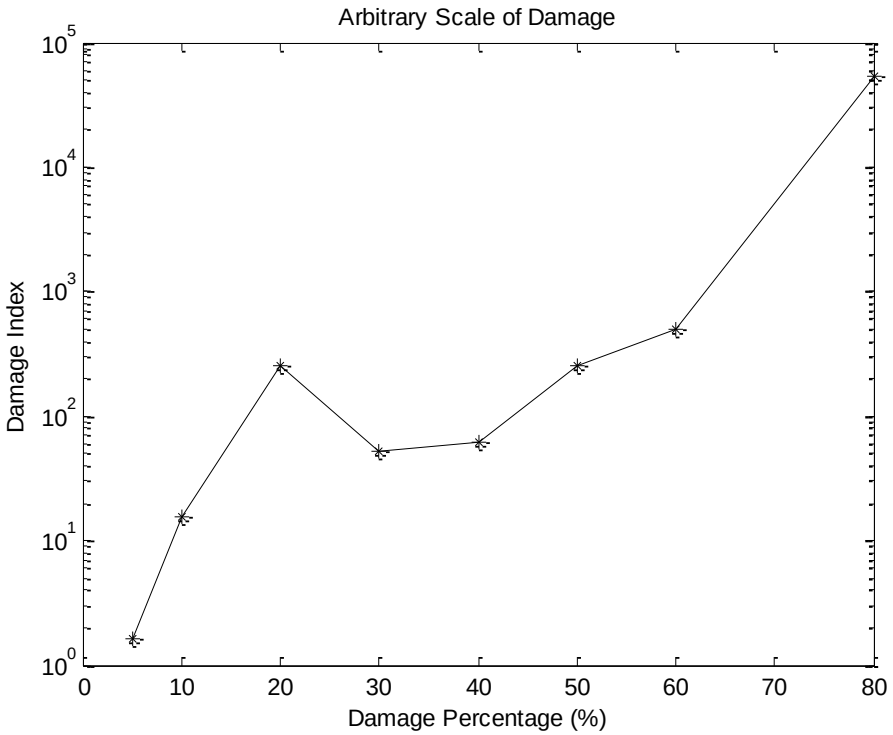

Figure 7.1.4.9 Relative Damage Index

7.2 Verification of Results

Verification of the natural frequencies gathered from the post processing program was completed using the FEA program ANSYS and simple calculations (ANSYS 2011) (Rao 2005). This was carried out to ensure the correct range of natural frequencies was detected and used in the damage detection process.

7.2.1 Finite Element Analysis Results

Finite element analysis was completed in the FEA program ANSYS. Modal analyses were completed for each damage level with the inclusion of the previous damages. The following show the natural frequencies gained from this analysis.

Table 7.2.1.1 Composite Member Natural Frequencies – Undamaged

Undamaged	
Natural Frequency Number	Frequency (Hz)
1	50.58
2	145.28
3	187.91
4	388.57
5	415.79
6	459.74

Table 7.2.1.2 Composite Member Natural Frequencies – 5 Percent Damage

5 Percent Damage	
Natural Frequency Number	Frequency (Hz)
1	50.22
2	145.58
3	187.12
4	388.55
5	413.85
6	457.73

Table 7.2.1.3 Composite Member Natural Frequencies – 10 Percent Damage

10 Percent Damage	
Natural Frequency Number	Frequency (Hz)
1	50.60
2	145.62
3	187.3
4	389.26
5	413.15
6	462.15

Table 7.2.1.4 Composite Member Natural Frequencies – 20 Percent Damage

20 Percent Damage	
Natural Frequency Number	Frequency (Hz)
1	50.87
2	145.73
3	188.74
4	389.24
5	414.41
6	461.27

Table 7.2.1.5 Composite Member Natural Frequencies – 30 Percent Damage

30 Percent Damage	
Natural Frequency Number	Frequency (Hz)
1	50.02
2	145.11
3	185.25
4	386.25
5	414.14
6	454.4

Table 7.2.1.6 Composite Member Natural Frequencies – 40 Percent Damage

40 Percent Damage	
Natural Frequency Number	Frequency (Hz)
1	49.15
2	144.89
3	178.48
4	387
5	406.67
6	461.35

Table 7.2.1.7 Composite Member Natural Frequencies – 50 Percent Damage

50 Percent Damage	
Natural Frequency Number	Frequency (Hz)
1	47.74
2	144.02
3	169.26
4	382.94
5	400
6	451.25

Table 7.2.1.8 Composite Member Natural Frequencies – 60 Percent Damage

60 Percent Damage	
Natural Frequency Number	Frequency (Hz)
1	43.99
2	142.84
3	150.62
4	376.27
5	384.04
6	451.84

Table 7.2.1.9 Composite Member Natural Frequencies – 80 Percent Damage

80 Percent Damage	
Natural Frequency Number	Frequency (Hz)
1	46.18
2	139.92
3	158.68
4	355.51
5	412.09
6	422.98

7.2.2 Natural Frequency Calculations Results

To further verify the correct natural frequencies were used by the damage detection process a simple pin-pinned beam natural frequency calculation was performed. The equation used can be viewed in Figure 5.1.2.1 and the operations taken to obtain the

first natural frequency can be found in appendix F.1. It was found that the first natural frequency of the beam was 200.51 Hz using this method.

7.3 Discussion

7.3.1 Post Processing

Accuracy and consistency of the acceleration and force data was important in the post processing operation. Achieving accuracy and precision in raw experimentation data assists in the accuracy of the various post processing steps. It was imperative that the acceleration and force data obtained from the apparatus, through experimentation, was of a particular precision. This would ensure the production of reliable velocity, deflection, FFT, FRF and damage detection results.

Vibration experimentation was performed at the 82 accelerometer position nodes at each of the 9 damage levels. The sensor gathered acceleration information pertinent to the oscillation of the composite member for later post processing. As can be seen Figure 7.1.1.1 the acceleration data gathered at node 23 at the undamaged level repeats a particular waveform. The signal appears to take the form of several summed sinusoidal waveforms creating the response of the member caused by forced oscillation. The repetition and uniformity of this signal led the researcher to believe it was an accurate and consistent representation of what was occurring in the member. Figure 7.1.1.5 was created using acceleration data gathered at node 40 at a 10 percent damage level. This data set is an example of the differing waveforms that were gathered in this experimentation. This node was positioned close to the centre of the composite member. The overall wavelength of the oscillation at the centre of the beam appeared to be larger than that of node 23 positioned a quarter down the member's length. Different waveforms relating to other node positions and damage levels may be viewed in appendices E.1 to E.3.

The force data gathered from the shaker appears to be consistent throughout all node points and damage levels. The oscillation force imparted upon the undamaged member when acquiring acceleration data at node 23 may be viewed in Figure 7.1.1.4. Although the input waveform of the shaker was sinusoidal in nature it appeared that the resulting output of the shaker was almost rectangular. This may have been caused by the shaker's attempt to create a sinusoidal output by gradually increasing the force on a relatively heavy member. The weight and rigid nature of the member may have caused the maxima and minima of the sinusoidal force signal to oscillate in an

undesirable fashion. However, the waveform generated was uniform and consistent in nature across all data collection points as can be seen in Figure 7.1.1.6. Generally the force oscillated between 6 N and -6 N at a constant frequency of 60 Hz. As each set of force data was practically identical only two were presented, additional force data can be viewed in appendices E.4 to E.6.

Velocity and deflection of the member at the particular points was successfully calculated using the acceleration data provided by the apparatus. This data was created using methods outlined in section 6.1. Typically the velocity and deflection profiles are similar in nature to their corresponding acceleration data, having similar wavelengths and waveforms.

The accuracy of the acceleration, velocity, deflection and force was of a high enough standard to graphically represent the response of the member. Although, it was thought that this accuracy was not of a high enough standard to correctly identify the damages in the system 100 percent of the time. This was due to the relatively low sample rate that was implemented. This sample rate affected the accuracy of the FFT and FRF analyses greatly. It achieved this by limiting the concentration of frequencies available for each FFT analysis. Therefore, with a low sample frequency, small frequency differences in the response waveforms were not identified. This allowed large damages to be identified while preventing smaller damages from being detected. The 5120 Hz sample rate that was chosen in section 2.5.4, was implemented in order to shorten computation time and memory usage. This sample rate allowed the post processing program to complete the 9 damage level analyses within 24 hours and required 4 gigabytes of memory. It was not possible to increase the sample rate due to the limitations of the computers available. To produce results accurate enough to perform this damage detection process it is recommended that one analysis be completed at a time with a large sample rate to verify findings. Small inaccuracies pertinent to the velocity and deflection data are also prevalent due to the interpolation required by Simpson's rule, outlined in section 6.1.2. Therefore the researcher suggests the use of a different sensor that gathers deflection directly in an attempt to remove these inaccuracies completely.

7.3.2 Fast Fourier Transformation

Fast Fourier transformation was used to create frequency response function data in order to carry out the vibration damage detection method. Force and deflection FFT

operations were completed for each data acquisition point and at each damage level. These analyses were performed successfully, however accuracy problems were prevalent.

Force fast Fourier transformations for all sets of data were identical as the form nature of the force data collected was uniform. An example of the fast Fourier Transformation of the oscillating force may be viewed in Figure 7.1.2.1, where the FFT of force at node 23 is presented. The frequencies that have been identified are a direct result of the phenomenon outlined in section 7.3.1. This phenomenon has caused the output of the shaker to be almost rectangular in fashion with small oscillations at the maxima and minima, see Figure 7.1.1.6. The frequencies of these maxima and minima oscillations have caused additional frequencies of 180 Hz, 300 Hz and 420 Hz to be present in the analysis. These extra oscillating forces, in addition to the 60 Hz main frequency, may cause inaccuracies in the damage detection method. However, as a frequency response function was created using a relationship between deflection and force, the inaccuracy caused by the extra oscillations was minimal.

Damage sustained directly on a data collection node had the greatest effect on the FFT processes. Several of the initial natural frequencies have been discovered as can be seen in Figure 7.1.2.2. The first of these natural frequencies was found to be slightly higher than 120 Hz, represented by the small heightening of the line at 120 Hz. This frequency was difficult to identify as the sample rate was not great enough to provide high frequency accuracy. After 5 percent damage had been implemented the frequency profile changed slightly, see Figure 7.1.2.3. The first natural frequency was then able to be easily identified as being close to 120 Hz. As this natural frequency is slightly smaller than the undamaged natural frequency, it is apparent that damage has occurred (Chen, Spyrakos & Venkatesh 1995). However, due to the inaccuracies associated with the small sampling frequency, natural frequency shifts did not occur again until the 80 percent damage level. Small amplitude shifts did occur between the 5 percent and 60 percent levels, however these were too small to visually convey in a graph. The similarity can be viewed by comparing the 5 percent and 60 percent damage levels at node 23, Figure 7.1.2.3 and Figure 7.1.2.4. At the 80 percent level the FFT at node 23 changes drastically. As can be seen in Figure 7.1.2.5 the first natural frequency has changed from being around the 120 Hz mark to being around 180 Hz. This would suggest that the member has sustained enough damage to allow it to act as though it were two shorter members increasing the natural frequency.

Damage sustained between nodes had far less effect on the FFT process. Damage was introduced gradually half way between nodes 54 and 55. These nodes acted in precisely the same fashion. Therefore only node 54 will be analysed in depth. The undamaged FFT analysis appeared to have identified the first natural frequencies correctly, (Figure 7.1.2.7). However, when damage was introduced into the system the frequency distribution did not change drastically. Amplitude changes did exist between the undamaged and damaged sections, but differences were minute. This can be found through a comparison between Figure 7.1.2.6, Figure 7.1.2.7 and Figure 7.1.2.8.

Fast Fourier transformations of nodes unaffected by damage were also completed. To achieve an identification of damage the deflection FFT of a node must change between damage levels. An example of an undamaged node was presented as a control. The FFT analyses at node 40 at undamaged, 5 percent and 80 percent damage levels were presented. These can be viewed in Figure 7.1.2.9, Figure 7.1.2.10 and Figure 7.1.2.11 respectively. As can be seen these frequency distributions do not differ in any way, suggesting no damage had taken place. The FFT analyses at node 54 and 40 at undamaged, 5 percent and 80 percent damage levels are similar. In this analysis they were similar as the natural frequencies did not change when different damage levels were applied. However, the damages between nodes 54 and 55 did cause an amplitude change in the FFT of node 54. This may suggest that this method may not be able to detect damages with accuracy between sensor data acquisition points, further research may verify this.

7.3.3 Frequency Response Function

Frequency Response Function data was produced using the FFT of force and the FFT of deflection outlined in section 6.2.1. This process was completed at each sensor location using each damage level. As the FRF process utilises the deflection FFT data, similar differences in results occur at the different damage levels. The FRF process appeared to exhibit a greater sensitivity to damages in comparison to the FFT process.

The frequency response function output differed drastically between damage levels pertinent to node 23, directly damaged node. As can be seen in Figure 7.1.3.1 the frequency response function has augmented the FFT data by removing the forced oscillation frequencies which highlighted the response frequencies. The 5 percent damaged FRF distribution, Figure 7.1.3.2, was vastly different to the undamaged. This difference in FRF was used to create the damage index values in order to determine

position and extent of damage. Therefore, a greater difference in FRF distribution causes a greater damage index reading. As can be seen in Figure 7.1.3.3 and Figure 7.1.3.4 the greater the damage the greater the difference in FRF in comparison to the undamaged specimen.

FRF output relating to the internodal damaged nodes, 54 and 55, between damage levels appeared to be relatively consistent. As can be seen in Figure 7.1.3.5 there is a peak around the 250 Hz mark with two smaller amplitude peaks at 150 Hz and 350 Hz. These peaks also existed when the member had been damaged at the 5 percent level, Figure 7.1.3.6, and at the 80 percent level, Figure 7.1.3.7. This suggests that the damage has not been detected using the FRF process nor the FFT process. This may be due to the small sample frequency problems previously discussed.

Nodes that remain undamaged, node 40, produced FRF data that was generally consistent. This can be seen by viewing the similarities between the undamaged FRF data of node 40, Figure 7.1.3.8, and the 80 percent damaged FRF data, Figure 7.1.3.10. As can be seen the peaks at the 250 Hz mark and the 350 Hz mark are consistent. However, in some circumstances the FRF data between damage levels of undamaged nodes was different. This produced incorrect large damage index values at these points where these differences occurred, causing incorrect damage position identification. An example of this difference between FRF distributions can be seen by comparing the undamaged and 5 percent damaged node 40 FRF data, Figure 7.1.2.8 and Figure 7.1.2.9 respectively.

7.3.4 Damage Index

Damage index is an arbitrary measure that was used to identify the location of the damages introduced into the composite member. This measure was created through the discovery of small differences between the undamaged and damaged FRF distributions at each data acquisition point, see section 6.2.2. With the use of the varying levels of damage imparted upon the member this arbitrary measure was used to form an arbitrary damage index scale. This scale quantified the damage index by relating a certain damage index to a level of damage. Therefore the position and extent of the damage sustained in a different structure may be identified using this method. However, this technique differed in reliability at varying levels of damage.

Damage index values were created for each data acquisition node and level of damage imparted on the composite member. The successful identification of the position of

damage increased with an increase in the damage sustained by the member when damage was directly applied to a node, node 23. When considering the 5 and 10 percent damage levels, Figure 7.1.4.1 and Figure 7.1.4.2 respectively, a damage index peak can be seen at node 23. However, these peaks can be rendered insignificant by the numerous large error peaks. At the 20 percent damage level, Figure 7.1.4.3, the damage index errors are several orders of magnitude larger than the damaged node. After the member had been damaged to the 30 and 40 percent levels, Figure 7.1.4.4 and Figure 7.1.4.5 respectively, the damage index at the true damage point begins to be comparable to the error readings. As seen in Figure 7.1.4.5 the damage index at node 23 has become larger than the other error values. At the 50 percent damage level, Figure 7.1.4.6, it can be seen that the true damage location at node 23 has a far greater damage index than the various error positions. This can also be seen at the 80 percent damage level, Figure 7.1.4.8, where the damage index at node 23 is several times larger than any other reading. However, the error readings reappear in the 60 percent damage level damage index distribution, Figure 7.1.4.7.

The detection of damages in between data acquisition nodes was less successful. As can be seen in Figure 7.1.4.1 and Figure 7.1.4.2 the 5 and 10 percent damage level analyses did not correctly identify the damage located between nodes 54 and 55. However, as can be seen in Figure 7.1.4.3 to Figure 7.1.4.7 a small damage index plateau was created at damage levels 20 to 60 percent. This would suggest that both nodes 54 and 55 had been affected by the damage in between them. However, the error and node 23 damage indexes render these readings insignificant if the damage locations were unknown.

The damage index errors significantly impinged upon the ability to correctly identify damage locations. These errors may be attributed to the error introduced into the post processing program by the Simpson's rule interpolation, problems with the sample frequency or existing damages in the structure. Previously existing 60 percent damages were located at nodes 30, 40, 48 and between nodes 15 and 16 and 60 and 61. This was completed in order to determine the effect existing damages would have on the damage detection system. By observing the damage index distributions from 5 to 80 percent, Figure 7.1.4.1 to Figure 7.1.4.8, it can be seen that these locations do not have significant damage index values. However, nodes 15 and 16 do occasionally gain a small damage index error. This led the researcher to believe that previous damages, of this form, in a structure would have little effect on the damage detection method.

However, delamination of the composite material may have occurred while the member was initially cut to size (Christensen 2009). Therefore, if this type of damage existed in the member at the time of damage detection data acquisition, large damage index values may exist at either end of the member. Due to the nature of this analysis, only one end of the member was analysed and was represented by node 82. Therefore, the large damage index values associated with nodes 64 and 73 may be attributed to delamination of the end of the member. The more insignificant error values located closer to the centre of the member were determined to be errors associated with the Simpson's rule interpolation and the low sampling rate issues.

The ascending nature of the damage index at node 23 through the damage levels would suggest that the damage index increases with the amount of damage sustained. Although the damage index values are considered as being inaccurate they were used to plot an arbitrary scale of damage. The damage index of node 23 at each damage level was used to create this scale. The damage indexes gathered from the 5 to 80 percent damage levels at node 23 may be viewed in Table 7.3.4.1.

Table 7.3.4.1 Damage Index at Each Damage Level

Damage Percentage (%)	Damage Index
5	1.61
10	15.51
20	251.6
30	52.21
40	62.15
50	252.5
60	500.9
80	53670

This data was graphed using a log scale on the vertical axis to assess whether any relationships between damage percentage and damage index exist. As can be seen in Figure 7.1.4.9 the damage index generally increases when the damage percentage increases. This seems to be linear with a logarithmic vertical axis, which indicates that the relationship between damage index and extent of damage is exponential in nature. However, the damage index resulting from a 20 percent damage level is larger than the 30 and 40 percent damage indexes. It is assumed that this anomaly is due to an error

associated with interpolation and issues with the sample frequency and would require further research for verification.

7.3.5 Verification

ANSYS and natural frequency calculations were performed in order to verify the range of frequencies used in the damage detection process. The ANSYS results provided the first 6 natural frequencies and the simple natural frequency calculation provided the first. These results varied in comparison to each other and the results obtained in the FFT analyses.

The ANSYS undamaged analysis performed produced a first natural frequency of 50 Hz and a second natural frequency of 145 Hz, (Table 7.2.1.1). As the first natural frequency obtained in this analysis was below the cut off frequency of the post processing program it could not have been identified in the FFT analyses. However, the FFT analysis at node 40 at the undamaged level, Figure 7.1.2.9, did indicate that there was a natural frequency between 120 Hz and 150 Hz. Therefore the FFT analyses correctly identified the second natural frequency relating to the ANSYS analysis. Throughout the entire set of ANSYS analyses it was also apparent that the natural frequencies of the system decrease as the damage extent increases, Table 7.2.1.1 to Table 7.2.1.9. This is confirmed in the FFT analyses and was discovered in by Chen et al. (1995), presented in Chapter 2.

The large 200 Hz first natural frequency calculated using simple natural frequency undamaged beam equations may be unreliable as the analysed member in this circumstance is completely undamaged and idealised. The previous damages imparted upon the member used in the experimentation were factored into the ANSYS analyses. This produced far smaller natural frequencies than were obtained using simple calculations. A phenomenon that affects the natural frequencies of a structure was outlined by Chen et al. (1995). As the damage introduced into a structure is increased the natural frequency of the structure decreases. Therefore, as the simple calculations related to an idealised perfect beam the previous damages were not factored in. This idealised beam would therefore have natural frequencies higher than in reality.

Although these verification methods differ slightly in comparison to one another and the FFT analyses it can be seen that they are in a similar range. Therefore as the frequencies gained through the FFT analyses were within the same range as the frequencies in the verification methods, the FFT analyses were completed correctly.

Chapter 8 **Conclusions**

The researcher has somewhat successfully utilised the frequency response functions of a glass fibre pultrusion composite to detect imparted damages in its structure. The use of processed acceleration and oscillating force data was used to conduct this non-destructive, comparatively less time and money consuming damage detection technique. Although the process was successful it was found that its accuracy was significantly affected by the data sampling frequency, Simpson's rule interpolation, operator fault and possible major initial damages.

Conduction of this damage detection method required data pertinent to the deflection and forced oscillation of the member. The deflection data was created by integrating acceleration data, provided by an accelerometer, twice. As Simpson's rule was used, interpolation was required which may have caused compounding inaccuracies in the deflection data. Sampling frequency was a major issue relating to this technique. As the researcher did not have access to a computer with a large memory capacity, the sampling frequency was limited in this analysis. This reduced the accuracy of the fast Fourier transformations which may have affected the damage detection process greatly. Delamination may have existed at one end of the pultruded member which may have also greatly affected the data at that end.

Regardless of the various errors associated with this initial analysis the system did detect damages in the structure. The experimentation successfully detected various levels of damages imparted upon a data acquisition node. However, this process had less success when attempting to detect damages between nodes. Through the conduction of this analysis with varying ranges of imparted damage levels, an arbitrary scale of damage was created. It was determined that this scale of exponential in nature.

With the use of a damage index plot and this arbitrary scale of damage plot the extent and position of damage may be estimated.

This avenue of damage detection may be a viable option in future engineering endeavours for real time updating of structural damages subject to dynamic loading. After addressing the issues pertaining to the current method such as code optimisation, error reduction and implementation of Microelectromechanical Systems, this method may be used in various engineering materials and applications. Ideally this method would be best applied to engineering endeavours that require reduced safety factors to increase performance such as aerospace purposes. When applied to such an application, this method may be used to detect anomalous damages which may have serious and catastrophic consequences if left undiscovered. Therefore this method may aid the maintenance process of dynamically loaded structures increasing the safety of the general public.

8.1 Achievement of Project

At the beginning of this research project a number of project specifications were created. It was the researcher's intention to fulfil all of these specifications in order to produce a well-rounded analysis of this damage detection method. All of the seven main project specifications were completed. These included the completion of extensive composite and vibration acquisition research which can be found in Chapter 2, the design and manufacture of the shaker attachment apparatus and several undamaged and damaged member data collections. The natural frequency signatures were then found using the numerical FFT process and were verified with computational FEA using ANSYS. This damage detection process was the deemed a plausible technique to detect damage in composite materials after certain problems had been addressed.

The specification that was to be completed if time permitted was not completed as the project grew far larger than was initially intended. The initial proposed project consisted of the performance of several FFT analyses at the centre of the composite member at differing levels of damage. This may have consisted of only 9 separate data acquisitions. The project grew into converting FFT data into FRF data at 82 locations at 9 different damage levels, or 738 data acquisitions. Therefore it would be almost impossible to analytically solve this system for each of these data points in the time allocated for the project.

Additional specifications were also completed. These included the creation of FRF data, the use of the FRF data to create a damage index at each node along the member, the creation of an arbitrary scale of damage using the damage index at node 23 at several damage levels. With the use of the arbitrary scale of damage the extent and position of damage along the composite member was then found. This method was considered as far more in depth than the initial proposed project as it would only indicate damage existed in the composite structure.

8.2 Further Research Recommendations

The method outlined in this dissertation is in its infancy and various issues must be addressed before it can be used and relied upon to detect damages. These mainly involve addressing inaccuracies, errors and computational requirements of the post processing program and apparatus used.

Errors in the system may be reduced easily and significantly through the use of a far higher sampling frequency. This would allow a far more accurate frequency distribution to be created in the FFT and FRF stages of the process. The minute frequency changes caused by small damages may then be revealed, creating far more accurate damage index values. It is thought that some of the large errors viewed in the damage indexes would also be reduced with an increase in sampling frequency.

The use of Simpson's rule may have introduced compounding errors in the deflection data. Other integration methods may be investigated to determine the ideal technique in this circumstance. Alternatively a different sensor may be used to detect deflection directly thus removing this step from the damage detection method.

Ensuring the structure being analysed has no prior damages is imperative. Damage indexes may have been correctly assigned to nodes that were continuing to be unknowingly significantly damaged. These results may be considered as large errors, causing confusion.

The application of Microelectromechanical Systems may also be investigated. The researcher was under pressure from strict timelines and was unable to investigate this type of apparatus.

List of References

ANSYS 2011, *ANSYS - Simulation Driven Product Development*, viewed 1 July 2011, <http://www.ansys.com/>.

Balachandran, B & Magrab, EB 2009, *Vibrations*, Cengage Learning, Toronto.

Bathias, C & Cagnasso, A 1992, 'Application of X-Ray Tomography to the Nondestructive Testing of High-Performance Polymer Composites', *American Society for Testing and Materials*, pp. 35-54.

Biomesh 2010, *FEA in biology*, viewed 1 September 2011, <http://www.biomesh.org/fea-basics>.

Castellini, P & Revel, GM 2000, 'An experimental technique for structural diagnostic based on laser vibrometry and neural networks', *Shock and Vibration*, vol 7, no. 6, pp. 1-17.

Chen, HL, Spyrakos, CC & Venkatesh, G 1995, 'Evaluating Structural Deterioration By Dynamic Response', *Journal of Structural Engineering*, vol 121, no. 8, pp. 1197-1204.

Christensen, RM 2009, *Failure Criteria.com*, viewed 24 May 2011, <http://www.failurecriteria.com/Media/Failure_of_Fiber_Composite_Laminates-_Progressive_Damage_and_Polynomial_Invariants.pdf>.

Dutta, D 2010, 'Ultrasonic Techniques for Baseline-Free Damage Detection in Structures', Dissertation, Carnegie Mellon University, Pittsburgh.

Faires, JD & Burden, R 2003, *Numerical Methods*, Brooks/Cole-Thomson Learning, Pacific Grove.

Fink, KD & Mathews, JH 2004, *Numerical Methods Using Matlab*, Pearson Education, Upper Saddle River.

FOES 2011, *ENG3003 Engineering Management Study Book 2*, University of Southern Queensland, Toowoomba.

He, J & Fu, Z-F 2001, *Modal Analysis*, Butterworth-Heinemann, Oxford.

James, G 2007, *Modern Engineering Mathematics*, Fourth Edition edn, Pearson Education Limited, Harlow.

Kim, JT & Stubbs, N 2002, 'Improved Damage Identification Method Based On Modal Information', *Journal of Sound and Vibration*, vol 252, no. 2, pp. 223-238.

LMS 2010, *Test.Xpress Software Manual*, LMS International.

Maia, NMM, Silva, JMM, Almas, EAM & Sampaio, RPC 2003, 'Damage Detection in Structures: From Mode Shape to Frequency Response Function Methods', *Mechanical Systems and Signal Processing*, vol 17, no. 3, pp. 489-498.

Martin, HC & Carey, GF 1973, *Introduction to Finite Element Analysis*, 1st edn, McGraw-Hill Book Company, New York.

MathWorks 2011, *Matlab - The Language Of Technical Computing*, viewed 1-10 2011, <http://www.mathworks.com.au/products/matlab/index.html>.

Munns, I 2009, *TWI*, viewed 13 May 2011, <http://www.twi.co.uk/content/ksijm001.html>.

Nise, NS 2008, *Control Systems Engineering*, Fifth Edition edn, John Wiley & Sons Inc, Danvers.

NVMS 2011, *Noise and Vibration Measurement Systems (NVMS)*, viewed 16 May 2011, <http://www.nvms.com.au/products/bksv/shakers.shtml>.

Orfanidis, SJ 2010, *Introduction to Signal Processing*, Prentice Hall, Inc.

Ortiz, J, Ferregut, C & Osegueda, RA 1997, 'Chapter4: Damage Detection From Vibration Measurements Using Neural Network Technology', *American Society of Civil Engineers*.

PCB 2009, *PCB Piezotronics Inc*, viewed 14 May 2011, <http://www.pcb.com/techsupport/tech_accel.php>.

Rao, SS 2005, *Mechanical Vibrations*, Pearson Education South Asia Pte Ltd, Bangkok.

Ricles, JM & Kosmatka, JB 1992, 'Damage Detection in Elastic Structures Using Vibratory Residual Forces and Weighted Sensitivity', *American Institute of Aeronautics and Astronautics*, vol 30, no. 9, pp. 2310-2316.

Salawu, OS 1997, 'Detection of structural damage through changes in frequency: a review', *Engineering Structures*, vol 19, no. 9, pp. 718-723.

Sampaio, RPC, Maia, NMM & Silva, JMM 1999, 'Damage Detection Using The Frequency-Response-Function Curvature Method', *Journal of Sound and Vibration*, vol 226, no. 5, pp. 1029-1042.

Shi, ZY, Law, SS & Zhang, LM 1998, 'Structural Damage Localization From Modal Strain Energy', *Journal of Sound and Vibration*, vol 218, no. 5, pp. 825-844.

Shi, ZY, Law, SS & Zhang, LM 2000, 'Structural Damage Detection From Modal Strain Energy Change', *Journal of Engineering Mechanics*, vol 126, no. 12, pp. 1216-1223.

SPS 2011, *Signal Processing Society*, viewed 08 October 2011, <http://www.signalprocessingsociety.org/>.

Storr, W 2011, *Electronics-Tutorials*, viewed 10 September 2011, <http://www.electronics-tutorials.ws/waveforms/waveforms.html>.

Tsuda, H 2006, 'Ultrasound and damage detection in CFRP usinf fiber Bragg grating sensors', *Composites Science and Technology*, vol 66, pp. 676-683.

USQ 2008, *ENG8803 Mechanics and Technology of Fibre Composites*, University of Southern Queensland, Toowoomba.

Vittorio, SA 2001, *MicroElectroMechanical Systems (MEMS)*, viewed 14 May 2011, <http://www.csa.com/discoveryguides/mems/overview.php>.

Wagners 2009, *Pultruded Structural Sections*, viewed 21 May 2011, <http://www.wagnerscft.com.au/documents/?2>.

Wagners 2011, *Wagners Composite Fibre Technologies*, viewed 21 May 2011, <http://www.wagnerscft.com.au/products/?electrical>.

Yao, GC, Change, KC & Lee, GC 1992, 'Damage Diagnosis of Steel Frames Using Vibrational Signature Analysis', *Journal of Engineering Mechanics*, vol 118, no. 9, pp. 1949-1961.

Appendix A: Project Specifications

Appendix A.1: Project Specifications

University of Southern Queensland

FACULTY OF ENGINEERING AND SURVEYING

ENG 4111/4112 Research Project

Project Specification

FOR: **Erin Heaton**

TOPIC: Use of vibration signature in structural health monitoring (Composites/Internal Damages).

SUPERVISORS: Dr. Jayantha Epaarachchi

ENROLMENT: ENG4111 – S1, 2011
ENG4112 – S2, 2011

PROJECT AIM: During the operational lifetime of a structure the vibration signature changes due to material property degradation. As such, vibration signatures can be used as an index of residual lifetime of the structure or component. The proposed project intends to investigate the change of vibration signature of a composite structure due to dynamic loading. Tasks to be completed consist of sample preparation, measurement of vibration characteristics of composite components and dynamic analysis using FEA.

PROGRAMME: **ISSUE A. 21st March 2011**

1. Research background material relevant to composite vibration modelling, the composite material being tested and vibration data acquisition.
2. The design and manufacture of a device that will be used to connect the excitation apparatus to the testing material.
3. Data collection pertinent to the forced vibration of defective and faultless fibre composite members.
4. After successful data collection numerically solve for the natural frequency signatures of the faultless material and the defective material.
5. Complete a computational finite element analysis of the members in order to confirm the numerical results.
6. After successful numerical analysis and finite element analysis, evaluate whether this process is accurate enough to be a viable means of defect detection in composite materials.
7. Submit an academic dissertation of research conducted.

Time permitting

8. Analytically confirm the numerical solution for the faultless member and the defective member.

Appendix B: Wagners Glass Fibre Pultruded Sections

Appendix B.1: Wagners Composite Pultrusion Specifications

(Wagners 2009)

WAGNERS

WAGNERS PULTRUDED FRP STRUCTURAL SECTIONS

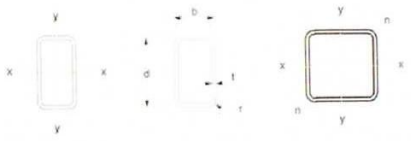

PRODUCT SPECIFICATIONS

75x100x5, 100x100x5, 125x125x6.5 SHS

SECTION PROPERTIES

Designation			Radii		Gross Section Area	About x-, y- and n- axis					
Depth d	Width b	Thickness t	Internal r_i	External r_e	A_g	Moment of Inertia about the x axis I_x	Moment of Inertia about the y axis I_y	Elastic Section Modulus for bending about the x axis Z_x	Elastic Section Modulus for bending about the y axis Z_y	Elastic Section Modulus for bending about the n axis Z_n	Torsion Constant J
(mm)	(mm)	(mm)	(mm)	(mm)	(mm^2)	($10^6 mm^4$)	($10^6 mm^4$)	($10^3 mm^3$)	($10^3 mm^3$)	($10^3 mm^3$)	($10^6 mm^4$)
100	75	5.25	4.75	10	1664.98	2.26	1.431	45.20	38.16	-	2.89
100	100	5.25	4.75	10	1931.68	2.86	2.86	57.20	57.20	42.83	4.65
125	125	6.5	4.75	10	3014.53	6.98	6.98	111.7	111.7	82.52	11.07

MECHANICAL PROPERTIES

Designation	Mass m	Density ρ	Ultimate Tensile Strength σ_T		Ultimate Compressive Strength σ_C		Shear Strength	Modulus Of Elasticity E		Moment Capacity M	
			Longitudinal	Transverse	Longitudinal	Transverse		Longitudinal	Transverse	X axis	Y axis
	(kg/m)	(kg/m^3)	(Mpa)	(Mpa)	(Mpa)	(Mpa)	(Mpa)	(N/mm^2)	(N/mm^2)	(kN.m)	(kN.m)
100x75x5 SHS	3.28	1970	650	41	550	104	84	35400	12900	13.17	9.44
100x100x5 SHS	3.81	1970	650	41	550	104	84	35400	12900	17.74	17.74
125x125x6.5 SHS	5.94	1970	650	41	550	104	84	35000	12900	33.85	33.85

MATERIAL REDUCTION FACTORS

Material Partial Safety Factor	Short Term Loading	Long Term Loading
Load Multiplier	1.3	3.16
Material Reduction Factor	0.79	0.32

EUROCOMP Design Code and Handbook, Edited by John L. Clarke,
1st edition, 1996, Published by E & FN Spon, London SE1 8 HN, UK

REV A

Appendix B.2: Wagners Composite Pultrusion Information

(Wagners 2009)

Wagners CFT Manufacturing Pty Ltd		MSDS No. WCFT 1004
Date of Issue: February 2009 Issue No.: 1	Page: 1 of 3	Pultruded Structural Sections

WAGNERS *CFT Manufacturing Pty Ltd*

ABN: **91 099 936 446**

Contact Details: **Ph** (07) 4637 7755 **Fax**: (07) 4637 7756

Street Address:
Corner Anzac Avenue and Alderley Street
Toowoomba Queensland 4350

Postal Address:
PO Box 151
Drayton North Qld 4350

HAZARDS IDENTIFICATION

This product is not classified as hazardous according to the criteria of the NOHSC Australia.

PRODUCT IDENTIFICATION

Product Name:	Hollow Pultruded Structual Sections of Varying Cross Sections.
Other Names:	Not Applicable
Manufacturers Product Code:	MPL004
Use:	Structural Pultruded Section
UN Number:	Not Applicable
Dangerous Goods Class:	Not Applicable
Hazchem Code:	Not Applicable
Poisons Schedule Number:	Not Applicable

Physical Data

Appearance:	Coloured fiberglass with hollow sections dimensions of varying lengths. Section sizes include:50 x 50, 100 x 75,100 x 100, 125 x 125.
Arm Density :	2000 kg / m^3 (3.5 kg per lineal metre)

Melting Point:	Not Applicable	**Flashpoint:**	Not Applicable
Boiling Point:	Not Applicable	**Flammabillity Limits:**	Not Applicable
Vapour Pressure:	Not Applicable	**Soluabillity in Water**:	Insoluable

Ingredients:

Chemical Entity	CAS Number	Proportion
Vinylester Resin	025036-25-3	20%
Glass Fibre	65997-17-3	76%
Other Non-Hazardous Ingredients	Proprietary	4%

This is a commercial product whose exact ratio of components may slightly vary. Minor quantities of other non-hazardous ingredients are also possible.

HEALTH HAZARD INFORMATION

Acute Health Effects

Swallowed: Unlikely under normal conditions of use, but swallowing dust from this product may result in abdominal discomfort.

Eye: Dust from this product may irritate the eyes causing watering and redness.

Skin: Dust from this product may cause irritation of the skin through friction but is not absorbed through the skin.

Inhaled: Dust from this product may cause irritation of the nose, throat and lungs causing coughing and sneezing.

Chronic Health Effects

No known long term effects

First Aid

Swallowed: Wash out mouth with water. If irritation persists consult medical advice.

Eye: Flush with clean water for 15 minutes. If irritation continues seek medical advice.

Skin: Wash with soap and water. Apply skin moisturizer.

Inhaled: Remove exposed person to fresh air.

Advice to Doctor: Treat symptomatically.

PRECAUTIONS FOR USE

Exposure Standards:	10mg / m3 Dust NOS (not otherwise specified) (NOHSC 1995)
Engineering Controls:	If dust is created when drilling or cutting the product in a poorly ventilated area local dust extraction is recommended.
Personal Protection:	If dust is generated, use a class P1 or P2 respirator conforming to AS/NZS 1715 and 1716
	Wear goggles or safety glasses if dust is likely to cause irritation.
	Wear suitable gloves when cutting and drilling this product (preferably elbow length)
Flammability:	Not Combustible, however decomposition in fire may cause toxic fumes.

SAFE HANDLING INFORMATION

Storage and Transport:	Store in a dry place, preferably out of direct sunlight. Not regulated for Transport Purposes.
Spills:	Remove bulk, then vacuum, avoid creating excessive dust.
Disposal:	Waste should be placed in containers or bags that prevent dust emission, and disposed of in accordance with the local waste disposal authority requirements.
Fire explosion / Hazard:	Not combustible, Fire fighters to wear self contained breathing apparatus.

OTHER INFORMATION

Emergency Numbers:

National Poisons Centre (24 hrs)	**13 11 26**
Wagners Group Safety Officer (8am to 5pm)	**(07) 4637 7880**

This MSDS summarizes at the date of issue Wagners CFT Manufacturing Pty Ltd 's best knowledge of the health and safety information of the product, and how best to transport, store and handle the product in the workplace. As Wagners has no control over the end use of its products, each user must, prior to acceptance of goods, review this MSDS in the context of how the product will be handled and used in the workplace. The user should contact this company should any clarification or further risk assessment be deemed necessary.

Appendix C: Experimentation Apparatus

Appendix C.1: Composite Member

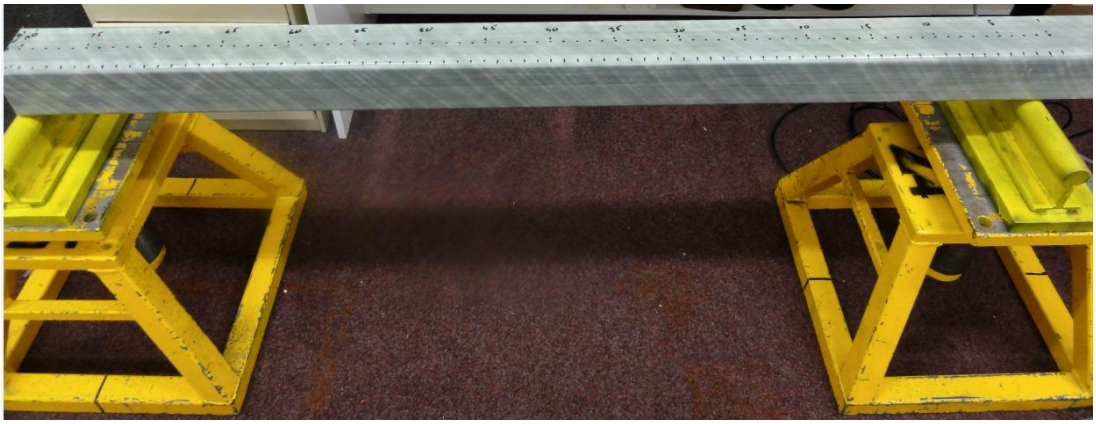

Appendix C.2: Shaker Attachment Apparatus

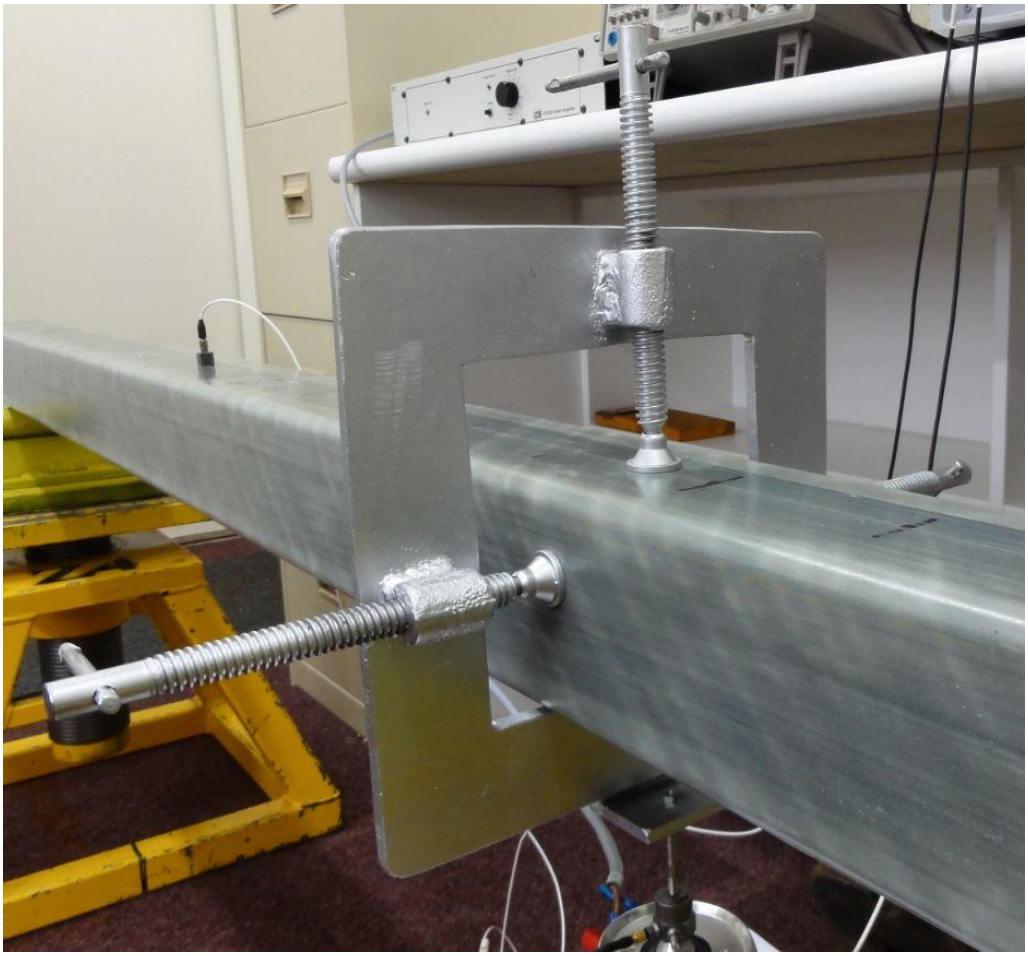

Appendix C.3: Shaker

Appendix C.4: Shaker Specifications

2.1 Specification - V200 Series Vibrators

		Metric		American	
Model		**V201/203**		**V201/203**	
Sine force, peak	(Note 2)	17.8 N		4.0 lbf	
Maximum Sine force peak	(Note 3)	26.7 N		6.0 lbf	
Armature Resonance Frequency		13000 Hz		13000 Hz	
Useful Frequency Range		5 - 13000 Hz		5 - 13000 Hz	
Effective Mass of Moving Element		0.020 kg		0.044 lb	
Velocity Sine Peak	(Note 2)	1.49 m/s		58.7 in/s	
Maximum Velocity Sine Peak	(Note 3)	1.83 m/s		72.0 in/s	
Maximum Acceleration Sine Peak Maximum Acceleration Sine Peak	(Note 2) (Note 3)	890 m/s^2 1335 m/s^2		90.7 gn 136 gn	
Amplifier rating		0.048 kVA		0.048 kVA	
LDS Amplifier		PA25E		PA25E	
Suspension axial stiffness (nominal) Stiffness with auxiliary suspension		2.8 N/mm 12.3 N/mm		16 lbf/in 70 lbf/in	*(11)*
Displacement (continuous) pk-pk		5.0 mm		0.2 in	
Max. Displacement (cont.) pk-pk		5.0 mm		0.2 in	
Cooling Air Flow Rate		0.001 m^3/s		2.1 ft^3/min	
Max. working ambient temperature		30^0C		86^0F	
Heat rejected to air		48 W		48 W	
Electrical requirement - Amplifier		0.13 kVA		0.13 kVA	
Max. acoustic noise (Ref. Figure 1.4)		75 dBA		75 dBA	
Impedance at 500 Hz	(Fig. 1.3)	2.0 ohm		2.0 ohm	
Vibrator mass, (mounting)	(base)		(trunnion)	(base)	(trunnion)
	1.81 kg		3.17 kg	4.0 lb	7.0 lb
Height	96 mm		128 mm	3.78 in	5.06 in
width	78 mm dia.		102 mm	3.06 in	4.00 in
Length	- - -		117 mm	- - -	4.63 in

Notes: 1. Details not applicable to this range of vibrator shown - n/a.
2. Performance available with LDS amplifier, naturally cooled.
3. Maximum performance with forced air cooling (with another amplifier)

Appendix C.5: Shaker Cross-Section Assembly Diagram

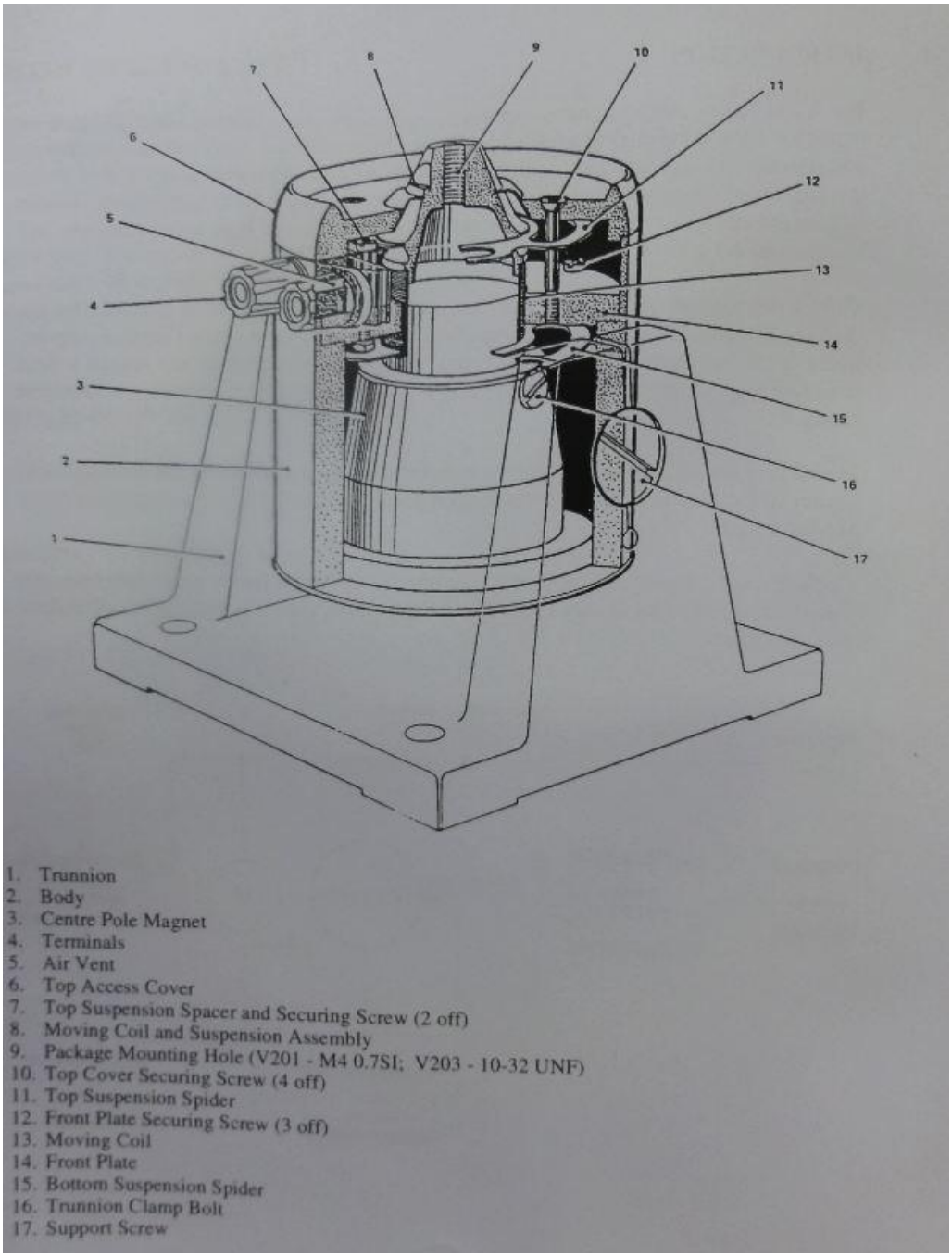

Appendix C.6: PCB Accelerometer Specifications

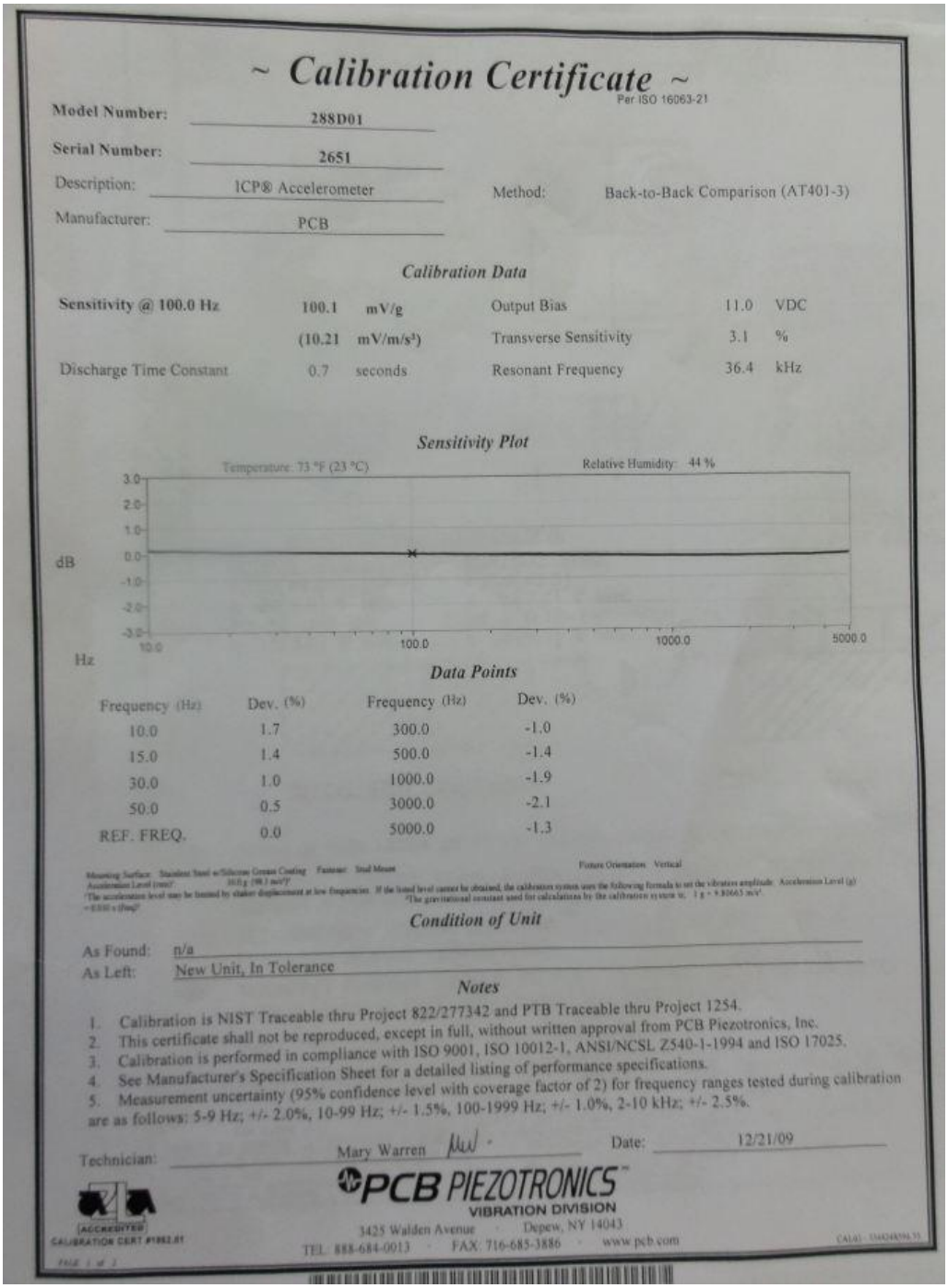

~ Calibration Certificate ~

Per ISO 16063-21

Model Number: 288D01

Serial Number: 2651

Description: ICP® Accelerometer Method: Back-to-Back Comparison (AT401-3)

Manufacturer: PCB

Calibration Data

Sensitivity @ 100.0 Hz	**100.1**	**mV/g**	Output Bias	11.0	VDC
	(10.21	**mV/m/s²)**	Transverse Sensitivity	3.1	%
Discharge Time Constant	0.7	seconds	Resonant Frequency	36.4	kHz

Sensitivity Plot

Temperature: 73 °F (23 °C) Relative Humidity: 44 %

Data Points

Frequency (Hz)	Dev. (%)	Frequency (Hz)	Dev. (%)
10.0	1.7	300.0	-1.0
15.0	1.4	500.0	-1.4
30.0	1.0	1000.0	-1.9
50.0	0.5	3000.0	-2.1
REF. FREQ.	0.0	5000.0	-1.3

Mounting Surface: Stainless Steel w/Silicone Grease Coating Fastener: Stud Mount Future Orientation: Vertical

Acceleration Level (min)*: 10.0 g (98.1 m/s²)*

*The acceleration level may be limited by shaker displacement at low frequencies. If the listed level cannot be obtained, the calibration system uses the following formula to set the vibration amplitude: Acceleration Level (g) = 0.030 x (freq)²

*The gravitational constant used for calculations by the calibration system is: 1 g = 9.80665 m/s².

Condition of Unit

As Found: n/a

As Left: New Unit, In Tolerance

Notes

1. Calibration is NIST Traceable thru Project 822/277342 and PTB Traceable thru Project 1254.
2. This certificate shall not be reproduced, except in full, without written approval from PCB Piezotronics, Inc.
3. Calibration is performed in compliance with ISO 9001, ISO 10012-1, ANSI/NCSL Z540-1-1994 and ISO 17025.
4. See Manufacturer's Specification Sheet for a detailed listing of performance specifications.
5. Measurement uncertainty (95% confidence level with coverage factor of 2) for frequency ranges tested during calibration are as follows: 5-9 Hz; +/- 2.0%, 10-99 Hz; +/- 1.5%, 100-1999 Hz; +/- 1.0%, 2-10 kHz; +/- 2.5%.

Technician: Mary Warren Date: 12/21/09

ACCREDITED CALIBRATION CERT #1982.01

PCB PIEZOTRONICS
VIBRATION DIVISION

3425 Walden Avenue · Depew, NY 14043

TEL: 888-684-0013 · FAX: 716-685-3886 · www.pcb.com

Appendix C.7: Signal Generator

Appendix C.8: Signal Amplifier

Appendix C.9: Data Acquisition Unit

Appendix C.10: Fully Assembled Experimentation Apparatus

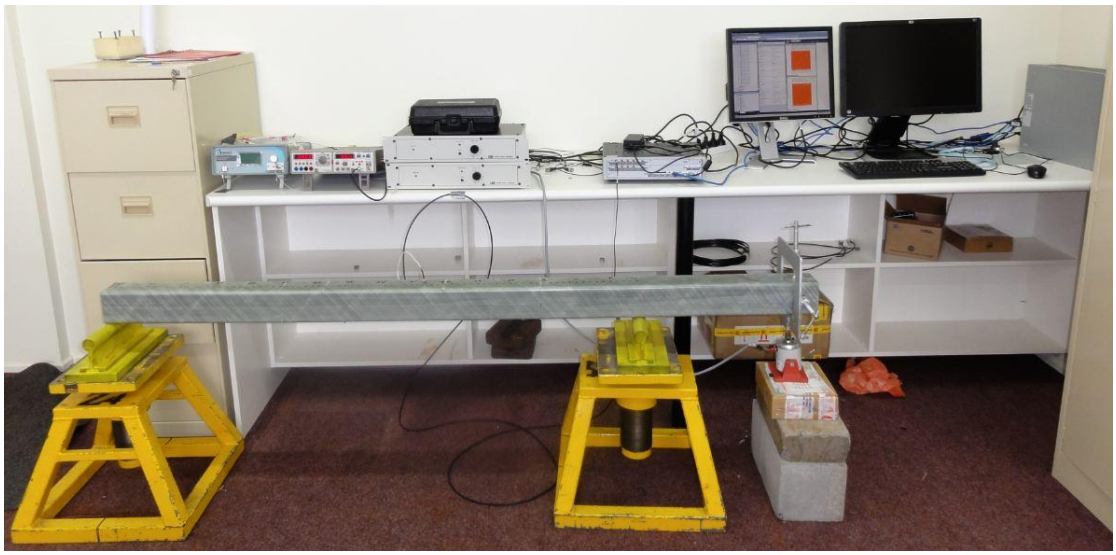

Appendix D: Matlab Post Processing Program

Appendix D.1: Matlab Post Processing Script

```
% Title: Data Importation, Post Processing and Damage Detection Script
% Created by: Erin Heaton - 0050085655

% This program was created to import data pertinent to the damage detection
% experimentation conducted by the researcher. The experimentation was
% conducted at varying damage levels, undamaged, 5%,
% 10%,20%,30%,40%,50%,60% and 80% damage, and at 82 equally spaced data
% acquisition nodes along a composite beam. This program initially imports
% the required data and then conducts a post processing process to provide
% FFT data of force and deflection from the raw force and processed
% acceleration data. The program then uses this FFT data to produce FRF
% data which was then used in a finite difference algorithm to produce
% a damage index at each node for each damage level.


clc
clear
close all
format long

% Simple input GUI

% disp('%-%-%-%-%-%-%-%-%-%-%-%-%-%-%-%-%-%-%-%-%-%-%-%-%-%-%-%-%-%-%-%-...
% %-%-%-%-%-%-%-%-%-%-%')
% disp(' ')
% disp('Program: Damage Detection With The Utilisation Of Frequency...
% Response Function')
% disp(' ')
% disp('Purpose: Determine the position and extent of any damage...
% present in a structure')
% disp(' ')
% disp('Creator: Erin Heaton, 0050085655')
% disp(' ')
% WW = input('Number of Data Sets Per Sample: ');
% disp(' ')
% h = input('Distance Between Nodes (m): ');
% disp(' ')
% Number_of_data_sets = input('Number of Damaged Data Sets: ');
% disp(' ')
% Win1 = input('Starting Time Value (s): ');
% disp(' ')
% Win2 = input('Finishing Time Value (s): ');
% disp(' ')
% Total_Time = input('Total Sampling Time (s): ');
% disp(' ')
% LP = input('Low Frequency Filter Level (Hz): ');
% disp(' ')
% HP = input('Higher Frequency Filter Level (Hz): ');
% disp(' ')
% disp('%-%-%-%-%-%-%-%-%-%-%-%-%-%-%-%-%-%-%-%-%-%-%-%-%-%-%-%-%-%-%-%-...
% %-%-%-%-%-%-%-%-%-%-%')
% disp(' ')
```

```
% Importing data from experimental data

% Multiple data sets:

WW = 82; % Number of sets of data

h = 0.020; % Distance between nodes (m)

Number_of_data_sets = 8; % Input number of data sets

Win1 = 1; % First windowing value

Win2 = 1.05; % Final windowing value

Total_Time = 3; % Sample time (s)

LP = 80; % Hz filter for low frequencies

HP = 500; % Hz filter for high frequencies

TT = 0.000000000000000001; % Filtering value

disp('Undamaged Initiated')
disp(' ')

for k = 1:WW

    Test_Data = ['C:\Data' num2str(k) '.txt'];

    Data_U(k,1) = importdata(Test_Data, ';', 11);

end

Time_Data = Data_U(1,1).data(:,2);

for i = 1:WW

    Acceleration_Data_U(:,i) = ((((Data_U(i,1).data(:,3)))')./9.80665)./...
        1000000; % Change data to m/s^2
    Force_DataA_U(:,i) = (Data_U(i,1).data(:,5))./1000000;
    Force_Data_U(:,i) = (Force_DataA_U(:,i) + (abs(0-(((abs(sum(...
        Force_DataA_U(:,i))))))/(length(Force_DataA_U(:,i)))))))';

end

% Create time data

Time_Full = [0:max(Time_Data)/(length(Time_Data)-1):max(Time_Data)];

WindowVal1 = ((length(Time_Full)/Total_Time)*Win1); % Windowing

WindowVal2 = ((length(Time_Full)/Total_Time)*Win2); % Windowing

Time_Data2 = Time_Full(WindowVal1:WindowVal2); % Time value windowing
```

```
t = Time_Data2; % reassignment of time data
Fs = length(Acceleration_Data_U)/Total_Time; % Sample frequency
%% Undamaged signal processing
T = 1/Fs;
L = length(t)-1;
% Data processing
for i = 1:WW
% Window data processing
% Assignment of acceleration data
DX2_U(:,i) = Acceleration_Data_U(WindowVal1:WindowVal2,i);
DX_U(:,i) = Simpsons(DX2_U(:,i),t); % Velocity data created
X_U(:,i) = Simpsons(DX_U(:,i),t); % Deflection data created
% Performing the Fast Fourier Transform to obtain frequency data:
NFFT = 2^nextpow2(L); % Resolution of frequency
D = fft(X_U(:,i),NFFT)/L; % This is deflection
f = Fs/2*linspace(0,1,NFFT/2+1);
AmpX_U(:,i) = 2*abs(D(1:NFFT/2+1));
% Filter the FFT to be above 80 and below 500 as above is considered as noise
AmpX_U(1:(LP/(Fs/NFFT)),i) = TT;
AmpX_U((HP/(Fs/NFFT):length(AmpX_U)),i) = TT;
end
% Assignment of force data:
for i = 1:WW
F_U(:,i) = Force_Data_U(WindowVal1:WindowVal2,i);
% Changing signal into its hertz constituents:
D2 = fft(F_U(:,i),NFFT)/L;
f2 = Fs/2*linspace(0,1,NFFT/2+1);
AmpF_U(:,i) = 2*abs(D2(1:NFFT/2+1));
```

```
% Filter the FFT to be above 80 and below 500 as above is considered as noise

AmpF_U(1:(LP/(Fs/NFFT)),i) = TT;

AmpF_U((HP/(Fs/NFFT):length(AmpF_U)),i) = TT;

% Therefore to obtain the Frequency Response of this situation the
% deflection is divided by the force:

FRF_U(:,i) = AmpX_U(:,i)./AmpF_U(:,i);

% Assignment of acceleration data:

AA = DX2_U(:,i);

% Changing signal into its hertz constituents:

D3 = fft(DX2_U(:,i),NFFT)/L;

A = Fs/2*linspace(0,1,NFFT/2+1);

AmpA_U(:,i) = 2*abs(D3(1:NFFT/2+1));

end

%% Damaged data import

% Several sets at once

j = 1; %

while j <= Number_of_data_sets


if j == 1

disp('5 Percent Damage Initiated')
disp(' ')

for k = 1:WW

    % Name of 5 percent data on HDD

    Test_Data = ['C:\Data\5_Percent\Data_D_' num2str(k) '.txt'];

    Data_D(k,1) = importdata(Test_Data, ';', 11); % Import 5 percent data

end

Time_Data = Data_D(1,1).data(:,2); % Creation of 5 percent time data

end
```

```
if j == 2

disp('10 Percent Damage Initiated')
disp(' ')

for k = 1:WW

    % Name of 10 percent data on HDD

    Test_Data = ['C:\Data_10_Percent\Data_D_' num2str(k) '.txt'];

    Data_D(k,1) = importdata(Test_Data, ';', 11); % Import 10 percent data

end

Time_Data = Data_D(1,1).data(:,2); % Creation of 10 percent time data

end

if j == 3

disp('20 Percent Damage Initiated')
disp(' ')

for k = 1:WW

    % Name of 20 percent data on HDD

    Test_Data = ['C:\Data\20_Percent\Data_D_' num2str(k) '.txt'];

    Data_D(k,1) = importdata(Test_Data, ';', 11); % Import 20 percent data

end

Time_Data = Data_D(1,1).data(:,2); % Creation of 20 percent time data

end

if j == 4

disp('30 Percent Damage Initiated')
disp(' ')

for k = 1:WW

    % Name of 30 percent data on HDD

    Test_Data = ['C:\Users\30_Percent\Data_D_' num2str(k) '.txt'];

    Data_D(k,1) = importdata(Test_Data, ';', 11); % Import 30 percent data

end

Time_Data = Data_D(1,1).data(:,2); % Creation of 30 percent time data
```

```
end

if j == 5

disp('40 Percent Damage Initiated')
disp(' ')

for k = 1:WW

    % Name of 40 percent data on HDD

    Test_Data = ['C:\Users\40_Percent\Data_D_' num2str(k) '.txt'];

    Data_D(k,1) = importdata(Test_Data, ';', 11); % Import 40 percent data

end

Time_Data = Data_D(1,1).data(:,2); % Creation of 40 percent time data

end

if j == 6

disp('50 Percent Damage Initiated')
disp(' ')

for k = 1:WW

    % Name of 50 percent data on HDD

    Test_Data = ['C:\Users\50_Percent\Data_D_' num2str(k) '.txt'];

    Data_D(k,1) = importdata(Test_Data, ';', 11); % Import 50 percent data

end

Time_Data = Data_D(1,1).data(:,2); % Creation of 50 percent time data

end

if j == 7

disp('60 Percent Damage Initiated')
disp(' ')

for k = 1:WW

    % Name of 60 percent data on HDD

    Test_Data = ['C:\Users\60_Percent\Data_D_' num2str(k) '.txt'];

    Data_D(k,1) = importdata(Test_Data, ';', 11); % Import 60 percent data

end
```

```
Time_Data = Data_D(1,1).data(:,2); % Creation of 60 percent time data

end

if j == 8

disp('80 Percent Damage Initiated')
disp(' ')

for k = 1:WW

     % Name of 80 percent data on HDD

    Test_Data = ['C:\Users\80_Percent\Data_D_' num2str(k) '.txt'];

    Data_D(k,1) = importdata(Test_Data, ';', 11); % Import 80 percent data

end

Time_Data = Data_D(1,1).data(:,2); % Creation of 80 percent time data

end

for i = 1:WW

    Acceleration_Data_D(:,i) = ((((Data_D(i,1).data(:,3)))')./9.80665)./...
        1000000; % Change data to m/s^2
    Force_DataA_D(:,i) = (Data_D(i,1).data(:,5))./1000000;
    Force_Data_D(:,i) = (Force_DataA_D(:,i) + (abs(0-(((abs(sum(...
        Force_DataA_D(:,i)))))/(length(Force_DataA_D(:,i)))))))';

end

% Active time data assigned

Time_Full = [0:max(Time_Data)/(length(Time_Data)-1):max(Time_Data)];

WindowVal1 = ((length(Time_Full)/Total_Time)*Win1);

WindowVal2 = ((length(Time_Full)/Total_Time)*Win2);

Time_Data2 = Time_Full(WindowVal1:WindowVal2); % Active time data windowed

t = Time_Data2;


%% Damaged signal processing

%Fs = length(Time_Data2)/max(Time_Data2);

T = 1/Fs;

%t = (0:L-1)*T;

L = length(t)-1;
```

```
% Data processing

for i = 1:WW

DX2_D(:,i) = Acceleration_Data_D(WindowVal1:WindowVal2,i);

DX_D(:,i) = Simpsons(DX2_D(:,i),t);

X_D(:,i) = Simpsons(DX_D(:,i),t);

% Performing the Fast Fourier Transform to obtain frequency data:

NFFT = 2^nextpow2(L);

D = fft(X_D(:,i),NFFT)/L; % Deflection

f = Fs/2*linspace(0,1,NFFT/2+1);

AmpX_D(:,i,j) = 2*abs(D(1:NFFT/2+1));

% Filter the FFT to be above 80 and below 500 as above is considered as noise

AmpX_D(1:(LP/(Fs/NFFT)),i,j) = TT;

AmpX_D((HP/(Fs/NFFT):length(AmpX_D)),i,j) = TT;

end

% Assignment of force data:

for i = 1:WW

F_D(:,i) = Force_Data_D(WindowVal1:WindowVal2,i);

% Changing signal into its hertz constituents:

D2 = fft(F_D(:,i),NFFT)/L;

f2 = Fs/2*linspace(0,1,NFFT/2+1);

AmpF_D(:,i,j) = 2*abs(D2(1:NFFT/2+1));

% Filter the FFT to be above 80 and below 500 as above is considered as noise

AmpF_D(1:(LP/(Fs/NFFT)),i,j) = TT;

AmpF_D((HP/(Fs/NFFT):length(AmpF_D)),i,j) = TT;

% Therefore to obtain the Frequency Response of this situation the
% deflection is divided by the force:

FRF_D(:,i) = AmpX_D(:,i,j)./AmpF_D(:,i,j);

end
```

```
%% Required FRF change:

FRF_U(:,WW+1) = FRF_U(:,WW);

FRF_D(:,WW+1) = FRF_D(:,WW);

% Windowing

FRF_U_W = FRF_U; %(200:300,:);

FRF_D_W = FRF_D; %(10:500,:);

for i = 2:WW

    AlphaX2_U(:,i) = (FRF_U_W(:,i+1) - 2.*FRF_U_W(:,i) + FRF_U_W(:,i-1))/...
        ((2*h)^2); % Creation of undamaged alpha values

    AlphaX2_D(:,i) = (FRF_D_W(:,i+1) - 2.*FRF_D_W(:,i) + FRF_D_W(:,i-1))/...
        ((2*h)^2); % Creation of active damaged alpha values

end

for i = 2:WW

AlphaX2_U(1,i) = sum(AlphaX2_U(:,i))./length(AlphaX2_U);

AlphaX2_D(1,i) = sum(AlphaX2_D(:,i))./length(AlphaX2_D);

end

%% Finite difference operation

% operation of the difference method:

for i = 2:WW

    % Creation of damage index data

   Beta(1,i) = ((AlphaX2_D(1,i).^2 + ((sum(AlphaX2_D(1,:)))).^2).*((...
       sum(AlphaX2_U(1,:))).^2))./((AlphaX2_U(1,i).^2 + ((sum(...
       AlphaX2_U(1,:))).^2)).*((sum(AlphaX2_D(1,:))).^2));

end

j = j+1; % Continue to next set of damaged data

end

%% Plotting of the data:

figure
Node_Number = [1:1:WW];
plot(Node_Number,Beta(1,:,1),'b',Node_Number,Beta(1,:,2),'g',...
    Node_Number,Beta(1,:,3),'r',Node_Number,Beta(1,:,4),'c',...
```

```
    Node_Number,Beta(1,:,5),'m',Node_Number,Beta(1,:,6),'y',..
Node_Number,Beta(1,:,7),'k',Node_Number,Beta(1,:,8),'-k') % percent damage

LEG = legend('5 Percent Damage','10 Percent Damage','20 Percent Damage',...
    '30 Percent Damage','40 Percent Damage','50 Percent Damage',...
    '60 Percent Damage','80 Percent Damage',7);

set(LEG,'Interpreter','none')

title('Damage Index')
xlabel('Node Number')
ylabel('Damage Index')
```

Appendix D.2: Matlab Simpson's Rule Function File

```
% Simpsons Rule for integrating

% Interpolates data points in sets of 9 points for accuracy and integration.

function Q = Simpson(F,a)

i = 1;

while i <= length(F)-8

    aa = a(i);

    bb = a(i+1);

    Fa = F(i);

    Fb = F(i+1);


     Fw = [F(i) F(i+1) F(i+2) F(i+3) F(i+4) F(i+5) F(i+6) F(i+7) F(i+8)];

     Fd = interp(Fw,100);

     if i > 1

    Q(i) = ((bb-aa)/6)*(Fa + 4*(Fd((1/18)*length(Fd)))+Fb);

     else

    Q(i) = ((bb-aa)/6)*(Fa + 4*(Fd((1/18)*length(Fd)))+Fb);

     end

 i = i+1;

end

while i <= length(F)-8
 if i >= length(F)- 8

     Fw = [F(length(F)-8) F(length(F)-7) F(length(F)-6) F(length(F)-5)...
         F(length(F)-4) F(length(F)-3) F(length(F)-2) F(length(F)-1)...
         F(length(F))];

      Fd = interp(Fw,1000);

     Q(i) = ((bb-aa)/6)*(Fa + 4*((Fd((1/18)*length(Fd))))+Fb);

    i = i+1;

 end
end
     while i <= length(F)-7
 if i >= length(F)- 8
```

```
    Fw = [F(length(F)-8) F(length(F)-7) F(length(F)-6) F(length(F)-5)...
        F(length(F)-4) F(length(F)-3) F(length(F)-2) F(length(F)-1)...
        F(length(F))];

     Fd = interp(Fw,1000);

    Q(i) = ((bb-aa)/6)*(Fa + 4*((Fd((3/18)*length(Fd))))+Fb);

   i = i+1;

end
    end
    while i <= length(F)-6
if i >= length(F)- 8

    Fw = [F(length(F)-8) F(length(F)-7) F(length(F)-6) F(length(F)-5)...
        F(length(F)-4) F(length(F)-3) F(length(F)-2) F(length(F)-1)...
        F(length(F))];

     Fd = interp(Fw,1000);

   Q(i) = ((bb-aa)/6)*(Fa + 4*((Fd((5/18)*length(Fd))))+Fb);

   i = i+1;


end
    end
    while i <= length(F)-5
if i >= length(F)- 8

    Fw = [F(length(F)-8) F(length(F)-7) F(length(F)-6) F(length(F)-5)...
        F(length(F)-4) F(length(F)-3) F(length(F)-2) F(length(F)-1)...
        F(length(F))];

     Fd = interp(Fw,1000);

    Q(i) = ((bb-aa)/6)*(Fa + 4*((Fd((7/18)*length(Fd))))+Fb);

   i = i+1;

end
    end
    while i <= length(F)-4
if i >= length(F)- 8

    Fw = [F(length(F)-8) F(length(F)-7) F(length(F)-6) F(length(F)-5)...
        F(length(F)-4) F(length(F)-3) F(length(F)-2) F(length(F)-1)...
        F(length(F))];

     Fd = interp(Fw,1000);

    Q(i) = ((bb-aa)/6)*(Fa + 4*((Fd((9/18)*length(Fd))))+Fb);

   i = i+1;
```

```
end
    end
    while i <= length(F)-3
if i >= length(F)- 8

    Fw = [F(length(F)-8) F(length(F)-7) F(length(F)-6) F(length(F)-5)...
        F(length(F)-4) F(length(F)-3) F(length(F)-2) F(length(F)-1)...
        F(length(F))];

     Fd = interp(Fw,1000);

    Q(i) = ((bb-aa)/6)*(Fa + 4*((Fd((11/18)*length(Fd))))+Fb);

   i = i+1;

end
    end
    while i <= length(F)-2
if i >= length(F)- 8

    Fw = [F(length(F)-8) F(length(F)-7) F(length(F)-6) F(length(F)-5)...
        F(length(F)-4) F(length(F)-3) F(length(F)-2) F(length(F)-1)...
        F(length(F))];

     Fd = interp(Fw,1000);

    Q(i) = ((bb-aa)/6)*(Fa + 4*((Fd((13/18)*length(Fd))))+Fb);

   i = i+1;

end
    end
    while i <= length(F) - 1
if i >= length(F)- 8

    Fw = [F(length(F)-8) F(length(F)-7) F(length(F)-6) F(length(F)-5)...
        F(length(F)-4) F(length(F)-3) F(length(F)-2) F(length(F)-1)...
        F(length(F))];

     Fd = interp(Fw,1000);

Q(i) = ((bb-aa)/6)*(Fa + 4*((Fd((15/18)*length(Fd))))+Fb);

   i = i+1;

end
    end
    while i <= length(F)
if i >= length(F)- 8

    Fw = [F(length(F)-8) F(length(F)-7) F(length(F)-6) F(length(F)-5)...
        F(length(F)-4) F(length(F)-3) F(length(F)-2) F(length(F)-1)...
        F(length(F))];
```

```
      Fd = interp(Fw,1000);

     Q(i) = ((bb-aa)/6)*(Fa + 4*((Fd((17/18)*length(Fd))))+Fb);

    i = i+1;

 end
     end
end
```

Appendix E: Data Produced by Post Processing Program

Appendix E.1: Acceleration Data, Node 55, 10 Percent Damage

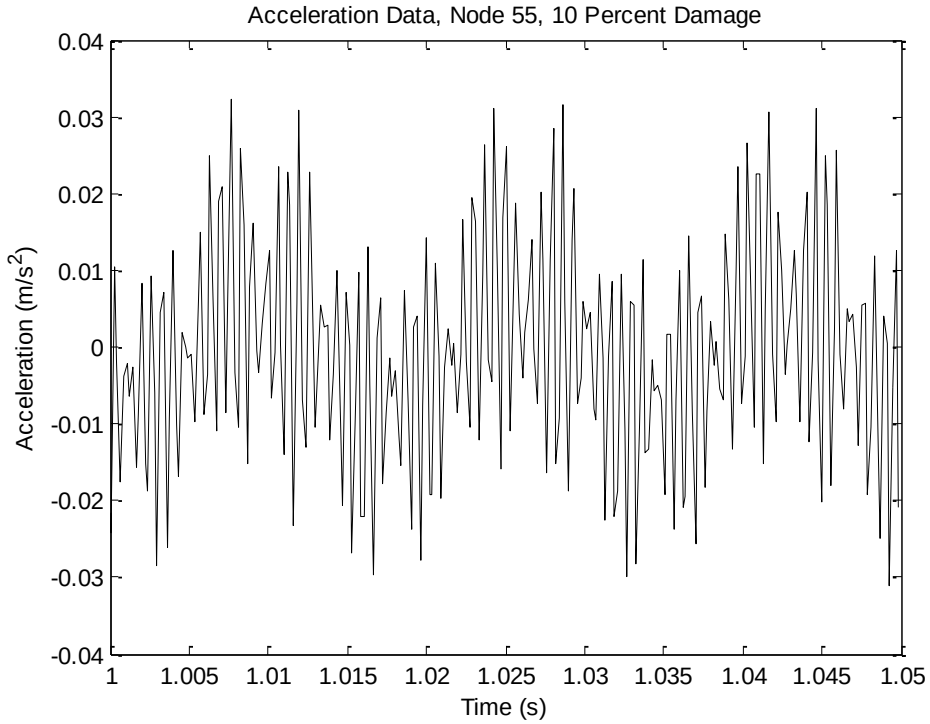

Appendix E.2: Acceleration Data, Node 55, 30 Percent Damage

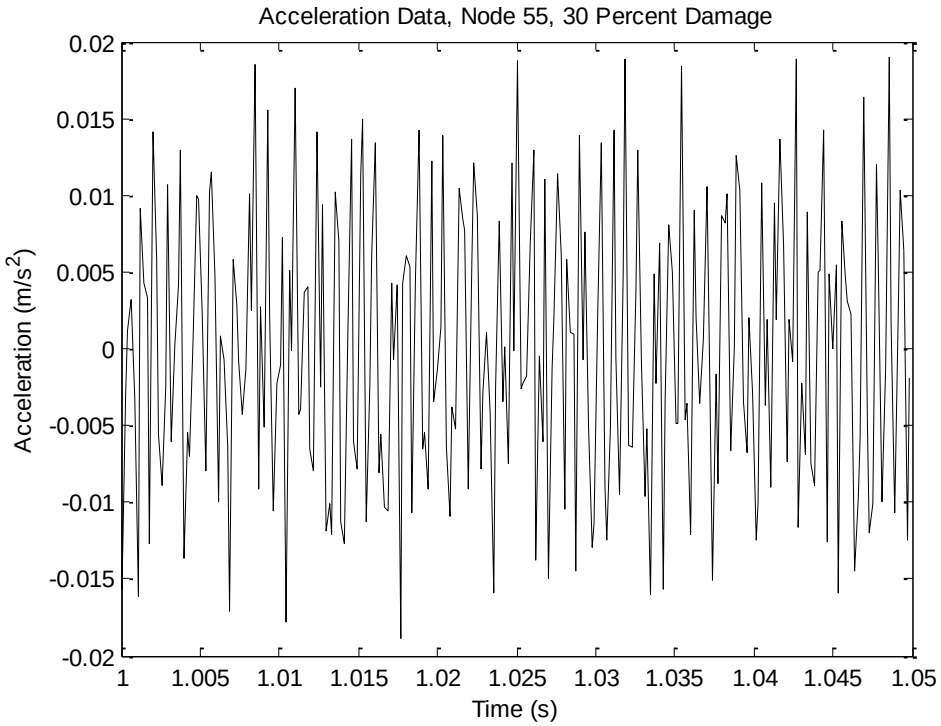

Appendix E.3: Acceleration Data, Node 23, 40 Percent Damage

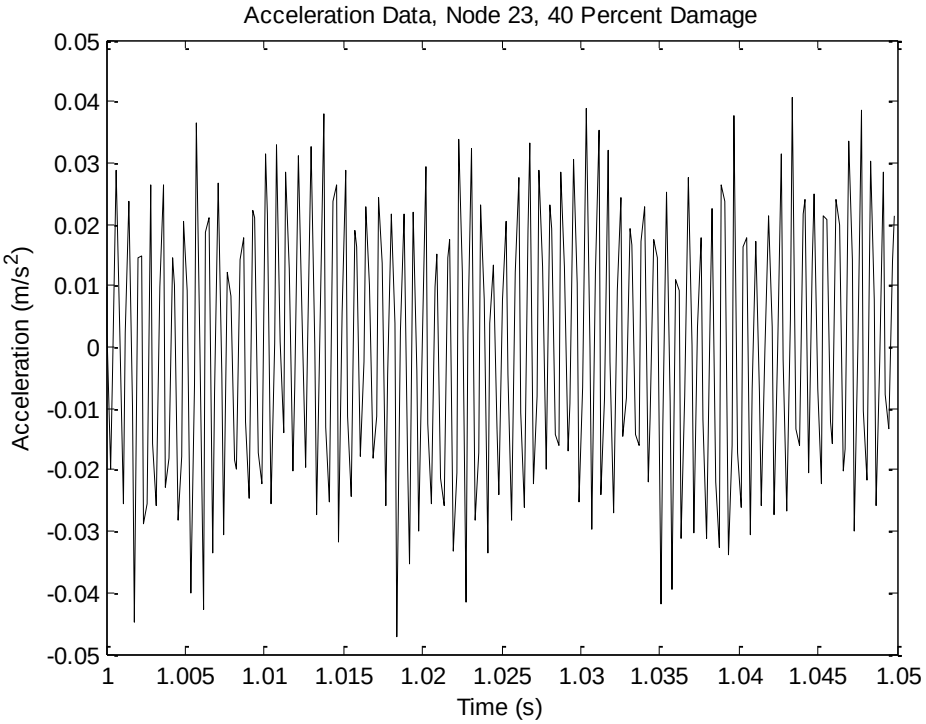

Appendix E.4: Force Data, Node 23, 10 Percent Damage

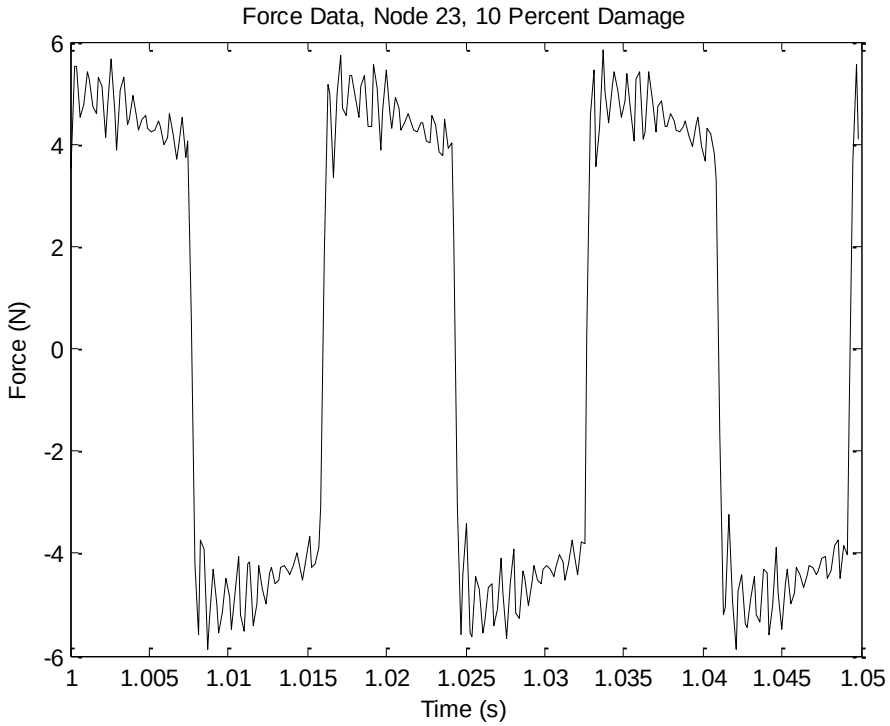

Appendix E.5: Force Data, Node 40, 40 Percent Damage

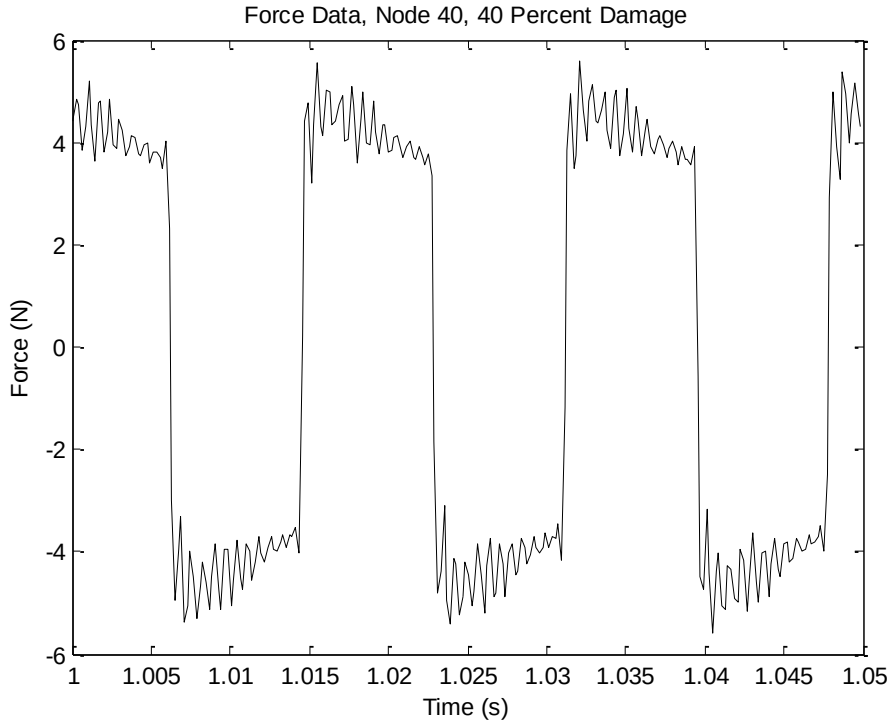

Appendix E.6: Force Data, Node 55, 50 Percent Damage

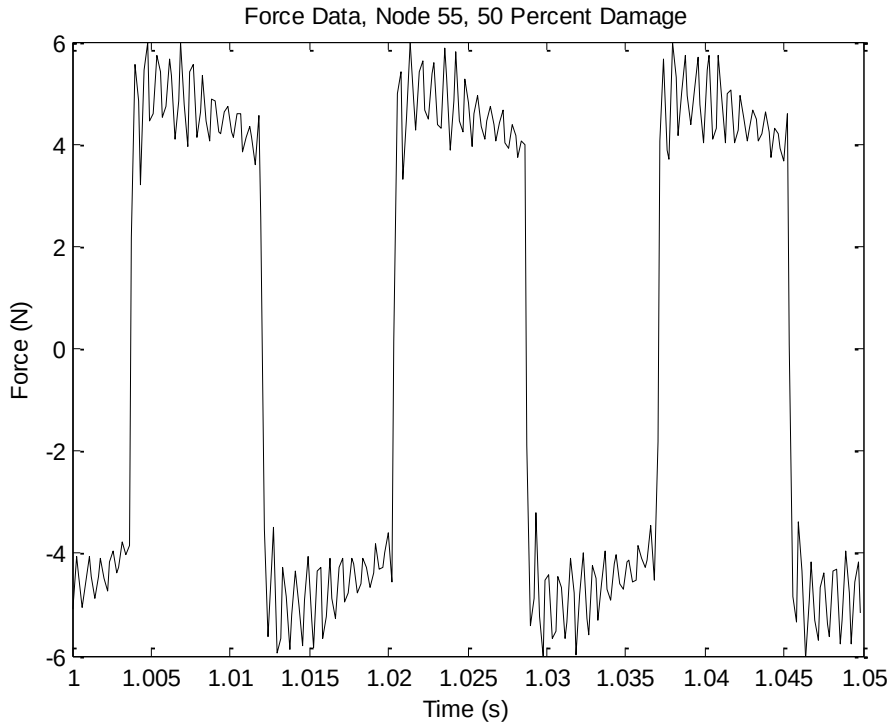

Appendix F: Natural Frequency Calculation

Appendix F.1: First Natural Frequency Calculations

To obtain the first natural frequency of the system the equation outlined in section 5.2 was used (Balachandran & Magrab 2009):

$$f_n = \frac{\left(\sqrt{\frac{E}{\rho}}\right)\left(\sqrt{\frac{I}{A}}\right)\Omega_n^2}{2\pi L^2}$$

Where the material properties are:

$E = 35.4$ GPa (obtained from appendix B.1 (Wagners 2009))

$\rho = 2000$ kg/m^2 (obtained from appendix B.2 (Wagners 2009))

$$I = \left(\frac{1}{3} \times 0.1^3 \times 0.1\right) - \left(\frac{1}{3} \times 0.09^3 \times 0.09\right) = 1.14633 \times 10^{-5} \text{ m}^4$$

$$A = 0.1 \times 0.1 - 0.09 \times 0.09 = 0.0019 \text{ m}^2$$

$\Omega_n = \pi$ (for the first natural frequency, obtained from table 9.3, pg 578, Balachandran & Magrab 2009)

$L = 1.6$ m (length of member)

Therefore:

$$f_n = \frac{\left(\sqrt{\frac{E}{\rho}}\right)\left(\sqrt{\frac{I}{A}}\right)\Omega_n^2}{2\pi L^2}$$

$$f_n = \frac{\left(\sqrt{\frac{35.4 \times 10^9}{2000}}\right)\left(\sqrt{\frac{1.14633 \times 10^{-5}}{0.0019}}\right)\pi^2}{2\pi 1.6^2}$$

$$f_n = 200.51$$

Therefore the first natural frequency of the system was 200.51 Hz for a perfect undamaged section of material.